Ultrasonic wave phase conjugation for air-coupled velocimetry : investigations of possible application on micro streams

Pavel Shirkovskiy

N° d'ordre : 119

ECOLE CENTRALE DE LILLE

INSTITUT DE RADIOTECHNIQUE, D'ELECTRONIQUE ET D'AUTOMATIQUE DE MOSCOU (MIREA-Université Technologique d'Etat)

THÈSE

présentée en vue
d'obtenir le grade

DOCTEUR

en
Spécialité : Micro et nano Technologies, acoustique et télécommunication

par

SHIRKOVSKIY Pavel

DOCTORAT DELIVRE CONJOINTEMENT PAR L'ECOLE CENTRALE DE LILLE ET L'INSTITUT DE RADIOTECHNIQUE, D'ELECTRONIQUE ET D'AUTOMATIQUE DE MOSCOU (MIREA)

Titre de la thèse :

CONJUGAISON DE PHASE ULTRASONORE POUR LA VELOCIMETRIE DES ECOULEMENTS GAZEUX. INVESTIGATIONS DES POTENTIALITÉS EN MICRO-FLUIDIQUE

Soutenue le 30 Avril 2010 devant le jury d'examen:

Président	Marc DESCHAMPS	Directeur de Recherche CNRS à Laboratoire de Mécanique Physique à l'Université Bordeaux 1
Rapporteur	Serge MENSAH	Maitre de conférences HDR à l'Ecole Centrale de Marseille
Rapporteur	Louis Pascal TRAN-HUU-HUE	Professeur à l'Ecole National d'Ingénieur de Val de Loire
Membre invité	Olivier BOU MATAR	Professeur à l'Ecole Centrale de Lille
Membre invité	Alain MERLEN	Professeur à l'Université de Lille 1
Directeurs	Philippe PERNOD	Professeur à l'Ecole Centrale de Lille
	Vladimir PREOBRAZHENSKY	Professeur à l'Ecole Centrale de Lille & Directeur de Recherche à l'Institut de Physique Générale de l'Académie des Sciences de Russie
	Yuri PYL'NOV	Professeur à l'Institut de Radiotechnique, d'Electronique et d'Automatique de Moscou (MIREA)

Thèse préparée dans le Laboratoire International Associé en Magnéto-ACoustique nonlinéaire de la matière condensée (LEMAC) de l'Institut d'Electronique, Microélectronique et Nanotechnologie (UMR CNRS 8520) et de l'Institut de Radiotechnique, d'Electronique et d'Automatique de Moscou (Russie)
Ecole Doctorale SPI 072

Acknowledgement

Ce travail a été réalisé au sein du Laboratoire International associé en Magnéto-Acoustique non-linéaire de la matière condensée (LEMAC), à l'Institut d'Electronique de Microélectronique et de Nanotechnologie (IEMN, CNRS/UMR 8520, France) en co-tutelle avec l'Institut de Radiotechnique d'Electronique et d'Automatique (MIREA, Université technique, Russie).

Je remercie vivement en premier lieu mes directeurs de thèse du coté français les Professeurs Philippe PERNOD et Vladimir PREOBRAZHENSKY de l'Ecole Centrale de Lille pour m'avoir accueilli dans leur équipe (LEMAC-IEMN), pour leur encadrement et pour la confiance qu'ils m'ont témoigné tout au long de ces trois années de travail.

Je remercie au même titre mon directeur de thèse du coté Russe le Maître de conférence Yuri PYL'NOV de l'Institut de Radiotechnique d'Electronique et d'Automatique de Moscou, je tiens à lui exprimer toute ma reconnaissance pour l'intensité de son partage et de son soutien.

J'associe également à ces remerciements le Professeur Louis Pascal TRAN-HUU-HUE de l'Ecole Nationale d'Ingénieur de Val de Loire et le Maitre de conférences Serge MENSAH de l'Ecole Centrale de Marseille d'avoir accepté de rapporter ce travail, ainsi que les membres du jury, le Docteur Marc DESCHAMPS, Directeur de Recherches au Laboratoire de Mécanique Physique LMP de l'Université Bordeaux 1 et les Professeurs Alain MERLEN de l'Université de Lille 1, et Olivier BOU MATAR de l'Ecole Centrale de Lille.

Je remercie aussi l'Ambassade de France à Moscou et le Ministère des Affaires Etrangères français pour la bourse de thèse qu'ils m'ont attribuée, ce qui m'a permis de venir en France durant la moitié de ce travail.

Cette thèse a enfin été rendue possible par le soutien et l'amitié de tous les membres présents et passés du LEMAC. L'environnement de recherche varié rencontré dans cette équipe a rendu mon expérience à Lille particulièrement enrichissante.

Je veux aussi exprimer ma reconnaissance à tous les personnels de l'IEMN qui ont permis ces recherches.

Table of figures

Figure 5.14 : The distribution of velocity in the air jet calculated from phase(a) and amplitude(b) distribution of ultrasonic PCW for turbulent flow.

Figure 5.15 : Results of simulation and experimental data of velocities distribution and phase shift in air jet. A - experimental data of phase shift of phase conjugate wave passed through air flow; B - numerical modeling of phase shift of phase conjugate wave passed through air flow; C –l numerical modeling of distribution of flow velocities.

Figure 5.16 : Phase shift distribution of the phase conjugate wave in cross-section of the flow received experimentally (points) and by means of numerical modeling (continuous lines): 1 — on distance about 5 mm from a nozzle (section 1 and 3 on fig. 5.12); 2 – on distance about 8 mm from a nozzle (section 2 and 4 on fig. 5.12).

List of tables

Table of contents

Introduction

Ultrasound is widely used for non-invasive diagnostics and for non-destructive testing in industry and medical applications: medical diagnostic, defect detection, for determining significant materials characteristics etc. Ultrasound and its applications have grown substantially. Highly desirable applications have attracted the attention of a wide range of industries. While ultrasound and its applications have grown phenomenally in the recent years, the mode by which it is propagated in a given test medium is severely limited. All conventional ultrasound is based upon the severe limitation of a physical contact between the transducer and the test medium by a liquid or semi-liquid couplants. For the past 20 years, few attempts have been made to change this mode of coupling to non-contact mode.

Air-coupled ultrasound has gained considerable attention over the past two decades thanks to its ability to eliminate the physical contact between the transducer and the material under inspection, especially in cases when humidity can change properties of the materials or even destroy the material, such as honeycomb structure. Also, liquid coupling cannot be used when water can fill defects and the detectability of the defects may be reduced. Use of contact ultrasonic systems is restricted in the case of complex geometry structures.

Air-coupled ultrasound in the low megahertz frequency range is becoming a real possibility for some particular applications: in nondestructive evaluation, distance and thickness measurements, testing, investigation of surfaces of the objects, imaging, flow measurements and etc. For example, in the composite industry, air-coupled ultrasonic inspection is starting to be applied to evaluate delaminations in laminates and sandwich

panels. The major advantages compared to the contact ultrasonic technique derive from the elimination of the risk associated with filling the composite delaminations with the coupling medium and heating the component during the drying procedures after inspection.

On the other hand, recent decade, the wave phase conjugation (WPC) of ultrasonic beams has become one of the forcefully developed lines of inquiry in physical acoustics and ultrasonics. Among the methods of generation of phase conjugate acoustic waves, practical significance was revealed by a numerical method of time reversal, based on multichannel receiver–emitter arrays, and the parametric phase conjugation of sound in acoustically active solid magnetics and piezoelectrics.

Parametric wave phase conjugation, based on magneto-acoustic interaction, is one of the most advantageous methods of acoustic wave transformation for various applications in ultrasonics. The above-threshold parametric phase conjugation of magnetoelastic waves in magnetostrictive ceramics is an effective way to produce phase conjugate waves (PCWs) with frequencies from several megahertz to several dozen megahertz for applications in medicine and defectoscopy.

The interest in acoustic PCWs stems from their properties to automatically focus onto objects that scatter the incident wave and to compensate the phase distortions of wave propagation in heterogeneous refractive media. Various uses of these properties for ultrasonic diagnostics, therapy, surgery, nondestructive control, and underwater communications have recently been intensely discussed. Due to this phenomenon a new unique possibilities in physical researches, nondestructive tests, and medicine become available.

The development of ultrasonic WPC methods is closely connected with applied studies demonstrating the possibilities of practical use of phase conjugate waves in modern ultrasonic technology. One of realized applications of conjugate waves is the acoustic microscope. Using of WPC method gives the noise reducing effect in a case of heterogeneous distortions placed near tested object. Hyperthermia is one of the very important medical testing methods. The method of magneto-acoustic WPC can be applied in principle for hyperthermia applications because of giant amplification (>80 dB) and high output intensity (>100 W/cm2) in the overthreshold (supercritical) parametric mode.

Development of effective methods for ultrasonic phase conjugation in the megahertz frequency range stimulated interest to the use of phase conjugation processes in ultrasonic tomography and diagnostics of inhomogeneous acoustic media. The most

actual applied line of inquiry is the development of novel systems of acoustic imaging based on the WPC engineering for medical diagnostics and nondestructive evaluation. The possibility to compensate for phase distortions both in conventional linear and novel nonlinear systems of acoustic imaging attracts particular attention.

Application of the phase-conjugation technique has opened new opportunities in phase velocimetry and flow mapping. The offered technics, unlike traditional doplerographie, does not use ultrasound scattering on particles transferred by a stream and is suitable for measurements of speed distribution in flow of homogeneous and non-homogeneous media. Velocimetry systems based on WPC do not demand precision adjustment, providing automatic confocality of measuring schemes, and allow to realise cartography of flow in the conditions of electronic scanning of a probing beam within WPC system aperture, without use of mechanical moving.

Problems of using phase conjugate waves in noncontact methods of acoustic diagnostics including air-coupled microscopy and velocimetry are rather urgent. For developing new application of WPC system to full scale non-contact mode is very important to connect new opportunities in phase velocimetry and flow mapping which gives the phase-conjugation technique with the possibilities of air-coupled ultrasound in low megahertz frequency range.

The main goal of the work was the realization of air-coupled wave phase conjugation technics for velocity measurements of gas micro flows. For achievement of the formulated goal following **research tasks** were assigned:

- The theoretical and experimental investigations of the features of the propagation of phase conjugate waves in gaseous mediums.
- The theoretical and experimental investigations of operating modes of the conjugator with small amplitude signals and different electromagnetic pumping time.
- Choice of advanced signal processing techniques to increase signal to noise ratio.
- The theoretical and experimental investigations of the requirement for efficient acoustical matching between transducer and air, active element of phase conjugation system and air.
- Investigation of possibility of application of wave phase conjugation technics for velocimetry of gas micro flow.
- Investigation of possibility of application of wave phase conjugation technics for air-coupled microscopy.

Methods of investigations. This work has been conducted with the help of the numerical simulation methods, ray acoustics methods, acoustical matching techniques, phase measurements methods, m-sequences phase coding technology, C-mode scanning acoustic visualization and finally magneto-acoustic WPC technology in the overthreshold (supercritical) parametric mode in a magnetostrictive ceramic.

Scientific and practical importance of obtained results.

- For the first time work of the air-coupled wave phase conjugation system is experimentally studied.
- The realization of efficient acoustical matching technique for active element of WPC system in the low megahertz frequency range is developed.
- For registration of weak acoustical phase conjugate signals for the first time was used the technology of phase coding by pseudonoise m-sequence.
- For the first time air-coupled methods of acoustic microscopy and velocimetry by means of phase conjugate waves are applied.

The main points presented to defence of a thesis.

- Mathematical model of phase conjugate wave passage through the interface active element of WPC system/air. This model allows to calculate the power loss per each passage of the air–ferrite (active element of WPC) interface and the intensity of ultrasonic beams with WPC.
- Technology of acoustical matching on base of thin polycorbonate porous oil impregnated membrane filters. This technology allows to optimise the conditions of wave transmission through the interface air–ferrite in the low megahertz frequency range.
- Method of phase coding by pseudonoise m-sequence for registration of weak acoustical phase conjugate signals. This method allows to work more effectively with strong noisy and being under noise level phase conjugate signals. Also this method has allowed to improve a gas flow velocymetry method.
- Experimental results of measurements of phase shift of phase conjugate wave propagating in moving air media. This experimental results allows to restore velocities distribution in an air stream and to create images of this distribution.
- Experimental results of measurements of amplitude and phase of phase conjugate wave propagating in air media on C-scan microscopy system. The results show

that a supercritical mode of parametric WPC can be successfully used in air-coupled acoustic imaging systems.

The practical importance of the work

Results of investigations of air-coupled wave phase conjugation technics can serve for drawing up of new methods ultrasonic velocimetry and microscopy in technical industrial applications. The elaborated methods can be used for development of devices of ultrasonic microscopy, tomography and velocimetry of gas microstreams.

The properties of phase conjugate ultrasonic waves such as compensation of phase distortions in the medium of propagation, autofocusing on ultrasound scatterers allow to design new techniques with better characteristics for acoustic imaging systems.

Phase sensitivity to moving media of air-coupled phase conjugate ultrasonic waves allow to create new techniques with better characteristics, possessing higher sensitivity.

Elaborated method of phase coding by pseudonoise m-sequence expands limits of application of air-coupled wave phase conjugation technics for microscopy and velocymetry.

Chapter 1: Generality of wave phase conjugation and air-coupled ultrasound

The first chapter presents description of different nature concepts of wave phase conjugation, properties and applications of phase conjugate ultrasonic beams; description of non-contact ultrasonic techniques and air-coupled transducers. Various ultrasonic techniques are presented for velocity measuring.

1.1. Acoustic phase conjugation

The problem of the ultrasonic phase conjugation (PC) has long attracted attention because of the unusual physical properties of phase conjugate wave beams and the unique possibilities offered by the PC technique in physical research, nondestructive testing, technology, and medicine. Phase conjugation means the transformation of a wave field resulting in the reversal of propagation of the waves conserving the initial spatial distribution of amplitudes and phases [1]. Unlike the usual specular reflection corresponding to the inversion of one of the spatial coordinates, PC represents the time inversion transformation.

The phenomenon of PC was first observed in a stimulated scattering of light [2]. After this discovery in 1972, phase conjugation has been extensively studied in optics [1, 3].

Studies in acoustics started in 1980's and several kinds of methods to generate phase conjugate waves have been proposed. It was found that some already known

physical phenomena contain the process of phase conjugation. Since then, a considerable number of studies on this matter have been reported. The range of study extends from the basic study to the application to practical ultrasonic instruments. The considerable progress in experiments on acoustic PC during the last decade has made these studies into a field of physical acoustics in its own right.

Despite the generality of the concept of phase conjugation for waves of different nature, PC in acoustics is characterized by silent features related to the wave properties of acoustic media, interactions involved in the PC process, the space-time structure of the acoustic beams being conjugate, and finally, to practical problems that can be solved using the PC phenomenon.

1.1.1. Phase conjugation in the time domain

The phase conjugation of sound waves at relatively low frequencies can be achieved by purely electrical methods [4 - 6] - using multichannel transmitting-receiving antenna arrays. Electronic channel control of the time delay of the received signal allows one to simulate on the array the amplitude-phase distribution corresponding to the phase conjugate wave. Recently, this approach was technically implemented [7, 8]. Modern microprocessors and the technology of matrix piezoelectric transducers permit the realization of PC schemes with hundreds of array elements and an operating frequency of about 5 MHz [9]. Among their advantages are the absence of fundamental restrictions on the shape of the pulse signals being processed and the possibility of deliberate correction of the synthesized amplitude-phase distribution. However, such electronic systems are still extremely complicated to control, cumbersome, and expensive.

Multichannel parametric systems provide some simplification of control and the possibility of operation in real time [4]. The principle of operation is analogous to the wave phase conjugation from a reflecting surface oscillating at double frequency [10 - 12]. The amplitudes of the phase conjugate acoustic waves generated upon such reflection are usually small because of the absence of accumulating parametric effects. A quasi-harmonic signal from a separate receiving transducer in the electronic parametric system is electronically mixed with the double-frequency pump, resulting in the generation of the phase conjugate signal in each channel. In this case, the spatial phase distribution over the array reflects that in the incident wave. The input and output signals are decoupled by means of two closely spaced piezoelectric transducers placed in each channel, operating

as a receiver and a transmitter, respectively. This principle has been used in a one-dimensional 300-kHz PC mirror consisting of 20 elements [4]. However, devices of this type have not gained wide acceptance because of the drastic complexity of construction of the parametric array with increasing operating frequency and the passage to two-dimensional arrays.

1.1.2. Purely acoustic phase conjugation methods and acoustic holography

Alternative physical principles of wave phase conjugation in acoustics were analyzed [13, 14]. Attention was devoted to processes in which the generation of phase conjugate sound waves was accompanied by amplification. Similarly to nonlinear optics [15, 3], mechanisms of phase conjugation based on the intrinsic nonlinearity of an acoustic medium were considered. It is known that four-wave mixing of holographic and parametric types can produce PC in a nonlinear medium. In the case of the holographic mechanism, information on the amplitude-phase distribution in the signal wave is recorded during its interaction with the pump wave of the same frequency. The recording occurs as the spatially inhomogeneous quasi-static perturbation of the medium. The conjugate wave is generated during reading the dynamic hologram by the second pump wave propagating toward the recording wave. In the parametric mechanism, the counter-propagating pump waves produce a spatially uniform modulation of parameters of the medium at double frequency. The conjugate wave is generated during parametric interaction of the variable perturbation of the medium with the signal wave. Both holographic and parametric mechanisms principally allow one to generate a phase conjugate wave which is amplified relative to the incident wave.

However, as was noted [14, 16], a practical implementation of wave phase conjugation on the hydrodynamic nonlinearity in common liquids is hindered by the silent feature related to the absence of ultrasound dispersion, which is typical of nonlinear acoustics as a whole [17]. When the pump-wave intensity is sufficient for producing noticeable PC effect, the processes of energy transfer 'upward' over the spectrum firstly develop, resulting in the generation of saw-tooth waves. To introduce dispersion and enhance nonlinearity, it was suggested to use liquids containing air bubbles [18]. In a system of such type, the nondegenerate three-wave generation of the phase conjugate wave was experimentally examined with an efficiency of about 1% [19]. The use of temperature nonlinearity was considered, which can only be applied for PC in special

cases of highly viscous liquids [20]. The holographic mechanism of wave phase conjugation in liquids containing suspended particles or gas bubbles capable of ordering under the action of acoustic pondermotive forces was discussed [14, 21]. PC of this type was experimentally realized with an efficiency of about 1% [26]. The holographic mechanism of PC based on the nonlinearity of the radiative pressure of sound on the liquid - gas interface was suggested and experimentally realized [22 - 24]. In this case, the PC efficiency in water was about 5% and was limited by side nonlinear effects of surface distortion caused by self-focusing of the sound. By changing the experimental conditions, the PC efficiency was increased almost to unity, which made it possible to observe active suppression of the sound field with the help of the wave phase conjugation considered earlier [25].

A cardinal change in the approach to the problem of the sound wave phase conjugation was associated with abandoning the acoustic pump for modulation of the parameters of a medium. The outlook for the development of parametric PC amplifiers using uniform modulation of the sound velocity by alternating fields of a nonacoustic nature was discussed [13]. However, the search for appropriate mechanisms in real liquids has not led to the desired practical result. Studies of the methods of ultrasonic wave phase conjugation produced in solid-state electro- and magneto-acoustic active media proved to be significantly more efficient.

1.2. Parametric wave phase conjugation

The first observations of the generation of phase conjugate sound waves in a solid were reported about thirty years ago [26]. Later, the effects of acoustic PC in crystals were often discussed, mainly in phonon-echo studies. Comprehensive references on this subject can be found in reviews and monographs [27 - 29].

1.2.1. Acoustic phase conjugation in nonlinear piezoelectric media

The simplest way of obtaining acoustic PC in a solid is by modulation of the sound velocity by an alternating electromagnetic field. Nonlinear piezoelectric method is based on the parametric interaction between acoustic waves at a frequency ω and an electric field at a frequency 2ω. Svaasand is reported on this effect [30] about forty years ago.

Thompson and Quate [31] studied this phenomenon extensively, with special interest in the generation of an electric field at 2ω as a result of the mixing of two acoustic waves at ω. In their work, and in the following studies in this field, the main interest was in the ‘‘convolving effect’’ of two acoustic waves. The phase conjugate effect involved in this phenomenon seems to have been paid little attention at that time.

In the 1980’s, after the prosperous research of optical phase conjugation, this nonlinear piezoelectric interaction attracted the attention of researchers with special interest in the wavefront of acoustic waves. It was pointed out that two acoustic fields in this interaction were in the relation of phase conjugation, and this phenomenon was nothing but a method of generating acoustic phase conjugate waves with the help of electrical field [32, 33]. Papers on phase conjugation using nonlinear piezoelectric materials such as LiNbO3 [34], CdS, BK7 glass [35] and PZT ceramics [36, 37] have been presented.

1.2.2. Magneto-acoustic phase conjugation

The use of the interaction of sound with soft modes of collective excitations of different physical nature substantially extends the possibilities of applications of solids for acoustic PC. The strong influence of the magnetic field on the sound velocity is observed in magnetostriction ferrites [38], a number of rare-earth compounds with giant magnetostriction [39, 40], and in some amorphous alloys [41].

It was reported that an acoustic phase conjugate wave at a frequency ω was generated as a result of the parametric interaction between the incident acoustic wave at a frequency ω and a magnetic field at 2ω in nonlinear magneto-acoustic media such as a-Fe2O3 and hematites. An outstanding feature of this method is that the conversion ratio from the incident wave to the phase conjugate wave is extremely high. Preobrazhensky et al. have reported on this method extensively [42 - 44].

Substantial parametric amplification of the bulk phase conjugate ultrasonic wave amounting to 35 dB at a frequency of 30 MHz was achieved in an antiferromagnetic hematite single crystal [45]. Earlier, parametric excitation of standing sound waves by an alternating magnetic field [46] and nondegenerate generation of the backward travelling ultrasonic wave in the acoustic pump field [47] were observed in this crystal. In the latter case, the generation was caused by the anomalous strong three-wave interaction of coupled magnetoelastic excitations [48].

The extremely high efficiency of the parametric PC of a travelling ultrasonic wave was found experimentally in a magnetostriction ceramics based on nickel ferrite [49]. The amplification coefficient of the backward wave at a frequency of 30 MHz exceeded 80 dB, its estimated intensity being hundreds of 100 W/cm2. The possibility of generation of highly intense phase conjugate ultrasonic waves by means of polycrystalline materials is of special interest because modern ceramic technology allows one to manufacture active elements for PC devices of any size and shape, which may be required for specific applications.

Ultrasound uses in the majority of practical applications are imposed by the obligation of use of ultrasound in low MHz range. Therefore development of ultrasonic PC methods has led to reduce working frequencies of WPC systems 5-10 MHz

In time of ultrasonic waves conjugation in the most of practical uses of WPC effect the liquid became the medium of wave propagation or became plays a role of immersion layer between conjugator, object of testing and transducer.

Development of the supercritical parametric technique of acoustic wave phase conjugation and interest in the implementation of nonlinear wave phenomena in acoustic imaging systems for medical purposes and nondestructive testing has noticeably quickened in the last few years.

The possible application of ultrasonic PCWs that are targets themselves to a scatterer for measuring the scatterer velocity is demonstrated [50, 51]. When PCWs of similar frequencies collided near a scatterer in experiments [52], they produced ultrasound of a low difference frequency, with its phase being anomalously sensitive to the movements of the scatterer.

The possibility of the giant amplification of PCWs in the above-threshold parametric mode permitted the natural expansion of the PCW technique to nonlinear acoustic imaging. The PCW technique has been combined with harmonic imaging [53, 54].

1.2.3. Properties and applications of phase conjugate ultrasonic beams

Despite the generality of the concept of phase conjugation for waves of different nature, PC in acoustics is characterized by silent features related to the wave properties of acoustic media, interactions involved in the PC process, the space-time structure of the

acoustic beams being conjugate, and finally, to practical problems that can be solved using the PC phenomenon.

Almost all known manifestations of the acoustic PC are of interest for applications. The most important among them are the compensation for phase distortions in an inhomogeneous, acoustically transparent medium, including the compensation for acoustic losses in elastic scattering, autofocusing or `self-targeting' of ultrasonic beams on scatterers, and the lensless formation of acoustic images. Figures 1.1 and Figures 1.2 illustrate these effects.

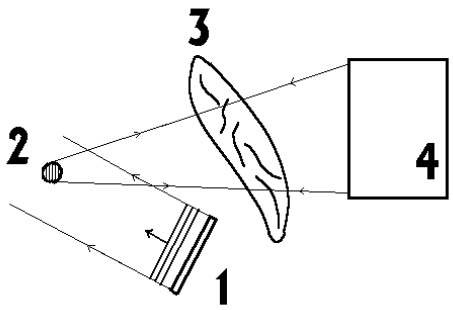

Figure 1.1. Schematic of autofocusing or 'self-targeting' of ultrasonic PC beams: (1) source of ultrasonic waves; (2) object; (3) phase-nonuniform medium; (4) PC mirror [150].

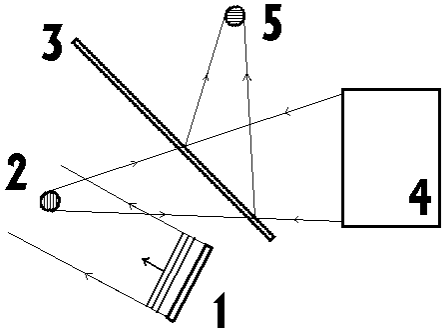

Figure 1.2. Schematic of lensless formation of acoustic images using PC effect: (1) source of ultrasonic waves; (2) object; (3) acoustic semitransparent mirror; (4) PC mirror; (5) real image of the object[150].

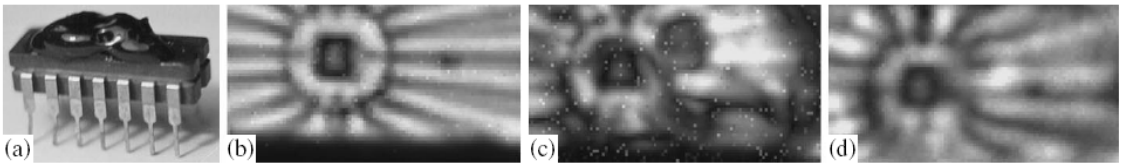

Figure. 1.3. (a) Photograph of a fracture microchip with a colophony aberration layer applied on top of it with a random shape and structure.(b) Image of the internal structure of the fracture microchip without the layer, with the use of the classical transmission scheme with two transducers. (c) Image of the same fracture microchip region that is distorted by aberrations introduced by the layer. (d) Image obtained using the effect of over-threshold phase-conjugation for the same conditions as in the case of image (c) [150].

Figure 1.3a presents a photographic picture of a fracture microchip with the aberration layer deposited on it. The image of the internal structure of the fracture microchip without a layer, which was obtained according to the classical "transmission" scheme with two transducers, is given in Fig. 1.3b. The image of the same fracture microchip region distorted due to the aberrations introduced by the layer is shown in Fig. 1.3c. Finally, Fig. 1.3d presents the image obtained using the effect of over-threshold phase conjugation for the same conditions as in Fig. 1.3c. From a comparison of Figs.

1.3b–1.3d, one can see that, although it was impossible to achieve a complete reproduction of the image in Fig. 1.3b in Fig. 1.3d, the image in Fig. 1.3d, obtained with the help of phase conjugation [150], demonstrates an evident increase in the quality of reproduction of even the fine details of the microcircuit's internal structure in comparison with the image in Fig. 1.3c, which was obtained by the conventional method.

The development of ultrasonic PC methods is closely connected with applied studies demonstrating the possibilities of practical use of phase conjugate waves in modern ultrasonic technology. One of the applications of the wave phase conjugation is acoustic microscopy. A substantial improvement in the quality of the object image was experimentally demonstrated in a scanning microscope containing a parametric piezoceramic PC mirror, when the object was surrounded by a medium with phase-distorting inhomogeneities [55, 56]. Note that the use of the supercritical parametric PC amplification allows one to additionally control the contrast and brightness of acoustic images.

The application of the PC method for the nondestructive testing of titanium alloys was demonstrated [57]. As a PC system in a B-type defectoscope, a two-dimensional electronically controlled matrix of 121 piezoelectric transducers with frequency 5 MHz was used. The use of PC permitted compensation for the phase distortions introduced by the complex surface of an object and detection of the accumulation of the α phase of titanium against a noise background caused by scattering from the granular structure of the medium.

One of the applications of acoustic PC in medicine is ultrasonic hyperthermia. Autofocusing of phase conjugate waves onto the model object through bony tissue was experimentally studied in connection with hyperthermia of a brain tumor [58].

Another promising medical application of ultrasonic PC beams is lithotrity. The self-targeting of powerful acoustic pulses to an object to be destroyed not only simplifies the system focusing but also principally allows one to continue crushing fragments of the object without any additional adjustment.

The possible application of ultrasonic PCWs that are targets themselves to a scatterer for measuring the scatterer velocity is demonstrated [50, 59].

The unusual effects of incomplete phase conjugation of sound in moving media are of some applied interest. The accumulating distortion of the wave front in a rotating cylinder placed between two PC mirrors was experimentally studied [60].

1.3. Ultrasonic velocimetry

Various ultrasonic techniques are available for velocity measuring. Each one has its advantages and disadvantages, and selecting a proper technique depends on its specific applications. The following methods describe the most common methods and techniques used for ultrasonic velocitmetry.

1.3.1. Ultrasonic velocimetry

Concerning the principles applied in flow velocity estimation the measurements methods can be divided into three groups. They are based on: (a) ultrasonic time propagation measurement, (b) Doppler's effect and (c) cross-correlation technique.

From the practical point of view, in industrial applications, the former methods are preferred. They are characterized by time propagation measurement in upstream and downstream directions and can be divided into three groups: direct time propagation measurement of the ultrasonic wave [61]; methods based on phase-difference measurement; sing-around techniques [62, 63]. But, their accuracy is not good enough, especially when low liquid flow velocities are estimated. Therefore, in practice, their modified versions known as the compensation methods are widely used because their accuracy and sensitivity is better [64]. Among them the most distinguished are the time-frequency and phase-frequency methods [65].

a) Ultrasonic time propagation measurement

Ultrasonic Transit-Time Method

The transit-time method is based on the physical legitimacy that a sound wave's propagation velocity within a medium in motion depends on its velocity. A typical transit-time flow measurement system utilizes two ultrasonic transducers that function as both ultrasonic transmitter and receiver. The flow meter operates by alternately transmitting and receiving a burst of sound energy between the two transducers and measuring the transit time that it takes for sound to travel between the two transducers. The difference in the transit time measured is directly and exactly related to the velocity of the liquid in the pipe.

Ultrasonic Phase Difference Measurement

The measurement is similar to transit-time measurement. Here, instead of the transit time of the sound, the phase difference angle is used for the determination of the average flow velocity. This is determined by the phase relationship between transmitted and received signals against the flow direction. The determined phase difference angle is proportional to the transit-time difference and is evaluated further as listed above.

b) Ultrasonic Doppler Method

The Doppler technique has traditionally been the method used to extract motion information from ultrasonic echoes reflected by moving tissues. The Doppler technique has been around for a long time, and has been extensively reviewed and analyzed in the literature [for example 66, 67].

The principle of the Doppler effect is based on transmitting a bundled ultrasound beam with a defined frequency and a well-known angle into a liquid. A part of the ultrasound energy is reflected by the solid particles or gas bubbles carried in the liquid. Due to the movement of the particles a frequency distortion occurs. This distortion is directly proportional to the particle velocity.

The ultrasonic Pulse Doppler Method represents a further development of the known Doppler method as a new measurement technique. Unlike the common Doppler method, using a continuous transmission frequency, the Pulse Doppler transmits a short frequency bundle with a defined length. The frequency distortion of the transmitted ultrasonic signal in a defined measurement window is a measure of the flow velocity corresponding to that measurement window. Reflections of particles in other areas don't have any influence on the velocity measurement.

c) Cross-correlation techniques

The concept of echo-shifting and cross-correlation to measure the arrival time and time delay of electronic signals is not new. These techniques have been in use since the 1950’s to estimate the range of objects by radar and sonar [68, 69]. Nonultrasonic cross-correlation flowmeters have been in use since the 1950’s and 1960’s with various types of transducers such as hot-wire sensors, thermal sensors, and capacitance or conductance transducers [70]. Early pre-digital industrial ultrasonic systems have also been used in various analog techniques to shift ultrasound echoes until they overlap in order to measure the thickness and velocity of sound in various materials [71, 72]. Industrial

ultrasonic transit-time crosscorrelation flowmeter were introduced in the early 1970's [73], and are commonly used to measure the flow of many substances, such as coal slurry and wood pulp [74, 75]. Ultrasonic cross-correlation is also widely used in nonflow applications such as the characterization of the mechanics of anisotropic solids [76] and in nondestructive evaluation [77, 78].

Flow measurement using cross-correlation techniques has long been reported in the literature. A significant advantage of the cross-correlation function lies in its ability to reject independent noise. The earliest descriptions of cross-correlation flow meters (e.g., Coulthard [79], Beck and Plaskowski [80]) focused on the physical mechanisms producing modulation of the ultrasonic signal and the signal processing aspects of the device.

One of the advantages of this method of estimating blood flow velocity is that the precision of the velocity estimate can be optimized by selection of which pairs of echoes are used in calculating the estimate for a given pulse repetition period [81]. The precision is defined as the standard deviation divided by the mean, and is a measure of the repeatability of the time shift measurements.

1.3.2. Ultrasonic velocimetry by Ultrasonic Phase Conjugation

Development of effective methods for ultrasonic phase conjugation in the megahertz frequency range stimulated interest to the use of phase conjugation processes in ultrasonic tomography and diagnostics of inhomogeneous acoustic media [82].

Medium motion violates the time invariance of an acoustic field that leads to distortions in an amplitude-phase distribution in a phase-conjugate wave with respect to the initial direct wave. In this case, in particular, the capability of a phase-conjugate wave to reconstruct independently of their propagation path, the phase of a direct wave at the radiation source is violated. As the result of wave propagation through moving regions of a medium an uncompensated phase shift is formed in a phase-conjugate wave. The value and sign of the phase shift carry the information on the value and direction for the motion velocity of a medium that can be used for velocimetry and diagnostics of liquid and gas flows including the ultrasonic studies of blood flows in medicine [50].

The possible application of ultrasonic PCWs that are targets themselves to a scatterer for measuring the scatterer velocity is demonstrated [59, 83]. The PCW principle assumes that the phase of the wave at the source is restored irrespective of the phase shifts

in the forward and the reverse directions. The phase is restored in both homogeneous and heterogeneous refractive media. Currents in the medium disturb the wave invariance under time reversal and thus result in a phase shift of the conjugate wave at the source-detector. A phenomenon of this nature observed earlier was the wave aberrations that accumulated during the repeated passage of conjugate waves through a vortex in a fluid [60]. An ultrasonic beam passing through a current was scanned, and the PCW phase shifts were analyzed [50, 83] in order to obtain the images of the velocity distribution of the water currents of various geometries. It was analyzed [83] not only the phases of the fundamental harmonic of PCWs but also the phases of the second harmonic and of the low difference frequency signals produced by the interaction of the phase-conjugate waves of similar frequencies. In this experiment, a low-frequency wave was generated by the interaction of the 20 MHz second harmonic of the conjugate wave with an additional 19 MHz pulse in the same direction, and the phase of the low-frequency wave was analyzed to produce the image. The use of the second harmonic doubled the registered phase shift, and the acoustic frequency subtraction increased the signal/noise ratio for digital processing of the registered signals by more than an order of magnitude.

Some principles of using the phase-conjugation phenomenon in ultrasonic velocimetry are considered [50] and is demonstrated that the presence of flows in the propagation region leads to an uncompensated Doppler shift in the phase of a phase conjugate wave at the source, which may be used for measuring the flow velocity with the help of phase conjugation.

Application of the phase-conjugation technique opens new opportunities in phase velocimetry and flow mapping. These opportunities are connected with the provision of automatic confocality in the case of spatial flow scanning by focused acoustic beams, compensation of aberrations from static inhomogeneities of a medium, and “embedding” for the fronts of phase-conjugate waves at their nonlinear interaction.

1.4. Air-coupled ultrasonic nondestructive testing

1.4.1. Non-contact ultrasonic techniques

NDT is divided into various methods of nondestructive testing, each based on a particular physical principle. These methods may be further subdivided into various techniques. The various methods and techniques, due to their particular natures, may lend

themselves especially well to certain applications and be of little or no value at all in other applications.

Non-contact techniques can make measurements in hot and cold materials and in other hostile environments, in geometrically difficult to reach locations and at relatively large distances from the test structure. Several non-contact acoustical techniques are presently available using air(gas)-coupling, electromagnetic acoustic transducers (EMATs), laser generation and optical holographic or interferometric detection.

Acoustic emission (AE)

AE is a naturally occurring phenomenon whereby external stimuli, such as mechanical loading, generate sources of elastic waves. AE occurs when a small surface displacement of a material is produced. This occurs due to stress waves generated when there is a rapid release of energy in a material, or on its surface. The wave generated by the AE source, or, of practical interest, in methods used to stimulate and capture AE in a controlled fashion for study and/or use in inspection, quality control, system feedback, process monitoring and others.

AE is related to an irreversible release of energy, and can be generated from sources not involving material failure including friction, cavitation and impact. Additionally, events can also come quite rapidly when materials begin to fail, in which case AE activity rates are studied as opposed to individual events. AE events that are commonly studied among material failure processes include the extension of a fatigue crack, or fiber breakage in a composite material.

The application of AE to non-destructive testing of materials in the ultrasonic regime, typically takes place between 100 kHz and 1 MHz. Unlike conventional ultrasonic testing, AE tools are designed for monitoring acoustic emissions produced within the material during failure, rather than actively transmitting waves then collecting them after they have traveled through the material [84]. Part failure can be documented during unattended monitoring. The monitoring of the level of AE activity during multiple load cycles forms the basis for many AE safety inspection methods that allow the parts undergoing inspection to remain in service.

The photoacoustic effect is a conversion between light and acoustic waves due to absorption and localized thermal excitation. When rapid pulses of light are incident on a sample of matter, they can be absorbed and the resulting energy will then be radiated as heat. This heat causes detectable sound waves due to pressure variation in the surrounding

medium. With the invention of the microphone and laser, the photoacoustic effect took on new life as an important tool in spectroscopic analysis and continues to be applied in an increasing number of fields.

The photoacoustic effect was first discovered by Alexander Graham Bell in his search for a means of wireless communication [85]. In 1938, M. L. Viengerov was the first to revive the use of the photoacoustic effect in gas analysis, which proved to be its most widespread application in the following decades [86]. However, his results were affected by the relatively low sensitivity of his microphone as well as undesired photoacoustic effects - a problem that persists in modern photoacoustic analysis.

The development of the laser in the early 1970s had critical implications for photoacoustic spectroscopy. Lasers provided high intensity light at a tunable frequency, which allowed an increase in sound amplitude and sensitivity. To this end, photoacoustics was able to be applied across a broader range of fields.

Electro Magnetic Acoustic Transducer (EMAT)

EMAT techniques are developing intensively in the world now [87]. Basic application branches are: Testing of steel bars, pipes and rods [88, 89]. An EMAT is a non-contact inspection device that generates an ultrasonic pulse in the part or sample inspected, instead of the transducer. The waves reflected by the sample induce a varying electric current in the receiver (which can be the same EMAT used to generate the ultrasound, or a separate receiver). This current signal is interpreted by software to provide clues about the internal structure of the sample.

An EMAT induces ultrasonic waves into a test object with two interacting magnetic fields. A relatively high frequency (RF) field generated by electrical coils interacts with a low frequency or static field generated by magnets to create the wave in the surface of the test material. Various types of waves can be generated using different RF coil designs and orientation to the low frequency field. The typical center frequency is 5MHz but could range from 2 to 8MHz depending on the scale thickness [90].

Disadvantages of both capacitance transducers and EMATs are: the surface of the material should ideally be electrically conducting, a situation not met for materials such as fibre-reinforced polymer composites, low efficiency compared to piezoelectric transducers, larger transducer size. One major problem with EMAT's is that their efficiency rapidly decreases with lift-off distance between the EMAT's face and the surface of the test object. The footprint of a generating EMAT transducer is much larger

than a detecting one. They can only be used for electrically conducting materials and are much better detectors than generators of ultrasound.

Laser ultrasonics

In 1963 White reported the generation of elastic waves in solid materials by transient surface heating [91] and research has continued in this field up to the present time. Pulsed lasers are able to simultaneously produce shear and longitudinal bulk waves as well as surface modes. Laser beam ultrasound generation and detection permits non-contact ultrasonic measurements in both electrically conducting and non-conducting materials, in materials at elevated temperatures, in corrosive and other hostile environments, in geometrically difficult to reach locations and at relatively large distances from the test object surface. Three different mechanisms account for the generation of ultrasonic waves by the impact of pulsed laser beams on a solid: radiation pressure, ablation and thermoelasticity. Radiation pressure is the least efficient and is, therefore, of little importance for practical applications. At the other extreme, when a laser pulse possessing high power density strikes the surface of a material the electromagnetic radiation is absorbed in a very thin layer and vaporizes it. The amplitude of the ultrasonic wave generated in the material by this ablation process can often be increased by placing a coating of a material possessing different thermal properties on the surface of the test object. Although the surface of the test object is slightly damaged when ablation occurs, in certain cases the amount of damage is acceptable when such a generation process is the only way to generate ultrasonic waves of sufficient amplitude in a non-contact manner. The thermoelastic process consists of absorption of a laser pulse possessing moderate energy in a finite depth of the material such that thermal expansion causes a volume change and consequently an elastic wave. Thus, the thermoelastic process is the only process which is truly non-destructive and still capable of generating an ultrasonic wave of sufficient amplitude for nondestructive evaluation purposes. Since a laser interferometer receiver is somewhat less sensitive than its piezoelectric counterpart, methods for enhancing sensitivity involve the use of very bright lasers for both the generating and receiving sources as well as new interferometer designs. More sophisticated methods such as laser generation of narrow-band, tone-burst signals and use of spatial arrays have also been investigated [92 - 96].

Acoustic microscopy

Acoustic microscopy is microscopy that employs high frequency ultrasound. Acoustic microscopes operate nondestructively and penetrate most solid materials to make visible images of internal features, including defects such as cracks, delaminations and voids.

In the half-century since the first experiments directly leading to the development of acoustic microscopes, at least three basic types of acoustic microscope have been developed. These are the scanning acoustic microscope (SAM), scanning laser acoustic microscope (SLAM), and C-mode scanning acoustic microscope (C-SAM) [97].

Because of its relatively small ultrasonic damping factor, water is mostly used as a coupling medium for the transmission of acoustic signals in ultrasound microscopy. Owing to the frequency dependent absorption, an increase of microscope resolution leads indirectly to a decrease of the distance between an ultrasonic lens and an investigated object, so that, for example, a microscope operating at 1.2 GHz in water has a typical working distance of about 50 μm. Of course, this is not a very great disadvantage but in special cases there is a demand for a larger working distance and a simplified mechanical set-up, as for example in robotics applications.

The use of air as a transmission medium can partially solve this problem. A scanning acoustic microscope operating in air at normal conditions has been presented [98-100]. Focusing transducers with and without impedance matching layers were manufactured and employed for the generation and spatially resolved detection of reflected or transmitted ultrasonic waves. Frequencies up to 11 MHz have been successfully employed. At 1.27 MHz a lateral resolution of about 220 μm is achieved. The distance resolution reaches 3 nm for 3 s total acquisition time in this case. At 5 MHz a lateral resolution of about 60 μm was measured.

1.4.2. Air-coupled transducers

The development of air-coupled transducer systems has taken place for reasons evident from the above discussion, where a method capable of generating and detecting ultrasonic signals in air would be of distinct advantage.

Over the last decades, noncontact and air-coupled ultrasonic techniques have experienced an enormous impetus. Materials characterization, nondestructive testing (NDT), and surface metrology are some of the areas in which these techniques are being

applied. Good reviews about developments of air-coupled transducers and noncontact techniques for NDT and materials characterization are given in [101–104]. More recently, successful use of air-coupled piezoelectric transducers has been reported for some particular applications [105–108]. However, design, fabrication, and applications of air-coupled piezoelectric transducers still suffer either from the limitation in materials availability for effective impedance matching or from the complexity of the proposed solution.

The propagation characteristics of ultrasound in the air and other gases have also received considerable attention. For example, Hickling and Marin describe phenomena that affect the use of l MHz sound signals in gauging and proximity sensing applications [109]. The physical phenomena of sound absorption in the atmosphere in the audio region are reviewed in great detail by H.E. Bass et al. [110], while the effects of turbulence on apparent attenuation are addressed by E.H. Brown and S.F. Clifford [111]. In the ultrasonic frequency region, above 20 kHz and below 1 MHz sound absorption information, as a function of frequency, relative humidity, and pressure, can be obtained by using published expression [112, 113]. The use of the published expressions is probably justified up to 10 MHz, and even higher, frequencies [114].

The potential advantages and limitations of using air-coupling in nondestructive material inspections have been recognized for a long time [115]. In particular, air coupling was found desirable in applications involving the inspection of materials that could not be immersed in water or that would be damaged by physical contact with an ultrasonic transducer.

Though much progress has been made in enhancing the transduction efficiency of transducers based upon piezoelectric and capacitive phenomena, from a practical standpoint these advancements have by no means reached a saturation point. In [148] is described the successful development of piezoelectric transducers which are characterized by extraordinarily high sensitivities in a frequency range from 80 kHz to 10 MHz. The evidence of the high sensitivity of these new transducers can be seen from the fact that even very high frequencies such as, 2 MHz to 5 MHz can be propagated through a number of solids in the NCU mode.

There are two main approaches to the design of air-coupled transducers, although others are possible. The transducers are a development of previous research into the use of capacitance transducers in air for ultrasonic ranging and manufacturing applications [117, 118]. Conventionally, these devices use a metallic backplate, over which a thin

polymer membrane is stretched, the membrane having a conducting grounded film on its outer surface. Application of transient voltages to the electrode cause motion of the membrane, and hence ultrasonic generation. Detection occurs via motion of the membrane causing charge variations on the hack electrode, on which a d.c. bias voltage is imposed. Much work has recently been reported on the effect of backplate surface condition and membrane properties on the resulting transduction performance [119], where it was shown that backplate roughness in particular had a pronounced effect on sensitivity and bandwidth. In [120, 121] was used the devices with a silicon backplate whose surface features can be precisely controlled. Air coupled transducers based upon capacitance (electrostatic) phenomena have also undergone substantial developments in recent years. Researchers at Kingston and Stanford Universities have successfully produced micromachined capacitance air transducers with the latter claiming a high 11 MHz frequency [122, 123]. These transducers - characterized by high bandwidths - have been used to evaluate composites and other materials. At the University of Bordeaux, ultrasound experts have reported the generation and detection of Lamb waves in noncontact mode in anisotropic viscoelastic materials by utilizing capacitive transducers [116].

V. Magori reviewed [124, 125] the characteristics of various practical air-coupled transducers that are used in propagation-path sensors, including gas-flow meters, and distance sensors in air-sonar applications. It is also important to include references to the pioneering work of L.C. Lynnworth [126], F. Massa [127], W.Kuhl and co-workers [128], W.W. Wright [129, 130] who developed the solid-dielectric microphone, and B.T. Khuri-Yakub [131].

The alternative approach is to use the conventional piezoelectric transducer, and so modify it that it becomes more sensitive to operation in air. In its normal state, PZT or other piezoceramics have a sufficiently different impedance to air that they are very insensitive in air-coupled applications. However, the use of composite materials, using a carefully-designed mix of polymer and piezoelectric ceramic can improve things markedly. The mechanical and electrical characteristics can be optimized for either generation or detection, using an appropriate volume fraction of ceramic in a 1-3 connectivity composite [132]. Sensitivity can then be increased further by the use of an appropriate impedance matching layer. Such devices tend to be more resonant than the capacitance devices, which are inherently broadband, and probably are of more use in

applications where increased signal over a narrow bandwidth is of interest. Other approaches using piezoelectric transducers have also been published [133, 134].

Researchers and transducer experts have been designing piezoelectric devices by manipulating the acoustic impedance transitional layers in front of the piezoelectric element. Initially, practical applications were confined to the 25-250 kHz frequency region [135]. Later, improvements in piezoelectric transducer-design technologies and electronics have made it feasible to operate in the 0.5-1.0 MHz frequency region [136, 137].

A precursor to high frequency non-contact transducers was the 1982 development of piezoelectric dry coupling longitudinal and shear wave transducers up to 25MHz frequency. Since 1983, these transducers have been commercially available for characterizing thickness, velocity, elastic and mechanical properties of green, porous, and dense materials [138-140]. Dry coupling transducers feature a solid compliant and acoustically transparent transitional layer in front of the piezoelectric materials such as lead meta-niobates and lead zirconate-lead titanate. These devices, which eliminate the use of liquid couplant, do require contact with the material.

An important by-product of dry coupling devices was the development of air/gas propagation transducers, which utilize less than a 1 Mrayl acoustic impedance matching layer of a non-rubber material on the piezoelectric material. Several workers are used: low-impedance and low-loss customized materials - aerogel and highly porous PMMA [141-143]; microspheres [144], but this has the disadvantage of increasing the attenuation and scattering within the material; balsa wood, cork [145] - all with varying levels of success. Air-coupled ultrasonic transducers using vinylidene fluoride/trifluoroethylene [P(VDF/TrFE)] piezoelectric films at 2 MHz is developed [146].

These commercially available transducers have been successfully produced in planar and focused beam configurations for transmitting ultrasound in air up to ~5MHz frequency and receiving up to 20MHz. Air/gas propagation transducers, between 250kHz to ~5MHz, quickly found applications in aircraft/aerospace industries for imaging and for defect detection in fibrous, low and high density polymers, and composites. For such applications these transducers have been used with high energy or tone burst excitation and high signal amplification systems. However, for applications such as level sensing and surface profiling, the low energy spike or square wave transducer excitation mechanism has been sufficient.

Similar transducers of 1MHz and 2MHz frequency were also produced at Stanford University by utilizing silicone rubber as the front acoustic impedance matching layer [147]. By using such a transducer at 1MHz, the distance in air could be measured from 20mm to 400mm with an accuracy of 0.5mm. Further improvements in transduction efficiency were shown by planting an acoustic impedance matched layer that is composed of tiny glass spheres in the matrix of silicone rubber on piezoelectric elements [144, 133]. Researchers at Strathclyde University [132] have reported air-coupling transducers based upon piezoelectric composites between 250 kHz to 1.5MHz frequencies. By utilizing tone burst transducer excitation, they have been successful in producing millivolt level transmitted signals through a composite laminated honeycomb structure at 500 kHz.

More recently, piezoelectric transducers featuring perfect acoustic impedance matched layers, made from filtration membranes (mixed cellulose esters and PVDF, polyethersulfone, nylon membranes), for optimum transduction in air have been successfully developed from <100 kHz to 5MHz [148, 149]. The sensitivity of these new transducers in air is merely 30dB lower than their conventional contact counterparts. As a result, ultrasound in the MHz region can be easily propagated through practically any medium, including even the very high acoustic impedance materials such as steel, cermets, and dense ceramics.

Conclusion

Air-coupled ultrasound has gained considerable attention due to its ability to eliminate the physical contact between the transducer and the material under inspection, especially in cases when humidity can change properties of the materials or even destroy the material, such as honeycomb structure. Though there are certain difficulties, air-coupled ultrasound in the low megahertz frequency range is becoming a real possibility for some particular applications.

The modern level of development above-threshold parametric phase conjugation techniques based on magnetostrictive ceramics allows realizing the applications in medicine and defectoscopy on frequencies from several megahertz to several dozen megahertz. The interest in acoustic PCWs stems from their properties to automatically focus onto objects that scatter the incident wave and to compensate the phase distortions of wave propagated in heterogeneous refractive media. Due to this phenomenon a new unique possibilities in physical researches, nondestructive tests, and medicine become available.

Development of effective methods for ultrasonic phase conjugation in the megahertz frequency range stimulated interest to the use of phase conjugation processes in ultrasonic tomography and diagnostics of inhomogeneous acoustic media. Application of the phase-conjugation technique has opened new opportunities in phase velocimetry and flow mapping. The offered techniques, unlike traditional dopplerographie, does not use ultrasound scattering on particles transferred by a stream and is suitable for measurements of speed distribution in flow of homogeneous and non-homogeneous media. Velocimetry systems based on WPC do not demand precision adjustment, providing automatic confocality of measuring setup, and allow to realize cartography of flow in the conditions of electronic scanning of a probing beam within WPC system aperture, without use of mechanical moving.

Developments of acoustic microscopy and velocimetry of liquids flow by using ultrasonic WPC and plentiful development of non contact methods in ultrasonic testing in air at low megahertz frequency range have shown good theoretical and experimental results at last years. It defines the main concept of the researches presented in this work: realization of air-coupled wave phase conjugation techniques for velocity measurements of gas micro flows and air-coupled microscopy. It is very important to connect new

opportunities in phase velocimetry and flow mapping which gives the phase-conjugation technique with the possibilities of air-coupled ultrasound in low megahertz frequency range for developing new application of WPC system to full scale non-contact mode.

Chapter 2: Features of ultrasonic wave phase conjugation system operating with weak signals.

This second chapter describes operating modes of ultrasonic wave phase conjugation system, methods for enhancing signal-to-noise ratio in ultrasonic measurements. The results of attenuation factor measurement of ultrasonic phase conjugate wave in air using pseudorandom codes in conjunction with cross correlation technique are presented.

2.1. Introduction

Electromagnetic pumping of parametrically active magnetic ceramics is one of the most advantageous methods of phase conjugation of ultrasound beams [49, 150] for various applications in ultrasonics. Its peculiarity is a possibility of operation in supercritical mode above the threshold of absolute parametric instability of phonons. This mode provides giant amplification of phase conjugate wave exceeding 80 dB with respect to the incident one [49].

The simplest way to get acoustic PC in a solid is to use the sound velocity modulation by an alternating electromagnetic field.

Let us consider the wave equation describing a case of not damped distribution of an acoustic wave:

$$\frac{\partial^2 u}{\partial t^2} = v^2(t)\frac{\partial^2 u}{\partial z^2}$$

Let's consider the velocity of sound *v(t)* is modulated by an electromagnetic field:

$$v^2(t) = v_0{}^2(1 + 2m\cos\omega_p t)$$

where $m = \Delta v/v_0$ — modulation depth, ω_p — frequency of pumping, v_0 — velocity of sound at constant value of magnetic bias field.

On figure 2.1 dependence of speed of a sound on the magnetic field for magnetostrictive ceramics made from polycrystalline nickel ferrite is presented.

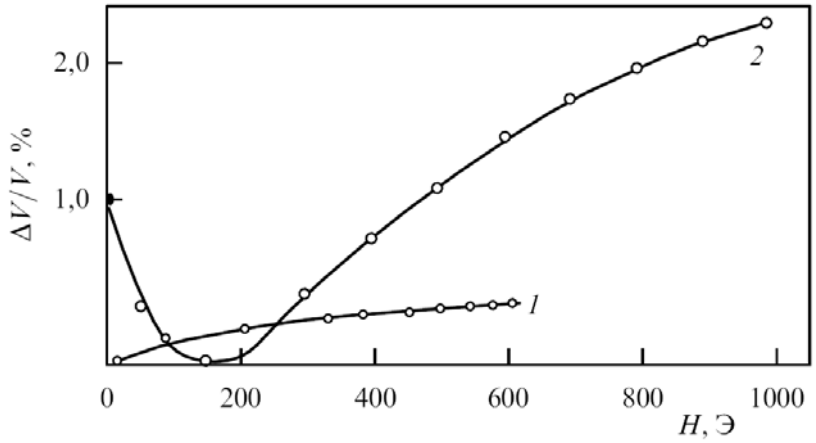

Figure 2.1. Dependence of relative change of speed of a sound on intensity of a magnetic field for longitudinal (1) and shear (2) ultrasonic waves in magnetostrictive ceramics on the basis of nickel ferrite (NiO-Fe2O3) [49].

Generally parametric wave phase conjugation uses an active material of limited length, a part of which (active zone) is under the effect of a pumping field. When an incident acoustic wave of frequency ω penetrates the active zone, a pumping field at double frequency 2ω (parametric resonance condition) is applied to the active material and the conjugate wave is created.

Let us consider the plane active zone with length L along the z-axis parallel to the direction of acoustic wave propagation. We assume that the acoustic field *u(z,t)* can be presented as a superposition of forward and backward waves with slowly varying amplitudes.

$$u(t,z) = A(t,z)\cdot e^{j(\omega t - kz)} + B(t,z)\cdot e^{j(\omega t + kz)} + c.c.$$

where A(t,z) and B(t,z) are slowly varying amplitudes of incident and conjugate waves. Generation of the PC wave can be described by means of system equations [31]:

$$\begin{cases} \dfrac{\partial A}{\partial t} + v_0 \dfrac{\partial A}{\partial z} = ihB^* \\ \dfrac{\partial B^*}{\partial t} - v_0 \dfrac{\partial B^*}{\partial z} = -ihA \end{cases}$$

where h = mω/2.

In the linear mode, the shape of conjugated acoustical pulse is defined by space allocation of amplitude of conjugate wave in active media at the moment of pumping termination. Within the asymptotic theory of the parametric interaction, the spatial distribution of the conjugate wave amplitude B^* at the linear stage of amplification is written as:

$$B^* = -iA_0 \frac{\sin(q(L-z))}{\cos(qL)}$$

where *L* is length of active zone, q = h/v0.

The condition $qL = \pi/2$ corresponds to threshold value of parametrical generation of a sound from thermal noise. The supercritical mode of giant amplification occurs when the pumping amplitude is higher than a threshold value, function, for a given material, of the length of the sample. The supercritical mode allows to realize giant amplification of PC wave propagated in a solid, for this reason this mode attract greatest attention.

Critical value of depth of modulation of speed of a sound in an active material *m* at which arises above threshold mode of amplification of PC wave, is defined by:

$$m = \frac{\lambda}{2L}$$

where λ — length of a wave of ultrasound. Threshold value of modulation of speed of a sound decreases at reduction of wavelength of ultrasonic bunch or at increase in the sizes of active zone L. Thus, at the fixed size of active zone efficiency of parametrical phase conjugation raises with frequency growth.

A simplified typical scheme of experimental setup for observation of water loaded wave conjugation is shown in figure 2.2 [152]. A wideband focused ultrasonic transducer with the focal distance of 30 mm and the diameter of 10 mm was placed in a water tank opposite a supercritical magneto-elastic phase conjugator (SMPC). The latter was introduced in the lateral wall of the tank through a rubber membrane. The distance between the transducer and the front surface of the conjugator was 85 mm. The active element of the conjugator has been fabricated from magnetostrictive ceramics and had a shape of cylinder 150 mm long and 29 mm in diameter. An acoustic burst at the frequency of 10 MHz radiated from the transducer propagated in water and got into the active element, whereupon the electromagnetic pump at the frequency double with respect to that of a sound was applied to the element via inductance coil. The delay between sound and pump bursts was 120 μs. In this process a conjugate ultrasonic burst was generated which propagated backwards and was registered by the same transducer. The period of repetitions of the process was 0.1 s. Duration of sound and pump bursts were 50 μs and 100 μs respectively.

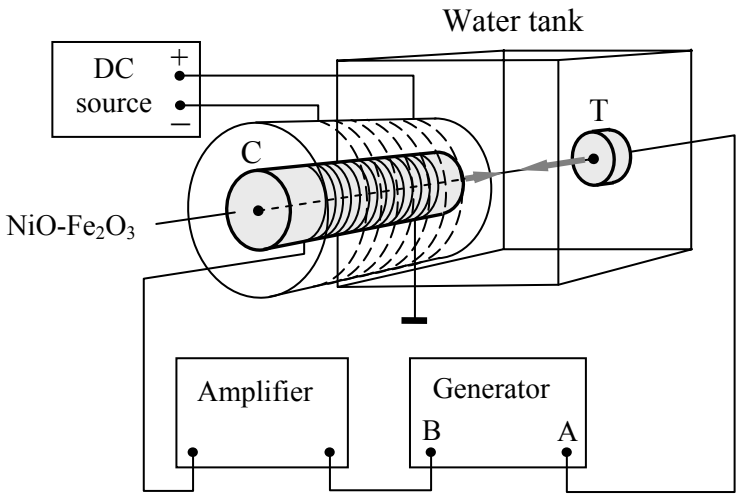

Figure 2.2. A simplified scheme of experimental setup for observation conjugate wave propagating in water [152].

In order to switch to air coupled mode the wave conjugation system needs to be modified. The experimental setup stays almost the same, however the water tank is removed and the air is used as medium of wave propagation instead. However this change poses some new challenges: strong sound wave attenuation on high frequencies, low density and velocity of sound in comparison with the same parameters in water.

The operation of PCW device (conjugator) loaded by air is deteriorated by strong ultrasonic waves attenuation in the air (16dB/mm at 10MHz frequency) and by giant ultrasonic wave power losses (≈40 dB) when the wave passes the interface between air and solid active element (magnetostrictive ferrite).

These two factors lead to very weak signals insufficient for efficient wave phase conjugation. It is necessary to reduce these losses as much as possible.

It is possible to reduce the attenuation of ultrasonic waves in air by decreasing the working frequency and by reducing the size of the air gap between solid-state active medium (polycrystalline nickel ferrite) and transducer. As a result the dimensions of the WPC system for practical applications have to be minimized, as well as the size of the active element (active zone). The decrease of active element reduces the efficiency of WPC and limits the durations of operating signals.

2.2. Operating modes of wave conjugation system

Air loaded wave conjugation system obtains some changes in comparison with water loaded systems.

To minimize the power losses of the conjugator, its working frequency was reduced from 10MHz to 7.5MHz. The airgap between solid-state active medium and transducer was reduced to 1 mm. The active element of the air loaded conjugator has been fabricated from magnetoacoustic ceramics and had shape of parallelepiped 40 mm long and 10*10 mm in the butt. The delay between sound and pump bursts has been changed to 10 μs. Duration of sound and pump bursts have been changed to 5 μs and 30 μs respectively. A two-channel Sony TEKTRONIX AWG 2120 arbitrary waveform generator was utilized to produce the signals for excitation of sound and pump bursts. Amplifiers were used to provide appropriate levels of pump and sound. The measurements were taken using Le Croy 9430 digital oscilloscope.

Optimization of the parameters of WPC amplifiers based on magnetostrictive ceramics is a complex problem. At the first step measurements were taken to find how in the certain experimental conditions the amplitude of conjugate wave depended on pump pulse duration.

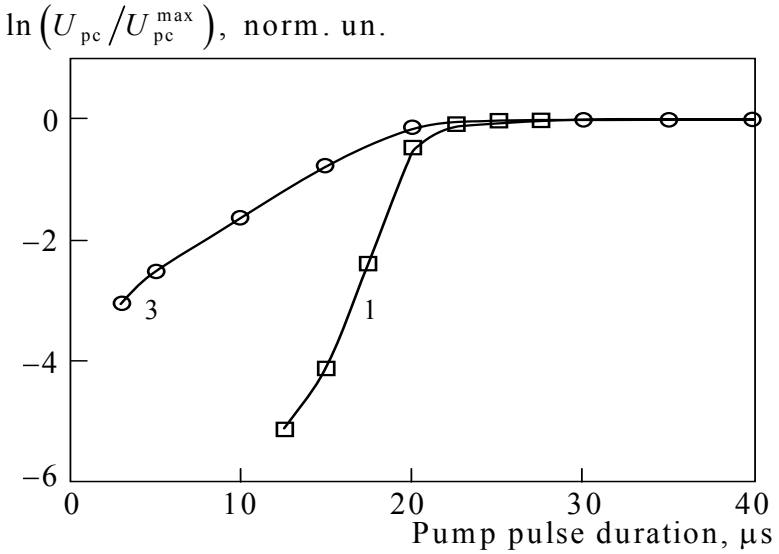

Figure 2.3. Dependence of the conjugate wave amplitude on the pump pulse duration for different samples [152]. U - the voltage excited at an ultrasonic transducer, U max - maximum output voltage of the conjugate wave.

Two characteristic modes can be distinguished in the overthreshold process of parametric WPC amplification. One of them is linear amplification with exponential growth of the WPC signal amplitude. The other is the saturation mode caused mainly by the inverse impact of the amplified incident and conjugate acoustic waves upon the pumping. The typical time of changing from one mode to the other as a rule does not exceed much the time of wave travel over the active zone. The typical dependence of PCW amplitude on time measured by means of variation of pumping pulse duration is presented in figure 2.3 [152].

In typical experimental conditions incident wave and electromagnetic pump are bursts with a proper delay and relatively long repetition period. The decrease of repetition period leads to essential decrease of output power of a parametric phase conjugator operating in the supercritical mode. This decrease is caused by mode competition [151] between the signal wave appointed to phase conjugation and reverberation noise that arises as a result of internal reflections of forward and backward waves in the finite parametrically active sample. When the pause between the two pumping pulses becomes short enough to be comparable with the lifetime of reverberations, the latter take part in parametric interaction and cause the mode competition with the signal wave.

In the case of comparatively weak input signals, the parametric amplification of thermal phonons proceeding simultaneously with amplification of the valid signal begins

to play a substantial role. The amplified thermal noise not only introduces additional restrictions on the achievable intensity of the phase conjugate wave, but also leads to amplitude-phase distortions in the supercritical PC mode. For this reason, taking noise into account becomes essential in the problem of supercritical PC quality.

Experimental observations and the simulation show that thermal noise is only observed for sufficiently long pump durations [151].

As the pump duration becomes longer, reflections of the amplified waves from the sample boundaries can become significant, forcing the conjugator operate in resonator mode. The return of the reflected waves to the active zone can result both in the increase and decrease of the backward wave amplitude, depending on the phase shift.

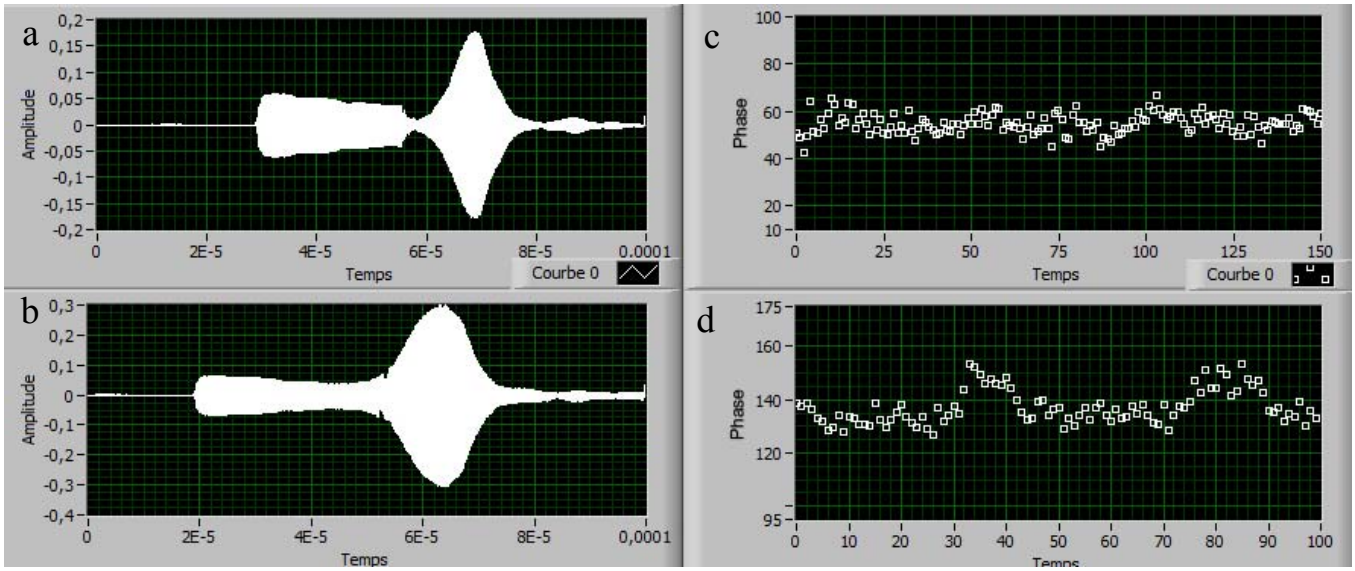

Figure 2.4. Dependence of WPC quality on pumping time. A,B - oscillograms of registered PC waves at various time of pumping - 20 and 40 micro seconds respectively. C,D – the phases of registered waves depending on transmitter/reseiver position at various time of pumping.

Figures 2.4a and 2.4b present oscillograms of registered PC waves with various pumping duration - 20 and 40 microseconds respectively. Figures 2.4c and 2.4d present the dependences of PC wave phases on transmitter/receiver position. The phase of conjugate wave does not depend on the transmitter/receiver position and that is reflected in figure 2.4c. The registered signal at 40μs pumping duration represents a mix of the PC wave and non-conjugated components; therefore the phase of registered wave depends on the transmitter/receiver position. It is shown in figure 2.4d and it corresponds to the resonator operation mode of conjugator.

Figures 2.5 present various cases of WPC system operation in resonator mode depending on boundary conditions of conjugator.

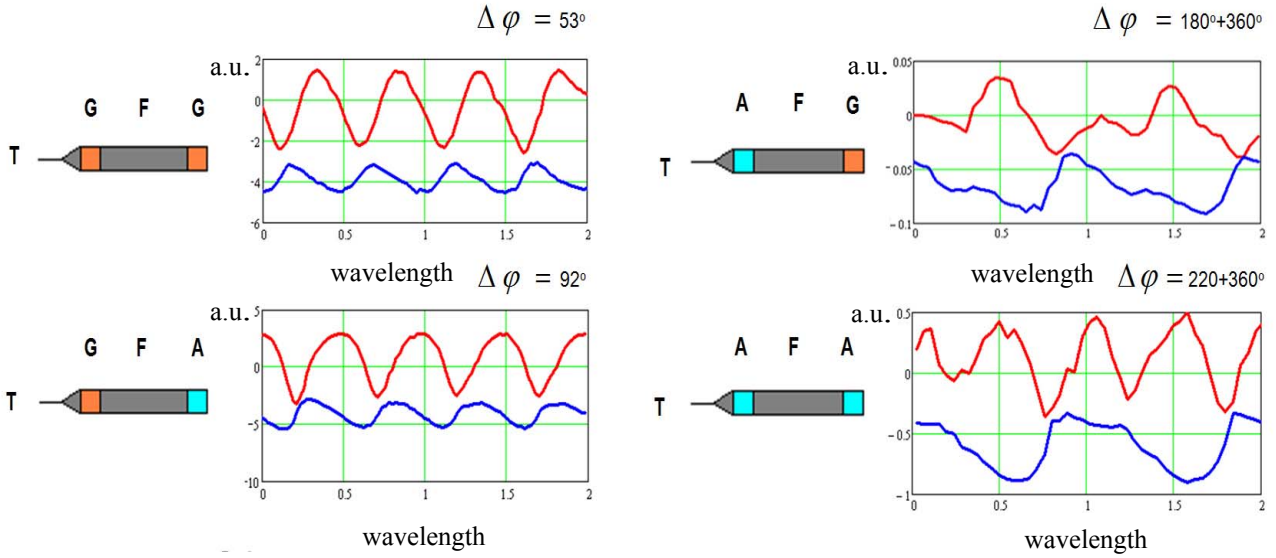

Figure 2.5. Various cases of WPC system operation in resonator mode. By letters are noted the boundary conditions: G - Acoustic gel; F- Ferrite ; A – Air. On figures dependences of phase(blue line) and amplitude(red line) of registered waves on a transmitter/receiver position are presented.

By letters are noted the transducer (T), ferrite (F) and boundary conditions: G - Acoustic gel; A – Air. Red lines present dependences of amplitude of registered signals on transmitter/receiver position, blue lines - dependences of phases of registered signals on transmitter/receiver position. Dominance of conjugate or nonconjugate components of the registered signal depends on boundary conditions (difference of acoustical impedances of adjacent mediums, parallelism of edges of active element of WPC system). At "rigid" (big difference of impedances) and parallel edges of active element resonance mode essentially prevails over conjugate mode on long pump duration (figure 2.6b). The use of resonance mode for practical applications in velocimetry and microscopy is not obviously possible.

In spite of "soft" (relative small difference of impedances) edges of active element loaded by water at long pump duration and short active element length registered signal will represent anyway a mix of conjugate wave and nonconjugate components. That will have influence on oscillation of phase of registered signal against the transmitter/receiver position. If this oscillation is less than 2π it is possible to consider that the signal is phase

conjugated (figure 2.6a). If this oscillation is more than 2π - the signal is not phase conjugated (figure 2.6b).

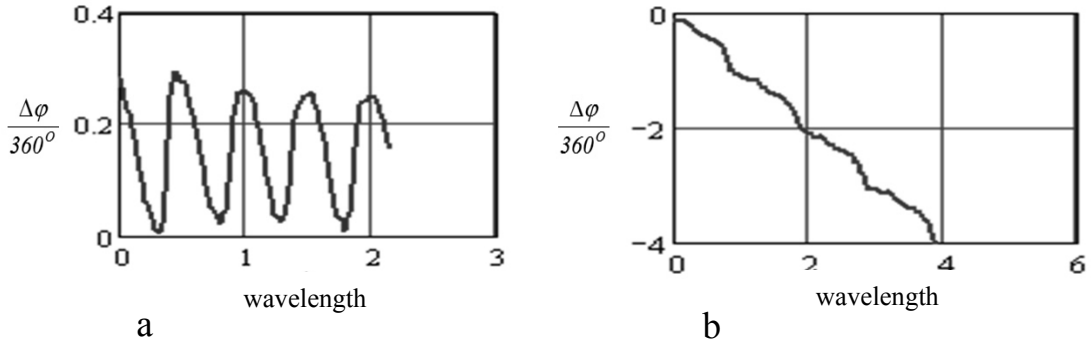

Figure 2.6. Dependences of phases of registered waves on a transmitter/receiver position .a – Prevalence of conjugate mode, b – Prevalence of resonance mode.

These features have been considered at realization of air-coupled WPC system. The layer of acoustic gel placed on the back side of the active element decrease sharp reflection from border of active element and doing resonator (active element) more opened. The 30 μs pump duration was chosen in order to achieve a maximum WPC signal gain in the absence of nonlinear saturation effects and other undesirable effects described above.

2.3. Linear and saturation modes of parametrical PCW generation.

As was shown above if the amplitude of the incident acoustic beam is very small it is necessary to increase the time of pumping up to limit level, practically up to appearance of the generation of resonator mode. When pumping duration is increased and the process of parametrical generation of PC wave is developed conjugator transfers to saturation mode of generation. This mode of conjugator operation is substantially nonlinear and it has to be taken into account for correct PC wave amplitude measurements. Application of appropriate corrections is necessary for trustworthy measurements. For example, measurement of attenuation factor of ultrasonic PC wave propagating in air is considered in this part.

Acoustic pressure and density, oscillating speed, changing in time and in space, define wave process in elastic liquid and gaseous mediums. These acoustic values are

connected by the physical laws characterizing change of condition of the elastic media during of wave propagation.

During of wave propagation in real solid, liquid and gaseous mediums the losses appear leading to reduction of energy, transferred by these waves. Losses are connected with viscosity and heat conductivity of elastic mediums. The part of energy passes in heat. The amplitude of an acoustic wave decreases along a distribution direction. It is physically caused by that the next particles of environment fluctuating under the influence of an acoustic wave propagate with various velocities and rub against each other, causing the raised heat emission.

Taking into account attenuation, wave equation for an acoustic wave in the viscous heat-conducting media may be written as:

$$\frac{1}{c^2}\frac{\partial p}{\partial t^2} - \nabla^2 p = \frac{b}{\rho_0 c^2}\frac{\partial}{\partial t}\nabla^2 p$$

Having presented $p = p_0 e^{j(\omega t - kz)}$, having substituted in (2) and having equated imaginary parts in paraxial beam conditions we receive

$$\frac{dp}{dz} = -\frac{b\omega^2}{2\rho_0 c^3} p = -\alpha p$$

where

$$\alpha = \frac{b\omega^2}{2\rho_0 c^3}$$

Principal cause of attenuation of acoustic waves is the force of viscous resistance between the next particles of environment possessing the various velocities. There it is because of influence of the internal friction acting on particles of environment in which the acoustic wave are propagated. Absorption of an acoustic wave because of losses on an internal friction varies proportionally to square of frequency and inversely 3 degrees of velocity of its propagation. The shift viscosity factor of water is 10^{-3} Pa*s and of air it is $1{,}9 \cdot 10^{-5}$ Pa*s. Considering densities of mediums and velocities of acoustic wave propagation, the attenuation factor in water is essentially less than in air (for example at

room temperature attenuation factor in water for 1 MHz frequency is equal to 0,22 dB/m, in air - 164 dB/m).

The contribution of attenuation of ultrasonic phase conjugate wave in air was studied experimentally at the first step. PCW amplitude and the amplitude of the emitted signal in the resonator mode were measured as a function of the distance between the transducer and the conjugator. The experimental results are shown in figure 2.7. It should be noted that on the background of the general decrease of amplitude of the resonator emission due to attenuation in air, oscillations are observed (curve (1) figure 2.7.). It results from the phase variation (depending on the transmitter/receiver position) of the incident ultrasonic wave at the interface of conjugator.

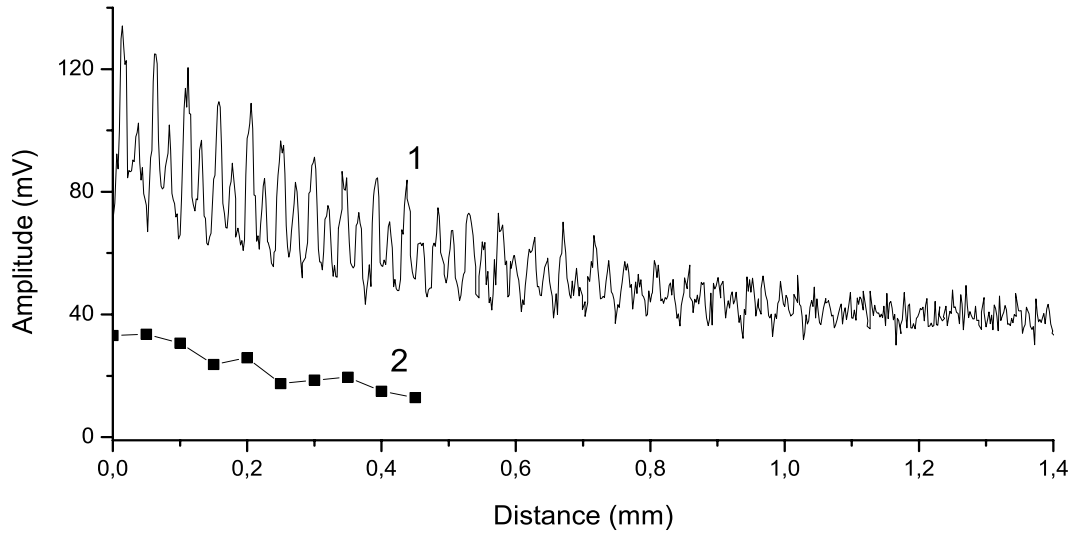

Figure 2.7. Attenuation in air for resonator (1) and WPC (2) modes.

To make a correct measurement of the attenuation factor α of the PCW in air, it is necessary to define precisely the working conditions of the conjugator. If the amplitude of the initial signal is $A_{in} = A_0 \exp(-\alpha z)$, the PCW has amplitude:

$$A_c = A_{in} T^2 f(A_{in}), \tag{2.4.3}$$

where T – transmission coefficient at the interface air-ferrite, $f(A_{in})$ - transfer function of parametrical generator. If find logarithm and trajectory derivative from Eq. (2.4.3) one can obtain the formula for the attenuation factor:

$$\alpha' = -\frac{\frac{\partial A_c'}{\partial z}}{1+\frac{\partial f'(A_{in})}{\partial A_{in}'}}\ , \qquad (2.4.4)$$

where all amplitudes are expressed in dB and α' expressed in dB/mm .

Dependence of this function on the amplitude of the incident signal is determined by the working condition of the parametric generator: if $\frac{\partial f'(A_{in})}{\partial A_{in}'}=1$ linear operation takes place, if $\frac{\partial f'(A_{in})}{\partial A_{in}'}=0$, generator works at saturation mode

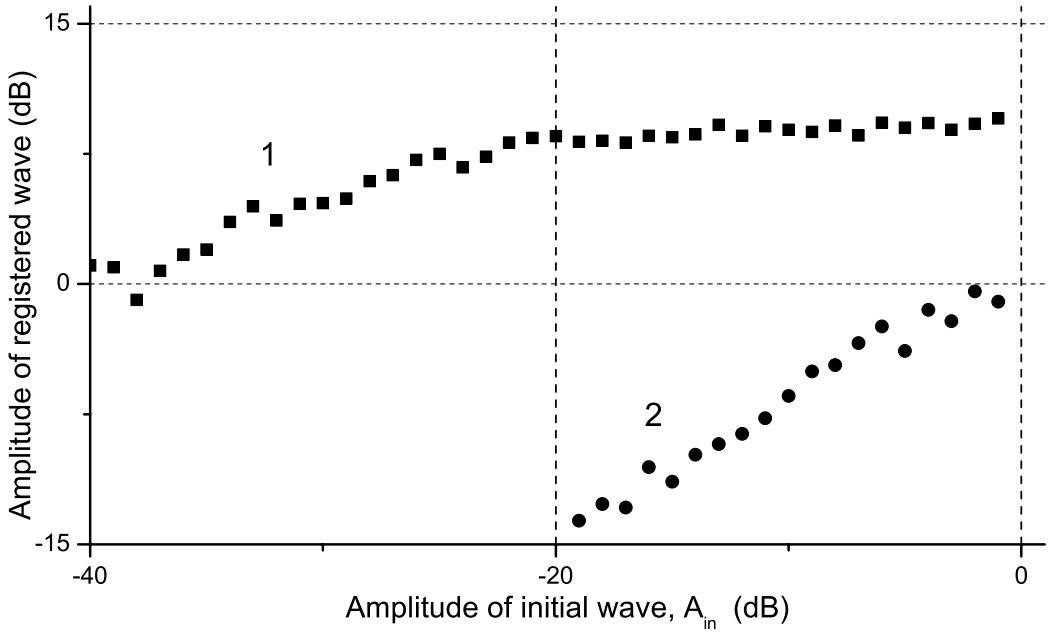

Figure 2.8. Transfer function of an active element for resonator (1) and conjugate (2) modes.

The transfer function of the conjugator was experimentally measured both for the resonator and the WPC modes (figure 2.8.) The results show that in each case an intermediate regime is realized. However in the case of the resonator emission the operation mode of conjugator is close to saturation ($\frac{\partial f'(A_{in})}{\partial A_{in}'}=0.22$), while in the case of WPC mode it is close to linear amplification ($\frac{\partial f'(A_{in})}{\partial A_{in}'}=0.78$). Taking into account

this result the attenuation factor for PCW at 7.5MHz was calculated by Eq.2.4.4. We obtained approximately the same results for resonator emission and for WPC: $\alpha_R = 9.2\, dB/mm$ and $\alpha_C = 9.6\, dB/mm$ respectively. Theoretical value of attenuation factor for PCW at 7.5MHz calculated by approximate expression 4.4.1 is 9.2 dB/mm .

2.4. Coded excitation

In spite of the frequency and airgap decreases, the phase conjugate acoustic signal is very weak and is lower than the noise level. The main technique used to maximize the performance of the WPC system is advanced signal processing.

It is well known that random or pseudorandom codes in conjunction with cross correlation measuring technique can enhance signal-to-noise ratio.

2.4.1. Codes

Over the past decade, coded excitation has gradually established itself as a practical technique for improving the sensitivity-resolution tradeoff in diagnostic ultrasound imaging. Various codes have been proposed as candidates for coded excitation, most of which can be categorized into continuous (linear and nonlinear frequency modulation chirps) and bi-phase (Barker, orthogonal Golay, m-sequences, etc.) codes.

Several other types of transmitted signals have been proposed by different authors. These include wide-band m -sequences [152, 153], random noise [155], chirp [156], Golay codes [157], Barker code [158].

In ultrasound imaging systems, a bi-phase code such as the Barker code, is always modulated by a base pulse sequence instead of being transmitted directly (direct sequence transmission). The encoding process can be described as a convolution of base pulse sequence with an oversampled code sequence.

A variety of codes are available for application in the ultrasound imaging system. In particular we shall emphasise factors affecting the choice of code are:

- the relative importance of the central lobe as compared to the side lobes of the correlation function, which is directly related to the dynamic of the imaging system (peak to side lobe ratio (Lp/Ls) in the correlation function),

- the width of the correlation peak which is directly related to the axial resolution of the system,

- the facility of the realization (ease in generation),

- the facility of the processing

Thus the main criterion is the value of peak to side lobe ratio (Lp/Ls). In order to allow easy comparison between the most common codes we will present hereafter a comparative study.

A-Type Codes

For Barker's codes the ratio (Lp/Ls)max is about 22 dB. This result can be improved by combined Barker's codes [159] but it is limited to a value of 30 dB. For our purpose the m-sequence and complementary Golay codes are better candidates.

Maximal Length Sequence: The m-sequence, simpler to implement, is a perfectly deterministic sequence of $N = (2n-1)$ binary digits which displays a certain number of properties of randomness approximating those of white noise. It is often referred to as a pseudorandom binary sequence or pseudonoise. In the case of nonperiodic emission of an N element sequence [160], the peak to side lobe ratio $Lp / Ls \le 20 \log N$. The ratio is equal to 30 dB for N = 31 when the m-sequence is transmitted continuously. This precludes however the use of a single transducer, which is not the case with Golay's codes.

Golay's Codes: Golay's codes are pairs of complementary binary codes [161]. The autocorrelation function of each code in a pair has a central peak and a range of side lobes of identical shape but of opposite sign. The addition of the autocorrelation functions from a pair of complementary codes produces a large triangular central peak with no side lobes ($Lp / Ls \to \infty$). The length of Golay's code usable by any correlation system is only limited by the generation capability of the system. Other codes have also been shown to have the same zero range side lobe property [162]. It is worth noting that because Golay's codes involve the sequential transmission of two related sequences, real time imaging of some systems is prohibited with this type of code.

B-Type Codes

Type B codes were generated as suggested by Frank [163]. Consider a code of N elements. Let j and m be two indexes with $0 \le j \le \sqrt{N}$ and $0 \le m \le \sqrt{N}$ The phase of each element $\varphi_{jm} = \left| 2\pi / \sqrt{N} \right| (j+m)$. The N elements of code are thus emitted in $\sqrt{N}$ subgroups. For each subgroup j is kept fitted while m runs from 0 to $\sqrt{N}-1$. For

sufficiently high values of N one can show [164] that $Lp/Ls = 20\log(\pi\sqrt{N})$. For $Lp/Ls \sim 50$ dB the phase is in units of $2\pi/\sqrt{N} \approx 3.6°$. This is hard to implement when the operating frequency is of the order of some Megahertz. That is why codes with only two phase values are more practical and appear more attractive.

C-Type Codes

Huffman has shown [165] that by varying the amplitude and the phase of each element of the coding sequence it is possible to increase significantly the peak to side lobe ratio. In spite of very promising results, however, implementation of Huffman coding sequences remains very delicate. Kretschmer and Lin [166] have shown that an error of 5% in the form of each of 64 binary elements of a Huffman sequence induces a loss of 20 dB in the peak to noise ratio. Such sensitivity makes it impractical to use.

It is apparent from previous discussion that only msequence and Golay's codes provide sufficient SNR and easy implementation to ultrasonic imaging. In the following we shall only consider this two types of codes and the corresponding SNR degradation due to Doppler effects.

2.4.2. Code choice and realization

Feature of the parametrical wave conjugation consists in that the phase of the conjugate wave is rigidly adhered to an initial phase of wave which has come to an active zone of the system of wave conjugation. At the moment of development of generation the wave conjugation system does not react to change of a phase in a setting signal. Therefore it is impossible to carry out intrapulse phase coding for wave phase conjugation.

To extract signals from noise, considering above described factors at a choice of a code and having made mathematical modeling, we have chosen phase coding of the excitation signals by five-order pseudo-noise sequence. Results of mathematical modeling are shown in table 2.1. Five-order sequences were investigated under the above described factors (side lobe ratio, signal-to-noise ratio).

We used M-sequence with five-order generator polynomial $f(x) = x^3 + x^5$. In this case M-sequence is generated by recurrence formula $a_i = a_{i-3} \oplus a_{i-5}$, where sign $\oplus$ means summation by modulus 2. Initiating sequence is 00101. The length of sequence

equals $L = 2^5 - 1 = 31$ elements, which theoretically allows to extract signals lying at -30dB under noise level.

Number	Polynom	Initial sequence	Side lobe ratio, dB	Signal-to-noise ratio , dB
1	x^4+x^5	00011	-11.76	-24.56
2	x^3+x^5	00101	-13.22	-29.35
3	x^2+x^5	01001	-17.87	-26.45
4	$x+x^5$	10001	-11.76	-25.33
5	$x^3+x^4+x^5$	00111	-3.31	-14.88
6	$x^2+x^4+x^5$	01011	-6.90	-25.45
7	$x+x^2+x^5$	11001	-3.36	-16.32
8	$x^2+x^3+x^4+x^5$	01111	-14.61	-18.76
9	$x+x^2+x^3+x^5$	11101	-15.84	-24.12
10	$x+x^2+x^4+x^5$	11011	-12.92	-23.58

Table 2.1. Results of mathematical modeling of the excitation signals by five-order pseudo-noise sequence.

Coding realization:

The incident ultrasonic signal was formed by reiteration of ultrasonic pulses with frequency 7.5MHz, duration 5 μs and repetition rate 15 Hz. Phase of each pulse was defined by equation $\phi_i = \pi \cdot a_i$.(the phase was coded by the chosen M-sequence). The ultrasonic beam passed through air and after phase conjugation in the active element of conjugator returned to the transducer. Impulse with duration 5 μs extracted from each conjugate signal was received by the Transducer. The sequence was made up from series of these pulses and its correlation function with emitted M-sequence was defined. From amplitude and phase of the correlation function we detected the changes of amplitude and phase of the conjugate wave passed through the airgap.

Demonstration of coding technics for wave extraction from under noise is presented in figure 2.9. Figure 2.9A presents the case of registration of the conjugate signal which is under noise level. Figure 2.9B presents the case of registration in the absence of the conjugate signal.

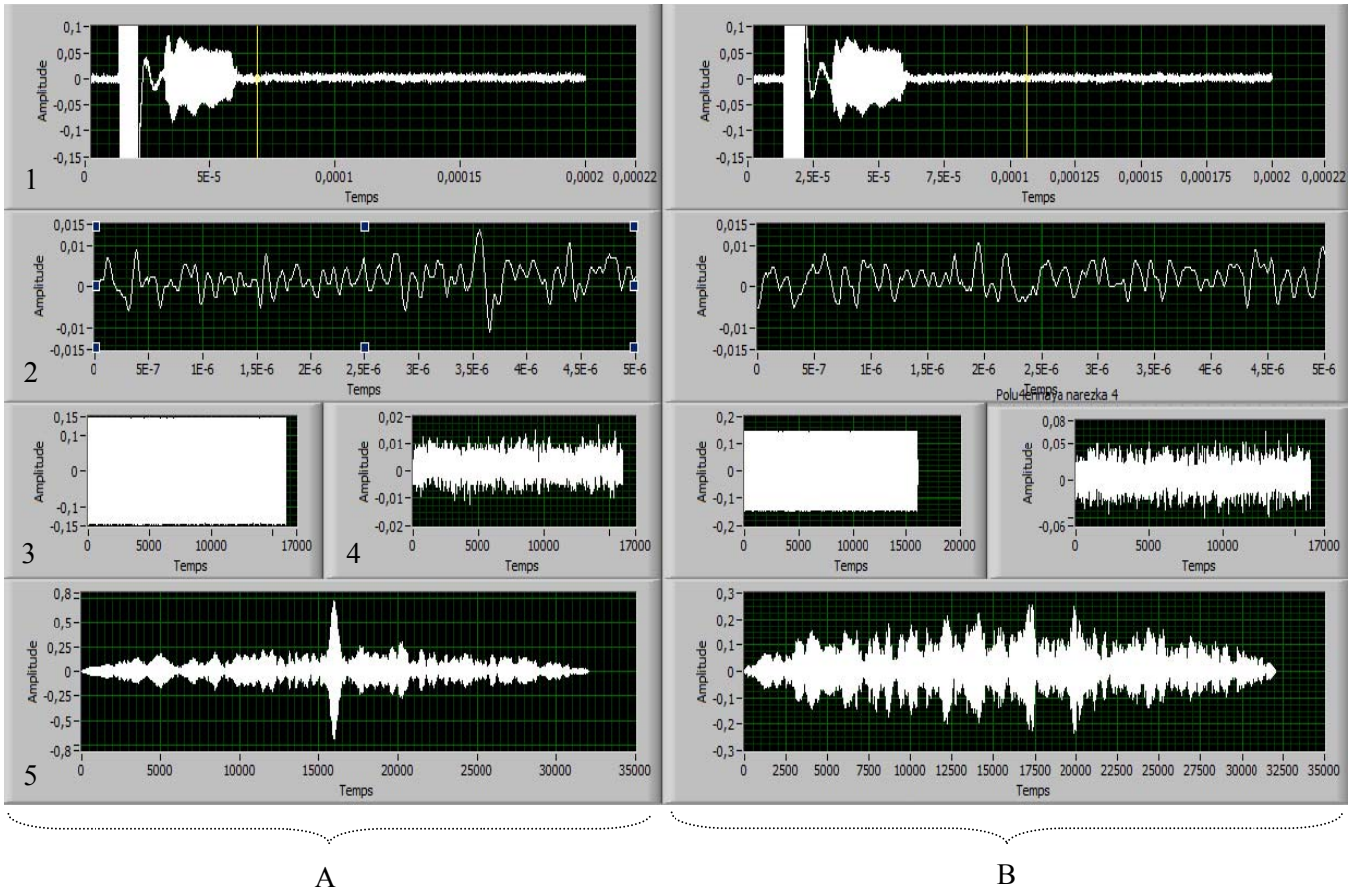

Figure 2.9. Demonstration of coding technics for extraction of a PC signal from under noise. Cases in presence(A) and absence(B) signal are presented. 1) received signal (conjugate signal is under noise); 2) Impulse extracted from conjugate signal; 3) incident sequence; 4) accepted coded sequence; 5) Convolution of an incident and accepted coded sequence.

In figure 2.9-1 one from series registered wave is presented. In figure 2.9-2 impulse with duration 5 μs extracted from conjugate signal is depicted. In figure 2.9-3 the incident sequence of ultrasonic signals made up from series of these pulses which phases was coded by the chosen M-sequence is shown. In figure 2.9-4 the sequence was made up from series of impulses extracted from registered conjugate signals is presented. In figure 2.9-5 the correlation function between incident and registered sequences is depicted.

From amplitude and phase of the peak of correlation function (figure 2.9-5) we can detect the changes of amplitude and phase of the conjugate wave passed through the airgap.

Conclusion

A feature of parametrical phase conjugation of weak incident ultrasonic waves is considered in this part. To improve efficiency of parametrical wave conjugation the increase of time of pumping is necessary. As shown in this chapter the growth of amplitude of WPC wave is limited by pumping power. Besides that, at the long time of pumping (exceeding a transit time of an ultrasonic signal on an active material) a resonant mode is generated. It is shown that the wave in resonant mode of generation is not phase conjugated to incident ultrasonic pulse and its amplitude essentially depends on boundary conditions at edges of an active element. Because of the part of pumping power is transformed to the amplitude of resonant mode the increase of time of pumping makes sense until the resonant mode does not develop strongly enough.

For the first time in WPC technique a phase coding of WPC wave by pseudonoise M - sequence was used to detect the weak conjugate signal. Physical principle of overthreshold parametrical phase conjugation do not make possible to change phase in the interior of the conjugate pulse. Therefore phase coding was made from pulse to pulse. The choice of optimal M – sequences was made and was allowed to obtain WPC signals from level -30dB relative to noise one.

With long time of pumping conjugator works in the mode close to saturation one. This fact should be taken into account if amplitude measurements of PC wave is carried out. The technique of correction of these types of experimental measurements is developed and described in this chapter. As example, the result of measurements of the absorption factor of ultrasound in air was adduced. The measurements were carried out at the frequency 7.5 MHz and value of absorption factor closed to theoretical one was obtained.

Chapter 3: Numerical simulations of propagation of ultrasonic phase conjugate wave in con-focal system

This third chapter presents the description of numerical model which describes the process of propagation of ultrasonic phase conjugate wave in con-focal system with air gap.

The angle dependence of transmission coefficient of ultrasonic wave of boundary surface "agar-air", boundary "air-ferrite", total angular dependence of transmission coefficient of ultrasound wave, trajectories of acoustical rays in con-focal system, intensity of acoustical rays in the line of it's propagation, evolution of the amplitude of ultrasonic wave passes the air gap in the con-focal system are studied.

3.1. Transmission angular characteristics

To develop mathematical model of process of propagation of ultrasonic PC wave in con-focal system with air gap it is necessary to take into account the loss by passing boundary surface of the propagation medium. In the case under consideration ultrasonic wave propagates in three medium: agar-air-active material (ferrite). We used transducer with long focal distance to provide a small angle of incident on ferrite. To avoid the huge absorption in air on big focal length we used a cylinder made from agar with acoustic properties close to water. The thickness of agar was selected so that exit of ultrasonic wave was directly before the focal point.

At the first step we study the angle dependence of transmission coefficient of ultrasonic wave of boundary surface agar-air. In this case three waves are under consideration: incident wave, transmitted and reflected waves (figure 3.2).

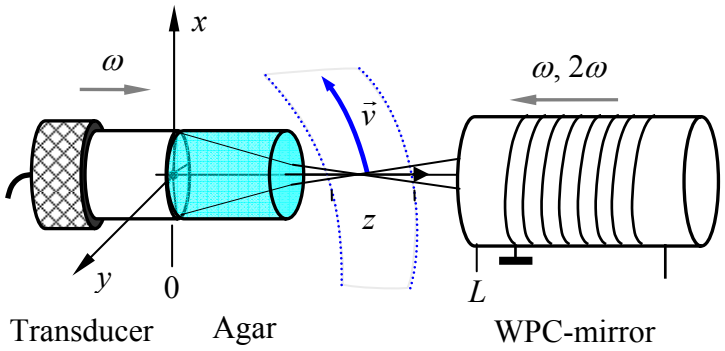

Figure 3.1. Propagation of ultrasonic phase conjugate wave in con-focal system: area of the air flow is represented by dotted line.

On the boundary surface of mediums the implementation of conditions of continuity of acoustical pressure and continuity of normal component of vibrational velocity of particles is necessary.

It can be expressed by following system of equations:

$$\begin{aligned} P_0 + P_R &= P_T \\ v_0 \cos\alpha - v_R \cos\alpha &= v_T \cos\beta \end{aligned} \qquad (3.1.1)$$

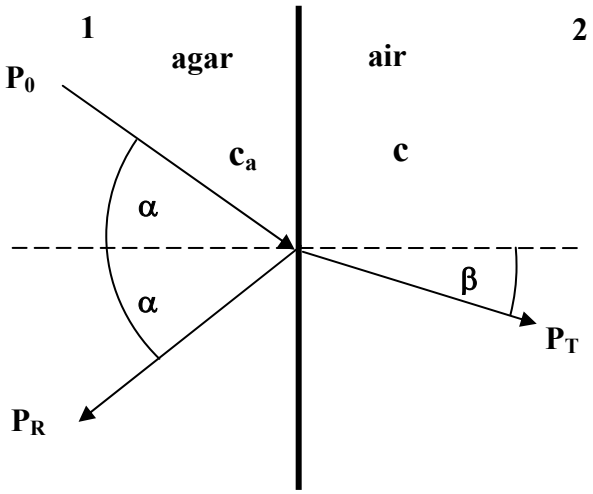

Figure 3.2. Propagation of ultrasonic wave the boundary surface "agar-air".

By introducing transmission and reflection coefficients (by pressure): $R_P = \frac{P_R}{P_0}$, $T_P = \frac{P_T}{P_0}$, respectively, and taking into account relation between pressure and vibration velocity: $P = Zv$, where Z - acoustical impedance of medium of propagation: $Z_1=\rho_a c_a$, $Z_2=\rho c$, ρ_a= 1014 kg/м^3, c_a= 1497 м/s, ρ = 125 kg/м^3, c = 340 м/s, from Eqs. (3.1.1) one can get system of equations:

$$\begin{aligned} 1 + R_P &= T_p \\ 1 - R_P &= T_P \frac{\cos(\beta)}{\cos(\alpha)} \frac{Z_1}{Z_2} \end{aligned} \qquad (3.1.2)$$

From these equations we evaluate pressure transmitted coefficient:

$$T_P = \frac{2 Z_2 \cos(\alpha)}{Z_1 \cos(\beta) + Z_2 \cos(\alpha)}$$

Energy transmitted coefficient we find by multiplying equations in the system (3.1.2)

$$1 - \left|R_P\right|^2 = T_P{}^2 \frac{\cos(\beta)}{\cos(\alpha)} \frac{Z_1}{Z_2} = T ,$$

and, finally,

$$T = \frac{2 Z_1 Z_2 \cos(\alpha)\cos(\beta)}{(Z_1 \cos(\beta) + Z_2 \cos(\alpha))^2} . \qquad (3.1.3)$$

It is to note that in the stationary medium the value of transmission coefficient for phase conjugate wave agree with the value of transmission coefficient for incident wave due to angular invariance of incident and passing waves. Angular dependence of ultrasonic transmission coefficient of boundary surface “agar-air” is presented in figure 3.3.

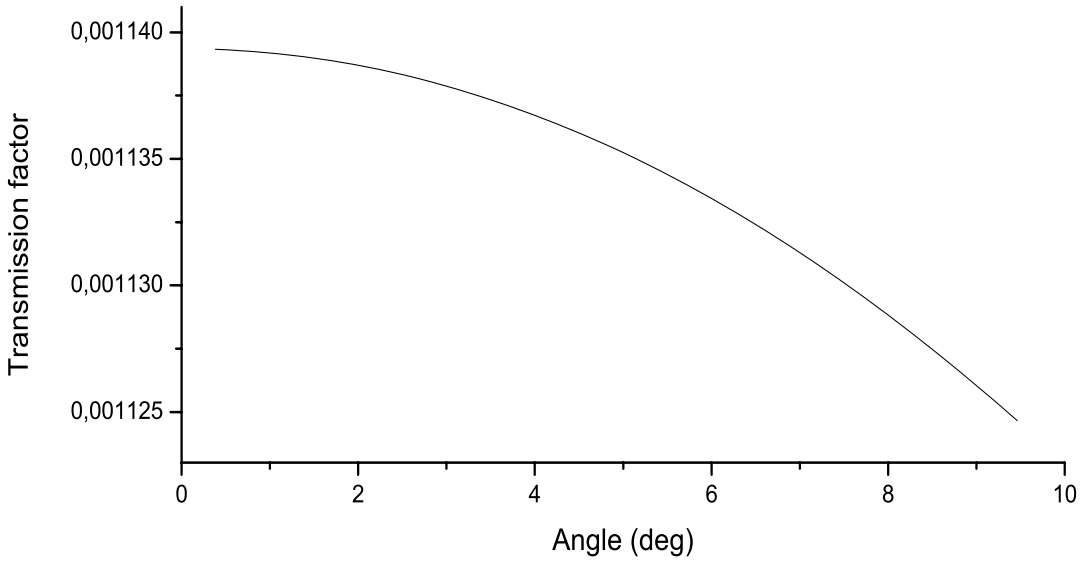

Figure 3.3. Angular dependence of ultrasonic transmission coefficient of boundary surface "agar-air".

When ultrasonic wave passes through boundary "air-ferrite" (figure 3.4) the process is more complicated. Besides of the longitudinal wave reflected from surface, transmitted shear wave is added to transmitted longitudinal wave. Velocity of shear wave is substantially smaller then velocity of longitudinal wave in an active material.

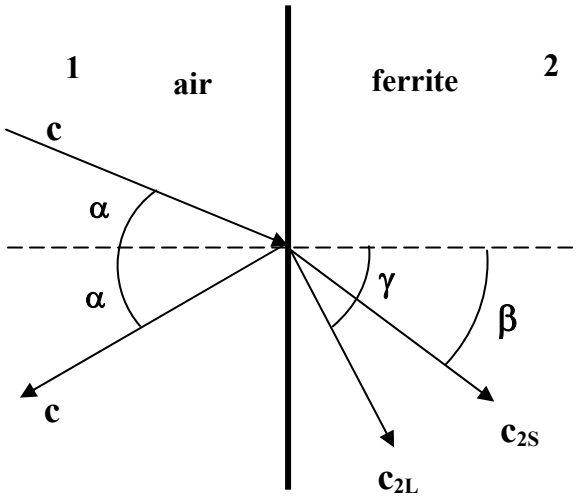

Figure 3.4. Propagation of ultrasonic wave the boundary surface "air-ferrite".

Taking into account requirement of continuity of the pressure and vibrational velocity we obtain following system of equations for transition coefficients shear wave

(t_P) and longitudinal wave (T_P), and also for reflection coefficient of longitudinal wave (R_P) [167]:

$$\begin{Vmatrix} \cos\beta & \sin\gamma & \sin\alpha \\ \sin\beta & \cos\gamma & \cos\alpha \\ \sin 2\beta & f & Z_1/Z_2 \end{Vmatrix} \cdot \begin{Vmatrix} t_P \\ T_P \\ R_P \end{Vmatrix} = \begin{Vmatrix} \sin\alpha \\ -\cos\alpha \\ Z_1/Z_2 \end{Vmatrix}, \qquad (3.1.4)$$

where $f = \frac{c_{2L}}{c_{2S}}(1 - 2\frac{c_{2S}^2}{c_{2L}^2}\cos^2\gamma)$, c_{2L}=6800 m/s и c_{2S}=3500 m/s – velocity of longitudinal wave and shear wave in ferrite correspondingly, $Z_1 = \rho c$ - acoustical impedance of air $Z_2 = \rho_2 c_{2L}$ - acoustical impedance of ferrite (for share wave). Because of ultrasonic parametrical wave phase conjugation realized substantially by shear wave in ferrite [49] in the first place the value of shear wave transmission coefficient t_P is of our interest. Equations for incident and refraction angles based on Snell's law:

$$\frac{\sin\alpha}{c} = \frac{\sin\beta}{c_{2S}} = \frac{\sin\gamma}{c_{2L}} \qquad (3.1.5)$$

Special feature of ultrasound passing through boundary surface "air-ferrite" is that total reflection occurs at first for passing longitudinal wave in ferrite. Critical angle for longitudinal wave "air-ferrite" equals $\alpha_{2L} = \arcsin\frac{c}{c_{2L}} \cong 2,9^\circ$. With further increase of incidence angle shear wave exist up to critical angle for shear wave in ferrite $\alpha_{2S} = \arcsin\frac{c}{c_{2S}} \cong 5,6^\circ$. In this angle range reflection and transmission coefficients connected by following equations:

$$\begin{aligned} t_P \frac{c_{2S}}{c} \sin\alpha + R_P \cos\alpha &= -\cos\alpha \\ t_P \frac{c_{2S}}{c} \frac{Z_2}{Z_1} \sin 2\alpha + R_P \cos 2\alpha &= \cos 2\alpha \end{aligned}, \qquad (3.1.6)$$

Eliminating R_p from system (3.1.6) we get pressure transmission coefficient:

$$t_P = \frac{c}{c_{2S}} \cdot \frac{2Z_1}{Z_2 tg\,2\alpha - Z_1 tg\,\alpha},$$

And also energy transmission coefficient:

$$t = \left(\frac{c}{c_{2S}} \right)^2 \cdot \frac{4Z_1 Z_2 \cos\beta}{(Z_2 tg\,2\alpha - Z_1 tg\,\alpha)^2 \cos\alpha}. \qquad (3.1.7)$$

After phase conjugation acoustical wave propagates on the same trajectory in the opposite direction. At the boundary surface one part of phase conjugate wave goes out from ferrite to aerial medium and another part reflects splitting into shear wave and longitudinal wave (figure 3.5).

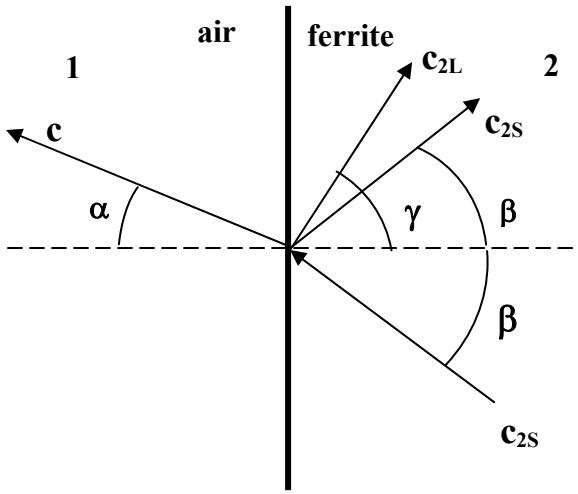

Figure 3.5. Propagation of ultrasonic wave the boundary surface "ferrite-air".

As in the case of passing ultrasound wave in ferrite in this case taking into account boundary conditions for continuity of pressure and vibration velocity lead to system of equations [167]:

$$\begin{Vmatrix} -\sin 2\beta & Z_1/Z_2 & f \\ \cos\beta & -\sin\alpha & -\sin\gamma \\ \sin\beta & -\cos\alpha & \cos\gamma \end{Vmatrix} \cdot \begin{Vmatrix} r_P \\ T_P \\ R_P \end{Vmatrix} = \begin{Vmatrix} \sin 2\beta \\ -\cos\beta \\ \sin\beta \end{Vmatrix}, \qquad (3.1.8)$$

where $f = \frac{c_{2L}}{c_{2S}} \cdot \left[1 - 2\frac{c_{2S}^2}{c_{2L}^2}\left(1 - \frac{c_{2L}^2}{c_{2S}^2}\cos^2\gamma\right) \right]$, and angles satisfy equations (3.1.5).

To find total angular dependence of transmission coefficient it is necessary to take into account that parametrical phase conjugation is realized only for shear wave. Parametrical wave phase conjugation of longitudinal acoustic wave is negligible [49]. Thereby one can get total transmission coefficient for ultrasonic phase conjugate con-focal system "transducer-agar-air-ferrite-WPC-ferrite-air-agar-transducer" Resulting angular dependence of transmission of con-focal system is shown on figure 3.6. At calculation we use the gain factor of WPC system equal 1.

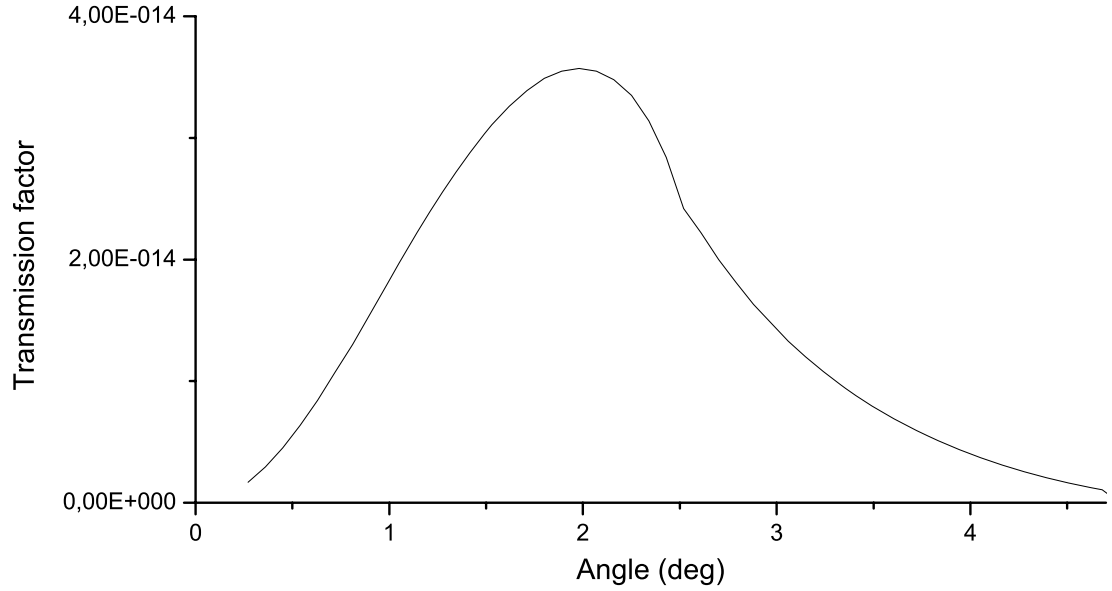

Figire 3.6. Resulting angular dependence of transmission of con-focal system "transducer-agar-air-ferrite-WPC-ferrite-air-agar-transducer".

3.2. Evolution of an amplitude and phase of PC wave in con-focal ultrasonic system in the framework of ray acoustics.

For paraxial acoustic beams propagates in moving medium with attenuation the wave equation can be transforms to next one [168]:

$$\pm\frac{\partial}{\partial\tau}\left[\frac{\partial P}{\partial z}-\frac{V_z}{c^2}\frac{\partial P}{\partial\tau}\right]+\frac{1}{c}\frac{\partial V_z}{\partial z}\frac{\partial P}{\partial\tau}=\frac{c}{2}\nabla_\perp^2 P+\frac{b}{\rho_0 c^4}\frac{\partial^3 P}{\partial\tau^3}, \qquad (3.2.1)$$

where $\tau = t \mp z/c$, $\nabla^2{}_\perp = \partial^2/\partial x^2 + \partial^2/\partial y^2$ — Laplace operator in the plane transversal to direction of propagation of acoustical beam. Upper and lower sign corresponds to forward and opposite directions of wave propagation.

To deduce equations for amplitude and phase of incident and conjugate wave we substitute $P^\pm = A^\pm \exp\left[i(\omega\tau+\phi^\pm)\right]+c.c.$ into equation (3.2.1) and extract the real part of equation in ray acoustics approximation:

$$\pm\omega\frac{\partial\phi^\pm}{\partial z}+\frac{\omega^2}{c^2}V_z+\frac{c}{2}(\nabla_\perp\phi^\pm)^2=0 \qquad (3.2.2)$$

Taking into account that $\vec{k}^\pm = \mp\vec{\nabla}\phi^\pm$, one can rewrite last equation as:

$$\mp\omega k_z^\pm+\frac{\omega^2}{c^2}V_z+\frac{c}{2}(k_\perp{}^\pm)^2=0 \qquad (3.2.3)$$

Let's denote the left part of equation (3.2.3) as $H^\pm(\vec{r},\vec{k})$ and work in parameter $t^\pm$, such as $\frac{dH^\pm}{dt^\pm}=0$.

Let's write out expression for total derivative of $H^\pm(\vec{r},\vec{k})$:

$$\frac{dH^{\pm}}{dt^{\pm}} = \frac{\partial H^{\pm}}{\partial \vec{k}^{\pm}}\frac{\partial \vec{k}^{\pm}}{\partial t^{\pm}} + \frac{\partial H^{\pm}}{\partial \vec{r}^{\pm}}\frac{\partial \vec{r}^{\pm}}{\partial t^{\pm}} = 0,$$

From this one can obtain:

$$\frac{d\vec{r}^{\pm}}{dt^{\pm}} = \frac{\partial H^{\pm}}{\partial \vec{k}^{\pm}}, \quad \frac{d\vec{k}^{\pm}}{dt^{\pm}} = -\frac{\partial H^{\pm}}{\partial \vec{r}^{\pm}}. \tag{3.2.4}$$

Let's find value of parameter t: $\frac{dz}{dt^{\pm}} = \frac{\partial H^{\pm}}{\partial k^{\pm}_{z}} = \pm\omega$, from this $t = \pm\frac{z}{\omega}$.

Further we find values of derivatives on z-coordinate from transverse component of radius vector of observation point at acoustical ray $\vec{r}_{\perp} = \vec{r}_{\perp}(z)$, wave vector $\vec{k}$ and phase of wave φ:

$$\frac{d\vec{r}_{\perp}^{\pm}}{dz} = \frac{d\vec{r}_{\perp}^{\pm}}{dt^{\pm}}\frac{dt^{\pm}}{dz} = \frac{\partial H}{\partial \vec{k}_{\perp}}\left(\pm\frac{1}{\omega}\right) = \pm\frac{1}{k_0}\vec{k}_{\perp}^{\pm}, \tag{3.2.5}$$

where $k_0 = \omega/c$ — wave number.

$$\frac{d\vec{k}_{\perp}^{\pm}}{dz} = \frac{d\vec{k}_{\perp}^{\pm}}{dt^{\pm}}\frac{dt^{\pm}}{dz} = -\frac{\partial H^{\pm}}{\partial \vec{r}_{\perp}^{\pm}}\left(\pm\frac{1}{\omega}\right) = \mp\frac{k_0}{c}\vec{\nabla}_{\perp}V_z.\nabla \tag{3.2.6}$$

$$\frac{d\varphi^{\pm}}{dz} = \frac{\partial\varphi^{\pm}}{\partial z} + \frac{\partial\varphi^{\pm}}{\partial \vec{r}^{\pm}_{\perp}}\frac{\partial \vec{r}^{\pm}_{\perp}}{\partial z} = \mp k_z^{\pm} \pm \vec{k}_{\perp}^{\pm}\frac{c}{\omega}\vec{k}_{\perp}^{\pm} = \mp\frac{k_0}{c}V_z \pm \frac{1}{k_0}\left(\vec{k}_{\perp}^{\pm}\right)^2 \tag{3.2.7}$$

To find equations for amplitude of acoustic wave we extract the imaginary part of equation (3.2.1):

$$\omega\frac{\partial A^{\pm}_1}{\partial z} + \frac{\omega}{c}\frac{\partial V_z}{\partial z}A^{\pm}_1 = \frac{c}{2}\left(\nabla_{\perp}k^{\pm}A^{\pm}_1 \pm 2k^{\pm}{}_{\perp}\nabla_{\perp}A^{\pm}_1\right) - \frac{b\omega^3}{2\rho_0 c^3}A^{\pm}_1. \tag{3.2.8}$$

Than working in denotation $u^{\pm}_{ij} = \frac{\partial k^{\pm}_i}{\partial x_j}$, one can transform equation for amplitude of acoustic wave as:

$$\frac{\partial A^{\pm}_1}{\partial z} \mp \frac{k^{\pm}{}_{\perp}}{k_0}\nabla_{\perp}A^{\pm}_1 = \left(\frac{1}{2k_0}\left(u_{xx} + u_{yy}\right) - \frac{1}{c}\frac{\partial V_z}{\partial z} - \frac{b\omega^2}{2\rho_0 c^3}\right)A^{\pm}_1, \tag{3.2.9}$$

Taking into account $\frac{d}{dz} = \frac{\partial}{\partial z} \mp \frac{1}{k_0}(\vec{k}_\perp^{\pm} \cdot \vec{\nabla}_\perp)$, we obtain:

$$\pm \frac{dA_1^{\pm}}{dz} = (-\delta_1 + F^{\pm})A_1^{\pm}, \tag{3.2.10}$$

where $\delta_1 = b\omega^2/2\rho c^2$, $F^{\pm} = \frac{1}{2k_0}(u_{xx}^{\pm} + u_{yy}^{\pm}) - \frac{1}{c}\frac{\partial V_z}{\partial z}$.

Further it is necessary to obtain equations for $u_{ij}^{\pm} = \frac{\partial k_i^{\pm}}{\partial x_j}$. To find these equations let's partial derive equation (3.2.6) on *x*-coordinate.

$$\frac{d}{dz}\frac{\partial k^{\pm}{}_x}{\partial x} = \mp \frac{\partial}{\partial x}\left(\frac{k_0}{c}\frac{\partial V}{\partial x}\right) = \mp\left(\frac{1}{c}\frac{\partial k_0}{\partial x}\frac{\partial V}{\partial x} + \frac{k_0}{c}\frac{\partial^2 V}{\partial x^2}\right).$$

and then:

$$\frac{d}{dz}u_{xx}^{\pm} = \mp \frac{1}{k_0}\left[(u_{xx}^{\pm})^2 + u_{xy}^{\pm}u_{yx}^{\pm}\right] - \frac{k_0}{c}\frac{\partial^2 V_z}{\partial x^2}. \tag{3.2.11}$$

In the same way, one can get following equations for another components of matrix $u_{ij}^{\pm}$:

$$\begin{aligned} \frac{d}{dz}u_{yy}^{\pm} &= \mp \frac{1}{k_0}\left[(u_{yy}^{\pm})^2 + u_{xy}^{\pm}u_{yx}^{\pm}\right] - \frac{k_0}{c}\frac{\partial^2 V_z}{\partial y^2}, \\ \frac{d}{dz}u_{ij}^{\pm} &= \mp \frac{1}{k_0}u_{ij}^{\pm}(u_{xx}^{\pm} + u_{yy}^{\pm}) - \frac{k_0}{c}\frac{\partial^2 V_z}{\partial x \partial y}, \quad i \neq j. \end{aligned} \tag{3.2.12}$$

Expressions (3.2.5)–(3.2.7), (3.2.10)–(3.2.12) make up closed systems of equations in the framework of ray acoustics for calculation of the evolution of fundamental harmonic of phase conjugate wave which propagates in the moving medium.

For velocimetry of gas flows the focused ultrasonic beams are of most interest, because it is possible to make local diagnostics of velocity distribution into various flows, using such kind of acoustical beams, for example such as in figure 3.1. To simulate focused beam let's work in Gaussian distribution of the phase at the transducer (located in the point $z = 0$). In the surface of conjugator (located in the point $z = L$) we use

conditions of phase conjugation and amplitude amplification by factor χ. Therefore boundary conditions for the system of equations (2.5)–(2.7), (2.10)–(2.12) have following view:

$$\begin{aligned}
&\varphi_+\big|_{z=0} = G(\omega) r_\perp^2 / \varepsilon^2 , \\
&A_1^+\big|_{z=0} = A_0(\vec{r}_\perp) , \\
&\varphi^-\big|_{z=L} = -\varphi^+\big|_{z=L} , \\
&\vec{k}_\perp^-\big|_{z=L} = -\vec{k}_\perp^+\big|_{z=L} , \\
&u_{ij}^-\big|_{z=L} = -u_{ij}^+\big|_{z=L} , \\
&A_1^-\big|_{z=L} = \chi A_1^+\big|_{z=L} .
\end{aligned} \qquad (3.2.13)$$

Where $G(\omega) = k_0\varepsilon^2/2d$, ε and d — radius of aperture and focal distance of transducer correspondingly. The lines from three to six of boundary conditions (3.2.13) show WPC transformation of incident wave.

It is to note that in the case of plane waves propagating in the moving medium one can get the phase shift of PC wave by next simplified formula:

$$\Delta\varphi = 2\frac{k}{c}\int_{d_1}^{d_2} v_z(z)dz , \qquad (3.2.14)$$

where d_1, d_2 — borders of air flow (figure 3.1). Thereby the phase shift defines by averaged projection of velocity of air flow to the direction of propagation of ultrasonic wave. If the case of non plane ultrasonic wave the phase is depend from amplitude distribution of phase conjugate waves on the surface of receiver and utilization of system of equations (3.2.5)–(3.2.7), (3.2.10)–(3.2.13) is necessary.

3.3. Results of numerical modeling

Mathematical model developed in the previous part is used for numerical calculation of trajectories of acoustical rays in con-focal system, which has parameters such as in experimental setup. Transmission coefficients obtained in part 3.1 are used for calculation of intensity of acoustical rays in the line of it's propagation. Diameter of

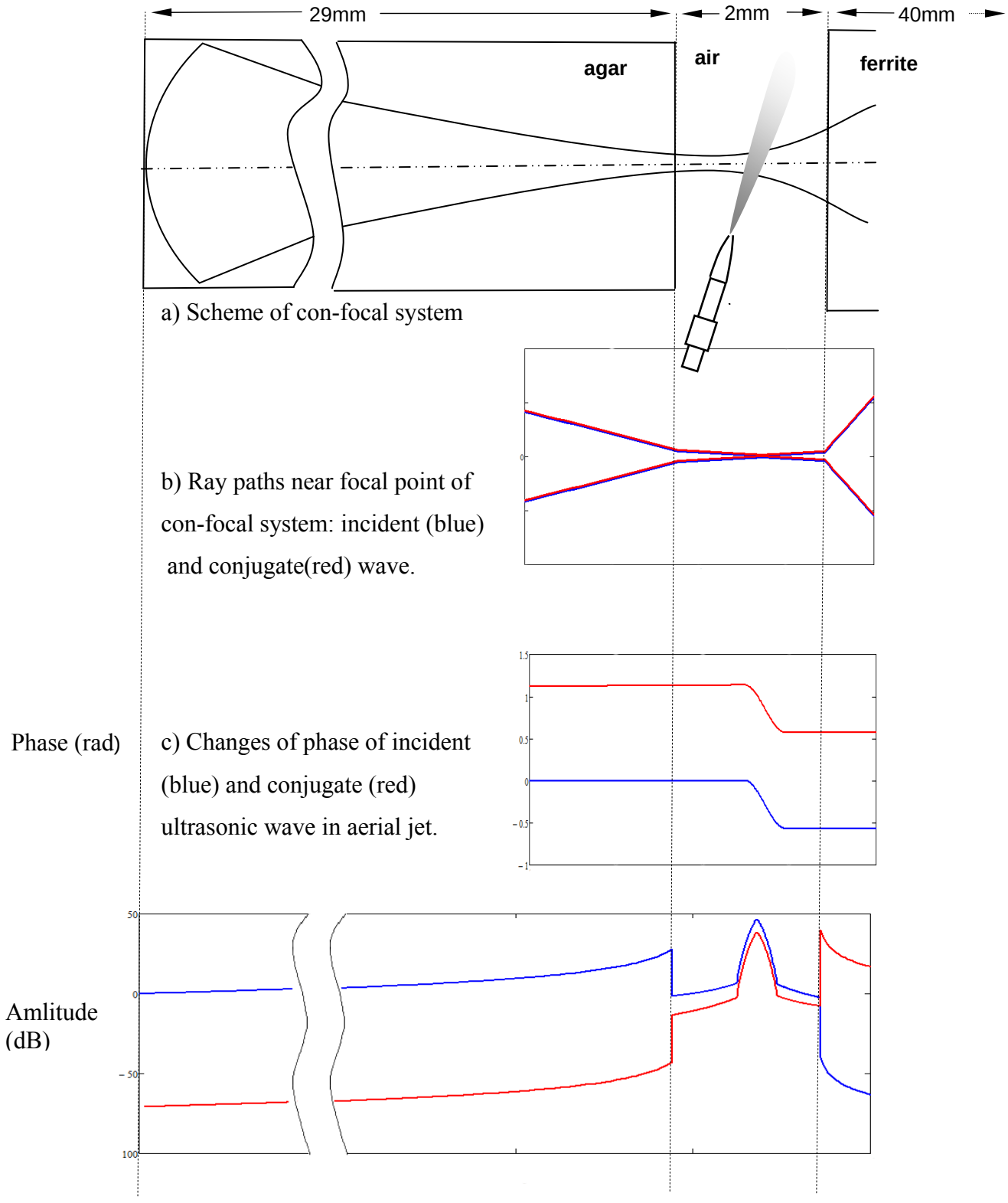

Figure 3.7. Results of numerical calculation of the ray paths (b), phase changes (c) and evolution of amplitude (c) ultrasonic wave in the phase conjugate con-focal system.

transducer and characteristics of the medium of propagation correspond to experimentally measured characteristics. In addition the evolution of amplitude and phase of conjugate waves depending on flow velocity is calculated. Results of this calculation are shown in figure 3.7. Figure 3.7(b) demonstrates paths of forward and conjugate wave.

Numerical simulation shows that length of cylinder made from agar must be a little bit smaller than the focal distance of transducer to minimize the distance of propagation of acoustical wave in the air and therefore minimize the distance with high attenuation. From the figure also follows, that even at the small incident angles on boundary surface "air-ferrite" (less than 2 degrees) refractive angles of shear wave in ferrite are very big and at the angle of 4 degree the total reflection of incident wave is coming. The change of the phase of acoustical wave on the path of propagation presents in figure 3.7(c). We observed sufficiently big phase shift (more then 1rad) due to small velocity of ultrasound in air. Air flow velocity in the model was equaled 1m/s and the inclination of air flow was 30 degree.

Evolution of the amplitude of ultrasonic wave in the con-focal system is shown on the figure 3.7(d). When ultrasonic beam propagates in agar amplitude of this wave increases due to focusing up to boundary surface "agar – air", where jump of amplitude appears because of passing boundary surface. When ultrasonic wave passes the aerial gap it's focalization is go on but the increase of it's amplitude compensates due to strong attenuation of ultrasound in air. In aerial flow grate increase of wave's amplitude occurs. It is connected with well known phenomenon in underwater acoustics – additional focalization of acoustical waves in water flows and sea currents [169]. In aerial flows this effect appears particularly strong because of a big ratio of velocity of moving medium to sound velocity.

When ultrasonic wave enter into ferrite the slump of amplitude of ultrasonic wave (more than 70dB) is happened but it is compensated by amplification of conjugate wave in conjugator. The gain factor used in the numerical model is equal 80dB that corresponds to real gain of experimental setup. Propagation of phase conjugate wave in the opposite direction and change of its amplitude qualitative corresponds to the change of intensity of forward wave. Therefore in the receiver we have acoustical wave which is depressed to level -70dB relative to initial signal.

Conclusion

Numerical model developed in Chapter 3 describes the process of propagation of ultrasonic phase conjugate wave in con-focal system with aerial gap. Carried out numerical simulation shown that this con-focal system has very high phase sensitivity to the change of gas flow velocity. The total lost of intensity in the system has value on the order of -70dB. Preliminary calculations show that this lost may by reduce to the level -40dB, with the help of adapted layers stick on the surface of an active element and agar. Such level signals can be successfully detected by using modern radio engineering equipment and techniques of signal enhancement by phase coding of the phase conjugate wave.

Chapter 4: Acoustical matching of the ultrasonic wave phase conjugation system

The fourth chapter presents the description of air coupled wave conjugation system. The ways for acoustical matching of air-coupled WPC system based on magnetostrictive ceramics are discussed. The results of experimental study of wide range of different filtration membranes for acoustical matching are shown.

4.1. Introduction

Typical operating frequencies of modern systems of the phase conjugation are 5-10 MHz. Air-coupled ultrasound in the megahertz frequency range is becoming a real possibility for some particular applications like: NDT and materials characterization.

The main drawback is that any solid-air interface is such a tremendous barrier for ultrasonic waves that the use of this technique is often impossible and, when possible, always requires high voltage excitation of the emitting transducers, filtering and amplification of the received signal and especially designed transducers.

The first problem of using phase conjugation systems loaded by air is very high attenuation of sound in air in the megahertz frequency range. The only one solution is to reduce as much as possible the dimension of the airgap. An approximate expression for the attenuation of ultrasonic waves in air at normal conditions is given by:

$$\alpha = 1.88 \cdot f^2 \cdot 10^{-11} \, Np/m \qquad (4.1.1)$$

Attenuation of ultrasonic waves in the low megahertz range is shown in figure 4.1. Dependence of factor of attenuation from frequency is calculated from equation 4.1.1.

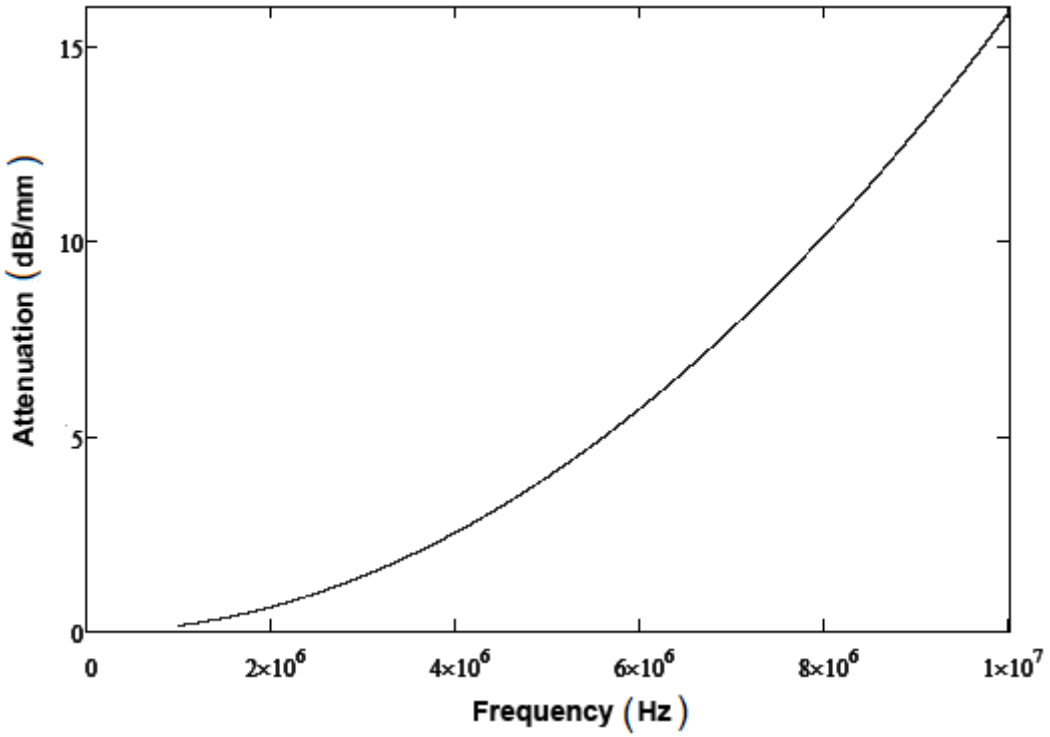

Figure 4.1. The dependency of the attenuation coefficient with the frequency in air calculated from equation 4.1.1.

One of the causes why it is difficult to make full use of the capabilities of active wave phase conjugating (WPC) elements operating with gaseous media is a great differences in the impedances of the solid-state active medium (polycrystalline nickel ferrite) and gaseous medium on the one hand and in the impedances between air and piezoelectric element of transducer on the other hand.

If a plane wave in one medium with impedance *Z1* is normally incident on a plane boundary of other media with impedance *Z2* the energy transmission coefficient *T* is given by the well known equation:

$$T = \frac{4Z_1Z_2}{(Z_1 + Z_2)^2}, \qquad (4.1.2)$$

Acoustic impedance of the air is about 410 Rayl while for most solids Z is in the range 1-50 MRayl. This is the energy loss between 28 and 45 dB at any solid/air interface. That is, most of the energy is reflected and any solid-air interface is always a problem. Such giant losses decrease dramatically the efficiency of the conjugator in spite of the giant gain factor of WPC.

As a consequence of the extremely high difference between velocities of sound propagation in air and solid materials, the angle of incidence of the acoustic radiation on the solid surface that provides total reflection (limit angle) is very low. This angle is calculated from the Snell's law:

$$\frac{\sin(\alpha)}{c_1} = \frac{\sin(\beta)}{c_2} \tag{4.1.3}$$

where c is the velocity of sound and α and β the angles. If wave is travelling from 1 to 2, α is the angle of incidence and β is the angle of refraction. It is clear that refraction depends only on the ratio of velocities of the two media involved. For example: for an air/ferrite interface it is about 4º. This fact has very important consequences when samples having rough or curved surfaces are to be inspected and for the design of focused transducers for through transmission operation.

4.2. Resonant λ/4 acoustical matching

The use of resonant λ/4 matching layers to reduce transmission loss in air-coupled ultrasonic systems is an old and well-known technique [170].

Let us consider an ultrasonic plane wave normally incident upon a thin layer on a thick substrate in air, as shown in figure 4.2. The incident wave is I_0.

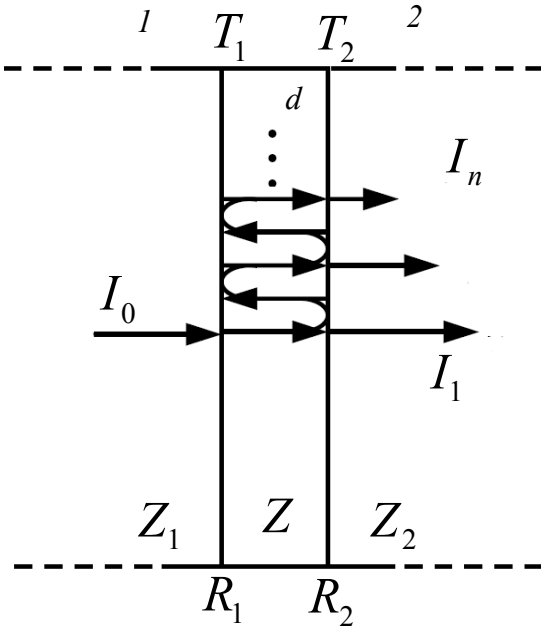

Figure 4.2: Various transmitted signals from a thin layer.

The substrate is thick enough so that only the first transmitted signal is taken into account, while the layer is so thin that the multiple reflected/transmitted signals from the front and back sides of the layer are difficult to separate in time domain. Then, the transmitted signals shown in figure 4.2 may be written as:

$$I_1 = I_0 T_1 T_2 \exp\left[-\left(\alpha + jk\right)d\right] \tag{4.2.1}$$

$$I_n = I_1\left(R_1 R_2 \exp\left(-\left(2\alpha d + j\left(2kd + \pi\right)\right)\right)\right)^{n-1} = I_1 q^{n-1} \tag{4.2.2}$$

Where

$k = \frac{2\pi}{\lambda}$; d - is the thickness of matching layer; $R_1 = 1 - T_1$ - is the reflection coefficient in medium 1 from matching layer 1; $R_2 = 1 - T_2$ - is the reflection coefficient in matching layer from medium 2; $T_1 = \frac{4Z_1 Z}{\left(Z_1 + Z\right)^2}$ - is the transmission coefficient from medium 1 into matching layer, $T_2 = \frac{4Z_2 Z}{\left(Z_2 + Z\right)^2}$ - is the transmission coefficient from

matching layer into medium 2; and Z_i is the acoustic impedance of medium *i*. In our experiments media with *Z1* - air, media with *Z* – matching polymer layer, and media with *Z2* - ferrite.

The total transmitted signal is given by:

$$I = \sum_{n=1}^{\infty} I_n = I_0 T_1 T_2 \, \mathrm{e}^{-\alpha d} \sum_{n=1}^{\infty} q^{n-1} , \tag{4.2.3}$$

where $q = R_1 R_2 e^{-2\alpha d}$

The total transmission coefficient is given by:

$$T = \frac{I}{I_0} = \frac{T_1 T_2 e^{-\alpha d} \left(1 + q\cos\left(2kd\right)\right)}{1 + 2q\cos\left(2kd\right) + q^2} \tag{4.2.4}$$

Multiple reflected/transmitted signals should be in one phase, for this purpose following implementation it is necessary:

$2kd = \pi$, therefore $d = \frac{\lambda}{4}$ and $T_{\max} = \frac{T_1 T_2 e^{-\alpha\frac{\lambda}{4}}}{1 - R_1 R_2 e^{-\alpha\frac{\lambda}{2}}}$

Maximum *T* is obtained at: $Z = \sqrt{Z_1 Z_2}$. In this case:

$$T_1 = T_2 = \frac{4\sqrt{Z_1 Z_2}}{\left(\sqrt{Z_1} + \sqrt{Z_2}\right)^2} \text{, and } T = \frac{T_1^2 e^{-\alpha\frac{\lambda}{4}}}{1 - R_1^2 e^{-\alpha\frac{\lambda}{2}}}$$

Dependence of transmission factor from an impedance of matching layer is shown in figure 4.3. Dependence is calculated from equation 4.2.4. Solid line corresponds to λ/4 matching layer; dotted line corresponds to nonresonant acoustical matching. It is visible from the figure 4.3 that is more important to choose correct thickness of matching layer, instead of an ideal impedance of matching layer.

Theoretically, it is possible to achieve efficiency more than 20dB by resonant λ/4 impedance matching layer.

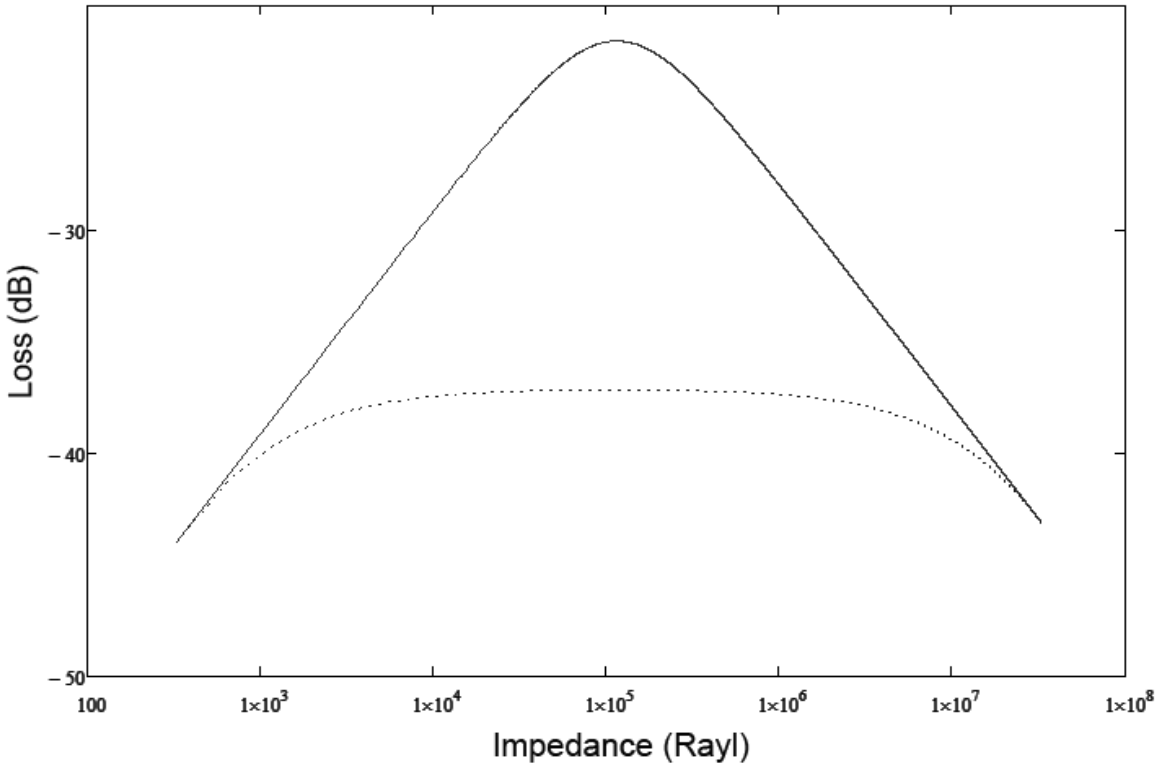

Figure 4.3. Transmission factor from air to ferrite from an impedance of matching layer. Solid line corresponds to λ/4 matching layer, dotted line – to nonresonant acoustical matching. Results are calculated from equation 4.2.4.

Several matching configurations have been proposed, examples are single quarter-wavelength (λ/4) layers and variations of this configuration such as λ/8 [171] and (n+1) λ/4, [172] stacks of λ/4 layers, half-wavelength configurations (λ/2) [173], and a stack of very thin matching layers whose total acoustic thickness is λ/4 [174]. In any of these configurations, a key aspect for the successful design of air-coupled transducers is the acoustic impedance of the outer layer. This is seriously limited by the availability of consistent materials having the required very low acoustic impedance, very low attenuation, and thickness for the designed configuration and working frequency.

Several researchers using a number of different approaches have considered the problems of achieving efficient mechanical matching to air. The basic problem affecting all of this work is that no homogeneous material with suitable characteristics is readily available. Silicone rubber has been attempted; however, this has an acoustic impedance of approximately 1 MRayl, significantly larger than that required for efficient λ/4 matching. One method of reducing this impedance is the inclusion of low-density, air-filled microspheres [144], but this has the disadvantage of increasing the attenuation and

scattering within the material. Other attempted materials include silica aerogels [141, 142], balsa wood, cork [145], and microporous membranes [144], all with varying levels of success.

4.3. Acoustical matching of wave phase conjugation system

The problem consists in the effective acoustical matching of a transducer with 30 mm focal length and an active material of the wave conjugation system. Acoustic impedances of piezoelectric and magnetostrictive ferrite are approximately equal 35 MRayl. The theoretically predicted acoustic impedance for the matching layer is in the range from 0.03-0.15 MRayl ($Zp \approx 35$ MRayl, $Za \approx 400$ Rayl). Unfortunately, such low-impedance values required are not always attainable in practice.

As acoustic impedance is given by $Z = \rho c$, this in turn imposes the condition of low density (ρ) and acoustic velocity (c) in the selection of matching layer materials. Such low-density solids are porous, for this kind of materials, the coefficient of acoustic attenuation is inherently high and increase with frequency. Low acoustic velocity leads to very thin $\lambda/4$ matching layers, especially for high frequencies. As a result, it is difficult to build piezoelectric transducers operating at frequencies higher than 0.5 MHz.

Some materials have acoustic impedance in the range 1–0.1 MRayl (e.g., some kinds of paper, rubbers, and silicone rubber loaded with micro-spheres), and a few in the range 0.1–0.01 MRayl (e.g., some foams and some polymeric filtration membranes). But there is almost no material (apart from very light aerogels and a few open cell foams) under 0.01MRayl. In addition, the practical use of such materials is questionable.

Moreover, not all materials with low acoustic impedance can be used to produce matching layers; most of them present a very high attenuation coefficient. So far, attenuation in the matching layer has attracted much less interest than it does the impedance, although attenuation is becoming the most restrictive.

Use of membrane filters is promising because there is a wide commercial offer of different materials, and grades; they all are highly porous, easy to handle, and have flat and parallel faces with a typical thickness between 20 and 200 μm. A recent work [104] shows that acoustic impedance of a wide collection of membrane filters are in the range 0.08–0.63 MRayl, attenuation per wavelength is within 0.1–0.6 Np, and $\lambda/4$ resonance lies within the range 0.3–2 MHz.

Previous studies [148, 149] of the acoustical properties of filtration membranes demonstrate that some of these materials exhibit very good properties to be used as quarterwavelength matching layers for air-coupled piezoelectric transducers. Best materials are polyethersulfone and nylon membranes because they exhibit the lowest attenuation coefficient and proper values of the acoustic impedance. For higher frequencies, some mixed cellulose esters and PVDF membranes can be used.

However, major limitation of filtration membranes as λ/4 matching layers is that thickness of the membrane cannot be changed. This means that each membrane (commercial type for a material and grade) could be used as λ/4 matching layer at one and fixed frequency.

For illustration the importance of a correct choice of a material for the acoustical matching figure 4.4 is shown.

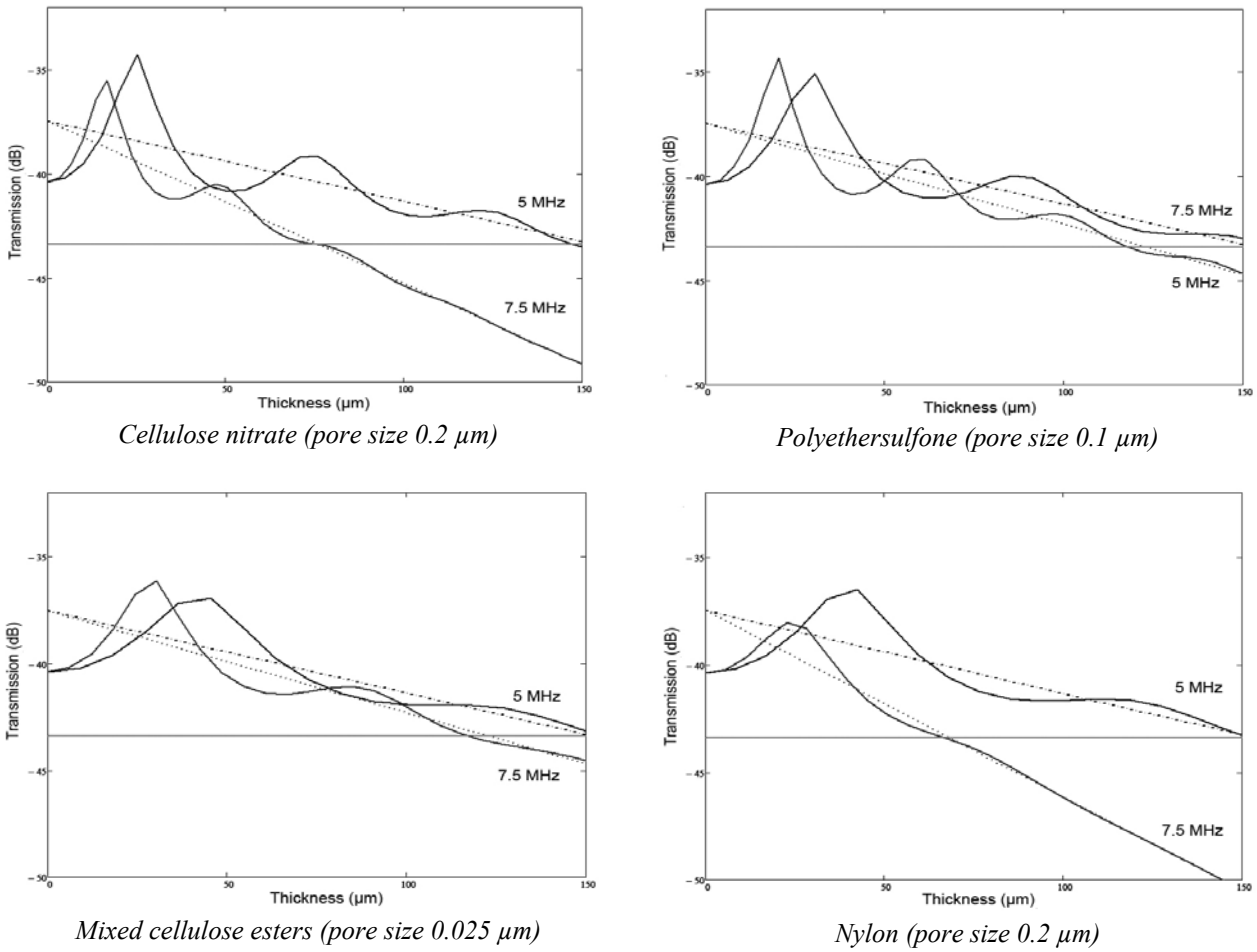

Cellulose nitrate (pore size 0.2 μm)

Polyethersulfone (pore size 0.1 μm)

Mixed cellulose esters (pore size 0.025 μm)

Nylon (pore size 0.2 μm)

Figure 4.4. Dependences of transmission factor of layer from its thickness (thickness resonance) for some materials for two frequencies. Solid lines - theoretical curves, dotted lines – reference lines.

The calculated dependences of transmission factor of layer from its thickness for some materials for two frequencies: 5 MHz and 7.5 MHz are presented in figure 4.4. Values of sound velocity in the material and attenuation factor of some materials are taken from research carried out earlier [148].

It is visible that each membrane can be efficiently used only at one minimum thickness corresponding to the first λ/4 resonance. The increase in thickness of matching layer leads to strong attenuation of a sound in it hence its use for the matching is doubtful. For some materials transmission factor without matching layer can be more than with it (in a consequence of strong attenuation in a matching material).

On the assumption of above-stated part it has been chosen the double matching layer configuration for impedance matching of piezoelectric transducers to the air for improvement of sensitivity and widening the frequency bandwidth. To avoid the huge absorption in air on big focal length we used a cylinder made from agar with acoustic properties close to water as the first nonresonant matching layer. The length of the cylinder was a little bit lower than the focal length, so that the ultrasonic beam was focused in air. The second external is λ/4 layer made of porous polycarbonate membrane.

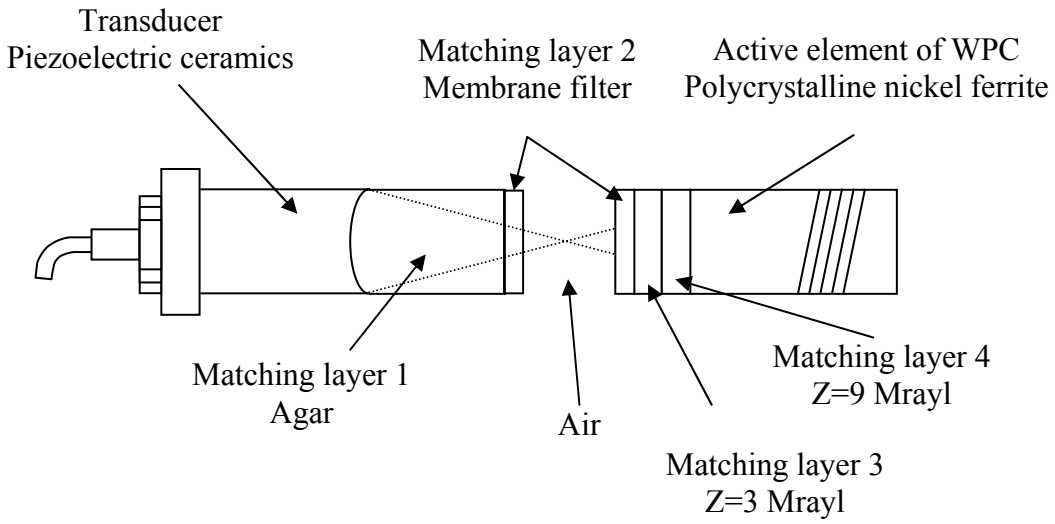

Figure 4.5. Offered scheme for acoustical matching of WPC system.

For matching of active element of wave conjugation system made from polycrystalline nickel ferrite it has been chosen the triple matching layer configuration. First and second layers are nonresonant layers with impedances 9MRayl and 3MRayl

respectively, the outer layer is λ/4 layer made of porous polycarbonate membrane. The offered scheme is of wave conjugation system is shown in figure 4.5.

The given scheme is chosen because: 1) the outer layer is made of the best available material (low impedance, low attenuation, and right thickness for the desired working frequency), 2) additional intermediate matching layers are determined to improve the bandwidth without significantly affecting the sensitivity.

4.4. Experimental results

For investigation of membrane filters experimental setup has been created. The installation scheme is presented in figure 4.6.

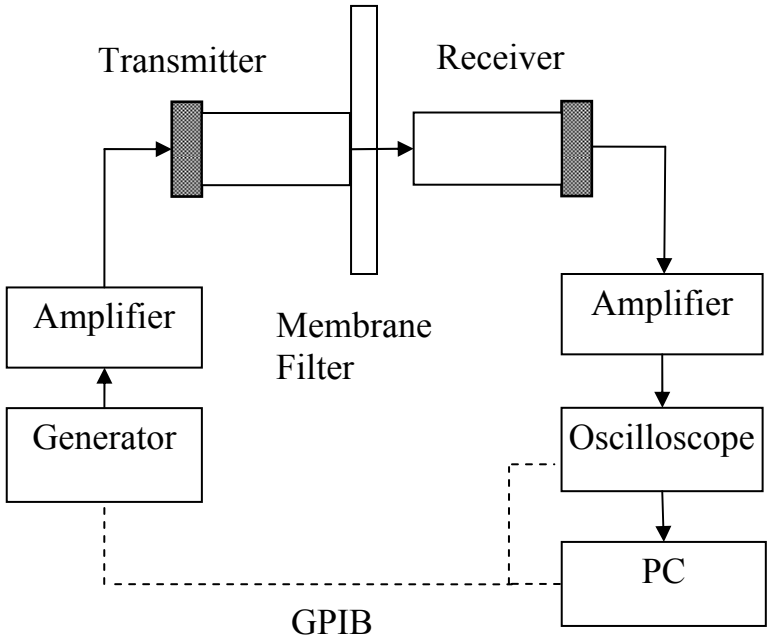

Figure 4.6. The setup for experimental study of set of filtration membranes.

The experimental setup consisted of an air-coupled through transmission technique. Transducers were driven by a tone burst (amplitude 16 volts) generated by a Tektronix AWG 2021. Frequency was changed in steps of 100 kHz in the range interesting us, for example from 0.3 MHz to 2 MHz (or from 5 MHz to 10 MHz). Received signal was amplified by a Sofranel 5052PR up to 40 dB and displayed in a digital oscilloscope TEKTRONIX TDS 5052. Frequency and amplitude were recorded at each step, first for the transmission through the airgap between transducers, which provides the reference level (e.g. line 1 in figure 4.9), and afterwards for the transmission through each sample

(e.g. line 2 in figure 4.9) positioned closely attached to emitter. The ratio of the amplitude transmitted through the sample to the reference level provides the square root of the transmission coefficient (T). Thus first resonance (λ/4) of T is observed. The λ/4 resonances for two different matching materials are presented in figures 4.7 and 4.10.

A wide set of different commercial filtration membranes are studied. Different manufacturers, materials, pore sizes, and other filtration properties were selected to have a wide collection of samples. The characterization of the material requires the measurement of thickness, density, velocity and attenuation of ultrasound in the material at the frequency of interest.

Membrane	**Ref number**	**Material**	**Pore Size (µm)**	**Porosity (%)**	**Thickness (µm)**	**Velocity (m/s)**	**Density (kg/m^3)**	**Impedance (MRayl)**	**λ/4 Resonant Frequency (MHz)**
Millipore	JVWP04700	Omnipore Membrane, PTFE	0.1	80	22	170	1150	0.200	1.95
Millipore	FHUP04700	Fluoropore Membrane, PTFE	0.45	NA	33	60	800	0.048	0.45
Millipore	VCTP04700	Isopore Membrane, polycarbonate	0.1	5–20	18	110	1120	0.120	1.47
Whatman	8182011	Polycarbonate Membrane	0.1	N.A.	20	80	520	0.038	0.9
Whatman	8078004	Cyclopore Membrane	0.2	N.A.	24	80	380	0.030	0.8
Whatman	70288	Membrene Filter	N.A.	N.A.	176	400	90	0.035	0.56
Whatman	6809-5012	Anodisc	0.1	N.A.	66	160	610	0.095	0.6
Whatman	6809-5022	Anodisc	0.2	N.A.	60	140	670	0.090	0.56

Table 4.1. Properties of investigated membrane filters.

Several porous materials have been investigated. Direct measurements of density and sound velocity in each matching material have been carried out. Some values have been calculated from the measured parameters. All measured and calculated values are presented in the table 4.1.

Such materials have low acoustic impedance due to their low density and ultrasound velocity. Quarter-wave layers made from this materials show good results up to frequency 2MHz. Theoretically calculated transmission coefficient from Eq. (4.2.4) and experimentally obtained results for the membrane with the highest λ/4 resonance are shown in the figure 4.7.

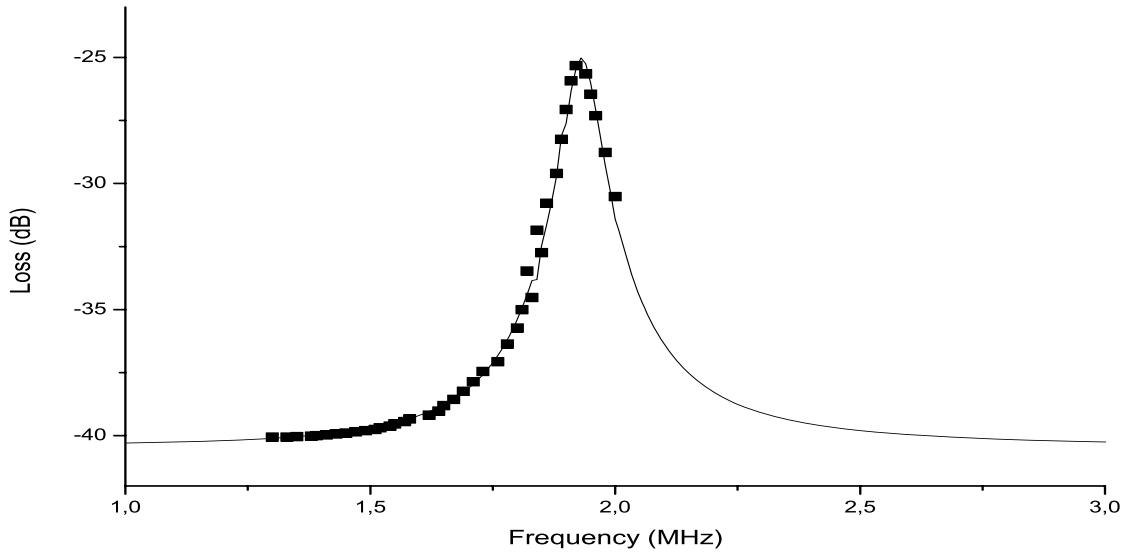

Figure 4.7. Frequency dependence of transmission coefficient for λ/4 JVWP04700 layer. Points – experimental data. Line - theoretical resonance curve calculated from equation 4.2.4.

Low resonant frequency is caused by low speed of a sound in samples. It is presumably possible to use the second (3λ/4) or third resonance (λ + λ/4) but as show calculations it does not give a big gain due to attenuation in a material (see figure 4.4 end figure 4.8).

An important point is the dependency of the attenuation coefficient with the frequency. Figure 4.8 is presented to illustrate the influence of the frequency of ultrasound on attenuation factor. It presents the theoretically calculated dependence of transmission factor from ultrasound frequency for JVWP04700 membrane (Table 4.1). It is visible that is possible to use the second resonance 3λ/4 but its efficiency reduces almost twice.

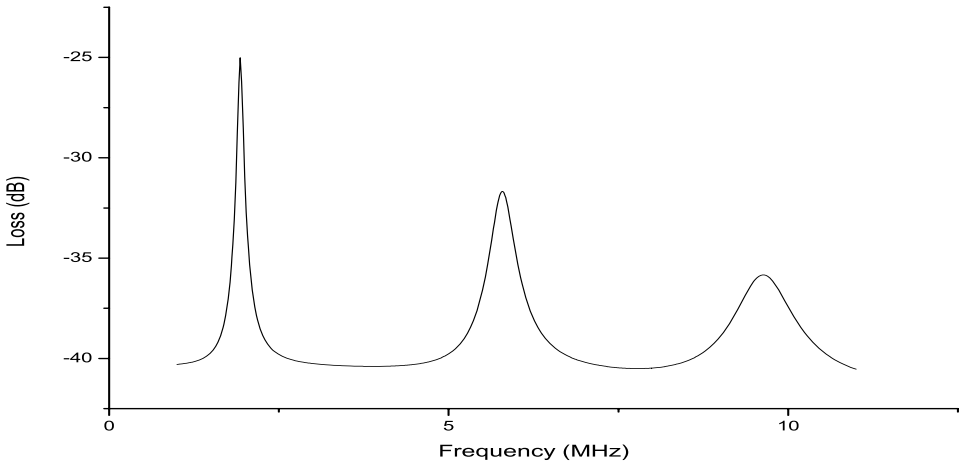

Figure 4.8. Theoretical dependence of transmission factor on frequency for membrane JVWP04700.

To raise the first resonance frequency of porous membranes up to the operational frequency of the conjugator, we proposed to impregnate the porous layer by oil, thus increasing speed of propagation of a wave in a membrane, raising frequency of a resonance. Several porous materials impregnating by oil were analyzed. The best for our frequency range became VCTP04700 membrane. After impregnating by oil the membrane has received following characteristics: thickness - not changed, density – 800 kg/m^3, velocity – 630 m/s; acoustic impedance – 0,5 MRayl, resonance frequency - 6.3MHz. The increase of impedance is compensated by reduction of absorption.

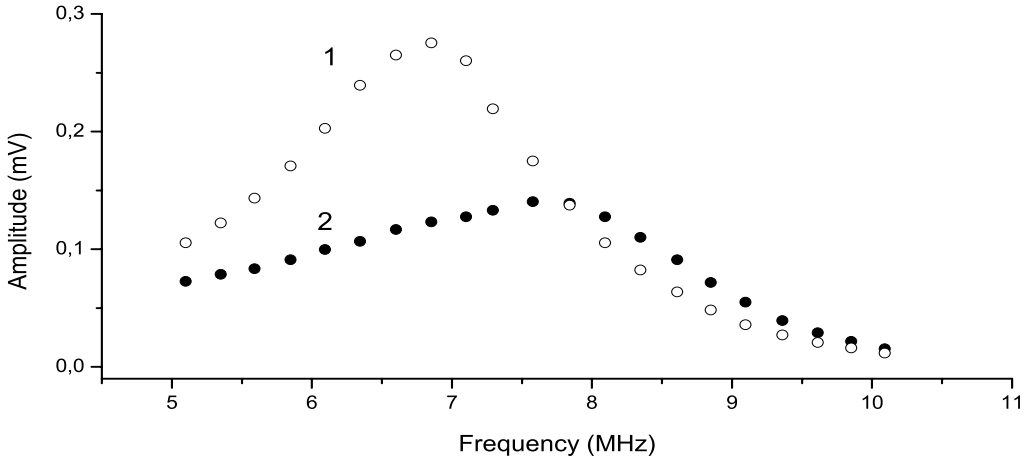

Figure 4.9. Frequency characteristics of 10MHz transducer-receiver:1 – with oil-impregnated layer , 2 - without matching layer.

The frequency dependence of the amplitude of the ultrasonic wave emitted by the transceiver with and without porous layer is shown in figure 4.9. On figure 4.10 the frequency response of the layer is shown without the frequency response of the

transceiver. The figure also shows the theoretical transmission coefficient calculated from Eq. (4.2.4). The resonance frequency of the matching layer is 6.3MHz.

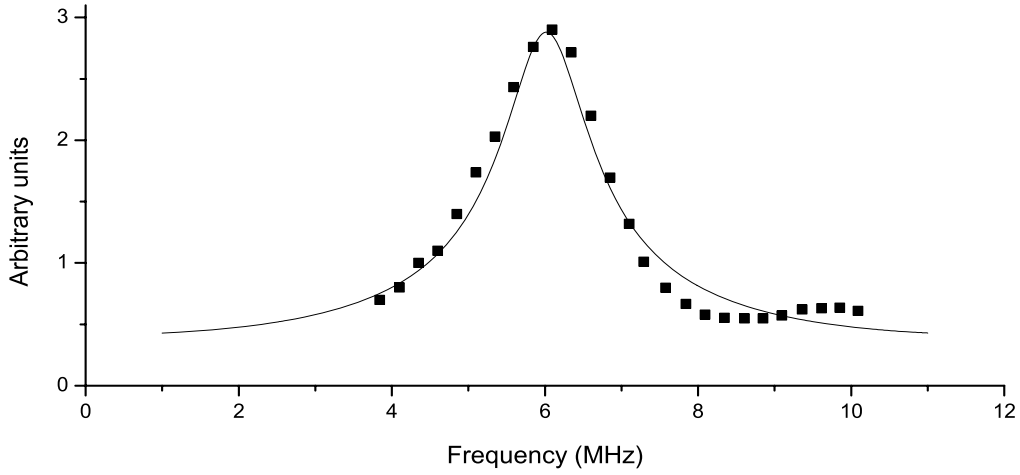

Figure 4.10. Frequency dependence of transmission coefficient for oil-impregnated λ/4 – layer. Points – experimental data. Line - theoretical resonance curve calculated from equation 4.2.4.

Also dependences of transmission factors for impregnated by oil filtration membrane attached to ferrite for two cases have been observed. The first case is attaching to "pure" ferrite. Frequency dependence of transmission coefficient for oil-impregnated λ/4 – layer attached on ferrite is shown in figure 4.11.

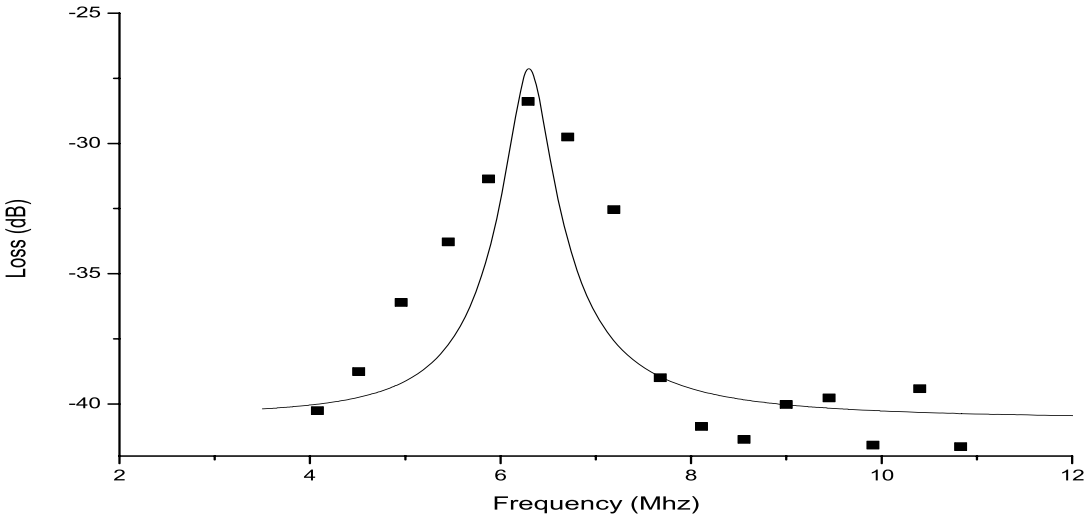

Figure 4.11. Frequency dependence of transmission coefficient λ/4 – porous layer (0.65 MRayl). Points – experimental data. Line - theoretical resonance curve calculated from equation 4.2.4.

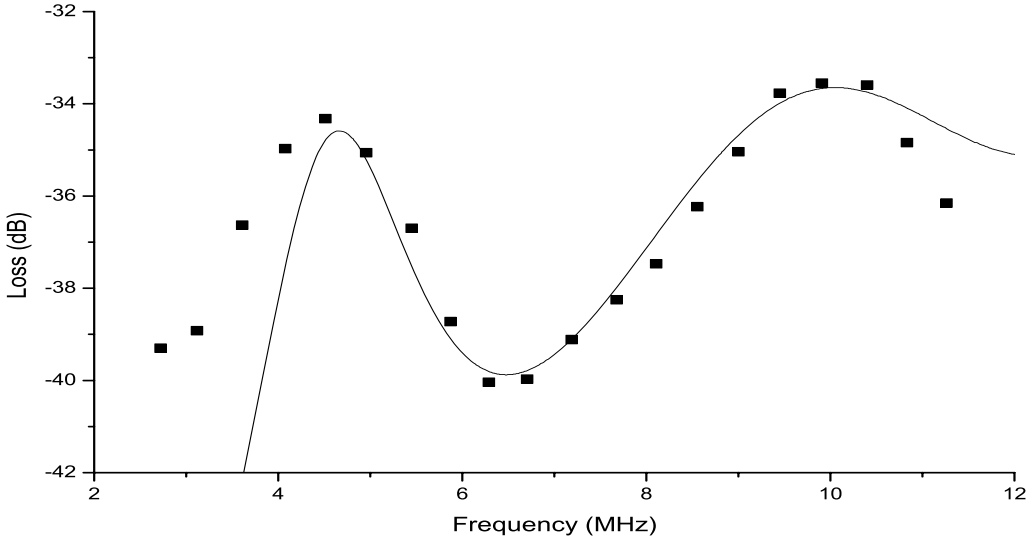

Figure 4.12. Frequency dependence of transmission coefficient: two λ/4 – layers (9 MRayl and 3 MRayl) and 10MHz transceiver. Points – experimental data. Line - theoretical curve.

Second case is attaching to the interface of the active element of conjugator witch was initially matched for water by two quarter-wave layers (adaption for f=10MHz; impedances: 9MRayl and 3MRayl). These layers have resonances at frequencies 5MHz and 10MHz. These resonances and also the resonance response of the matching layer for ferrite are shown on Fig.4.12.

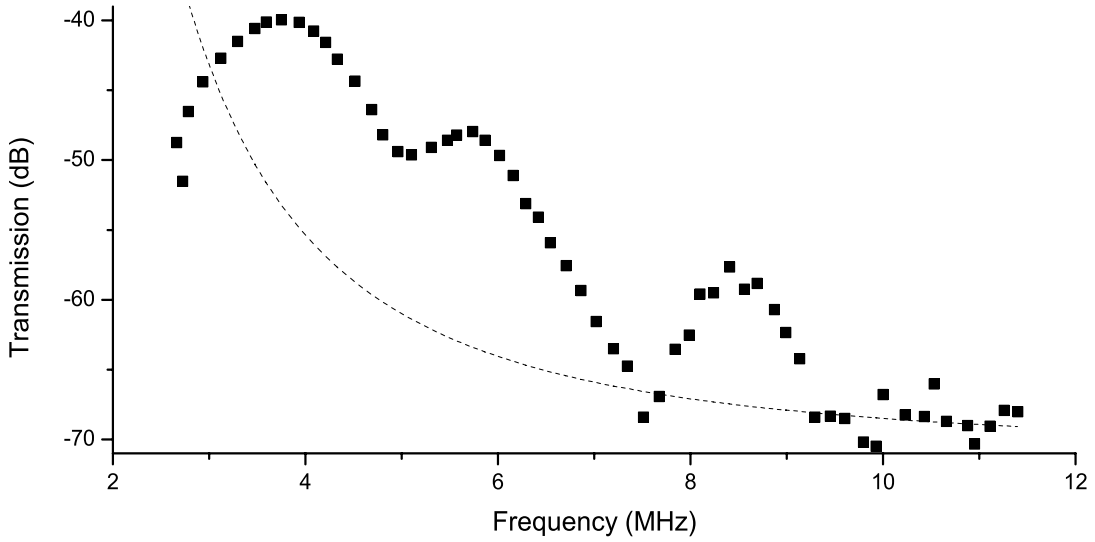

Figure 4.13. Frequency dependence of transmission coefficient for the system transducer – layer – air – layer – ferrite. Experimental data (points). Absorption in air (line).

Thus the scheme of the acoustical matching of wave phase conjugation system remained same as in paragraph 4.3 only the external layer of the matching scheme became impregnated by oil. We used the same layers for the acoustic matching of the conjugator than for the transceiver with resonance frequency 10MHz.

The frequency response of the system “transducer-matching layer-air-matching layers-conjugator” is shown on figure 4.13.

Thus the most suitable material for loading by air the system “transceiver-conjugator” on required (6-10 MHz) frequency range are porous polycorbonate membranes (VCTP04700 (Millipore)) with resonance frequency 6.3MHz impregnated by oil. As a consequence, all the experimental setup was retuned to this frequency.

Next step is to find out the way to attach the matching layer to the transducer or to the sample. The proposed procedure is to simply press the external layer to the transducer or to active element. Due to impregnations by oil, the external layer well sticks to a surface providing good acoustic contact. Matching layers so produced can be easily attached to any solid.

Conclusion

For improvements of characteristics of WPC system besides using coding by m-sequences use an acoustical matching of WPC was necessary.

For acoustical matching of the ultrasonic wave phase conjugation system several matching configurations and matching materials have been analyzed. As an external layer for the matching porous membrane filters have been chosen. For investigation of membrane filters experimental setup has been created. A wide set of different commercial filtration membranes are studied. Thus first thickness resonance λ/4 is observed.

For raising the first λ/4 resonance frequency of porous membranes up to the operational frequency of the conjugator for the first time the method of acoustical matching for low MHz range by oil impregnate filtration membranes is offered.

The chosen multilayer matching scheme of wave phase conjugation system has been realised using of the investigated materials. Acoustical matching of transducer has allowed to gain 10 dB in emitting and reception; acoustical matching of the active element of WPC system has allowed to gain 10 dB on 6.3 MHz. All the setup of phase wave conjugation was retuned to this frequency. That has allowed to gain on factor of attenuation which became 6.4 dB/mm.

Together with coding use, the acoustical matching has allowed to increase distance between the transducer and an active element of WPC system to 4 mm. It has given the chance to make experiments on velocimetry of air streams and acoustic microscopy.

Chapter 5: Examples of application of air coupled phase conjugate waves

The fifth chapter presents the examples of application of phase conjugate waves in air. In this chapter the results of application of supercritical magneto-elastic phase conjugation to imaging in C-scan acoustic air coupled microscopy are presented. Also is demonstrated that the presence of air flow in the wave propagation region leads to an uncompensated Doppler shift in the phase of a phase conjugate wave at the source, which may be used for measuring the flow velocity with the help of phase conjugation.

5.1. Experimental setup for demonstration the applications of PC waves in air

The scheme of experimental setup for demonstration the applications of PC waves in air is presented on figure 5.1. The active element of the air loaded conjugator has been fabricated from magnetostrictive ceramics and had shape of parallelepiped 40 mm long and 10×10 mm in the butt. A wideband focused ultrasonic transducer with the focal distance of 30 mm and the diameter of 10 mm was placed opposite a supercritical magneto-elastic phase conjugator (SMPC) and was used to emit an ultrasonic wave at frequency 6.3MHz. To avoid the huge absorption in air on big focal length a cylinder made from agar which acoustic characteristics are close to the water ones is used. The length of the cylinder was a little bit lower than the focal length, so that the ultrasonic beam was focused in air. The air gap between agar and the active material of the

conjugator was 2mm. For realisation of spatial scanning of objects the two-co-ordinate system of positioning controlled by computer is included in experimental setup. The transducer emitted a series of ultrasonic bursts of 4 μs duration and 6.3 MHz central frequency. They are formed by the generator (Generator 1) Tektronix AWG 2012. The phase was coded by the chosen M-sequence. The time interval between bursts was equal to 100 ms. Interfaces between agar and ferrite were covered by the matching layers described in part IIII. The ultrasonic beam passed through air got into the active element, whereupon the electromagnetic pump generated and amplified by Tektronix AWG 2012 (Generator 2) and power amplifier (Amplifier 2) at the frequency double with respect to that of a sound was applied to the element via inductance coil. After phase conjugation in the active element of conjugator ultrasonic beam returned to the transducer (figure 5.1). Impulse with duration 4 μs extracted from each conjugate signal was received by the Transducer. They arrive on an input channel of a digital oscilloscope Tektronix TDS 5052 (Oscilloscope)**.** The sequence was made up from series of these pulses and its correlation function with emitted M-sequence was defined with the help of personal computer (PC). From amplitude and phase of the correlation function we detected the changes of amplitude and phase of the conjugate wave.

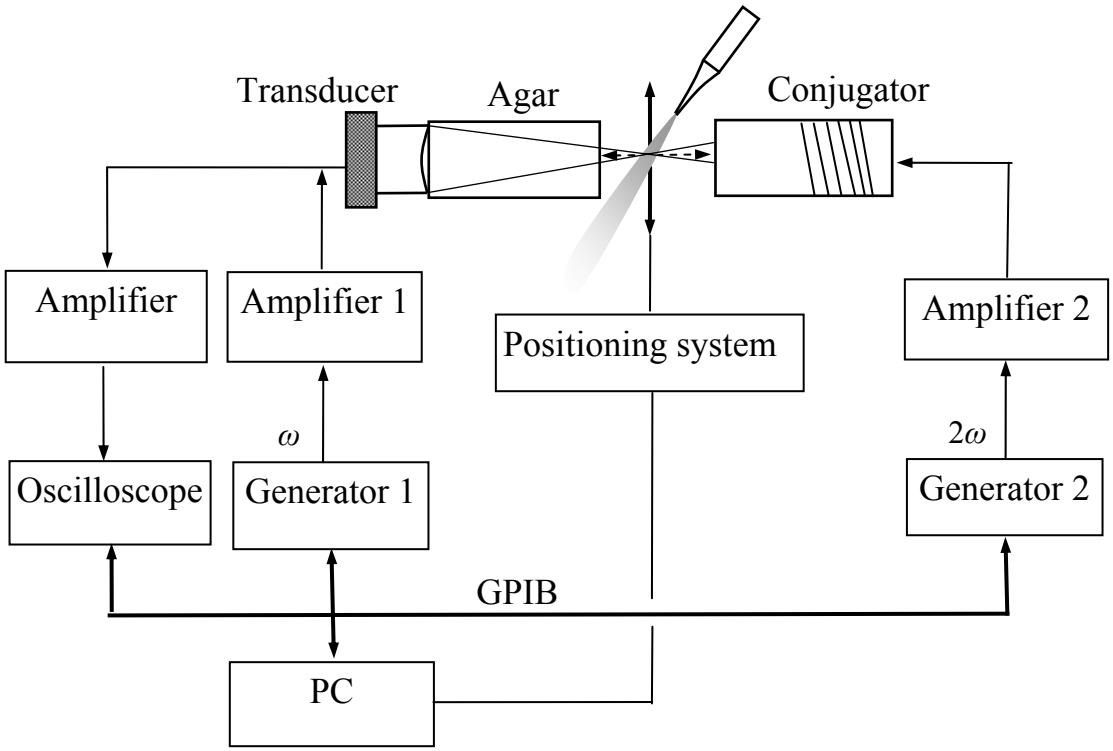

Figure 5.1. Functional scheme of the flow velocity measurement experiment.

Experiment is carried out under control of the personal computer by means of LabVIEW.

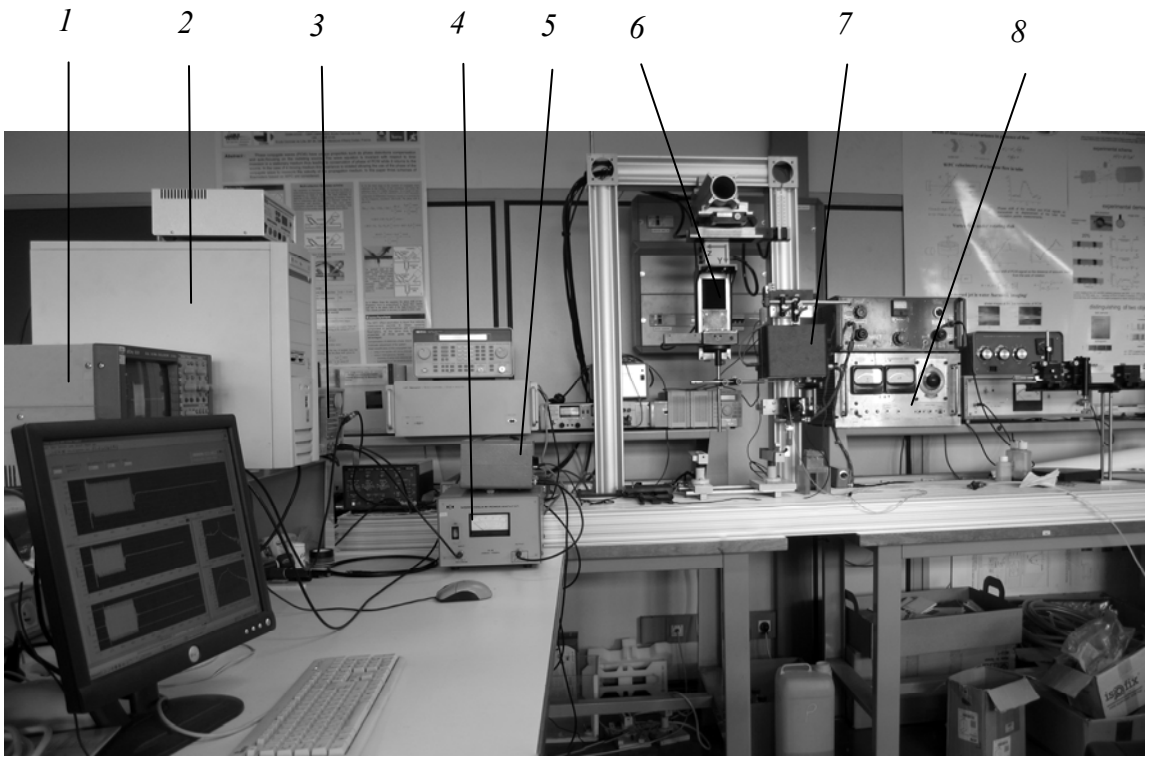

Figure. 5.2. Experimental installation : 1 – Scope; 2 – Personal Computer; 3 - Generator of initial signal; 4 – Amplifier of initial signal; 5 - Amplifier of Phase Conjugate signal; 6 - Positioning system; 7 – Conjugator; 8 – Pumping amplifier.

5.2. Air-coupled acoustic C-scan imaging (acoustic microscopy) by means of supercritical parametric wave phase conjugation.

The scheme of this experiment is presented on figure 5.1. The object to be imaged was made of two crossed thin wires of 200 microns diameter. Crossed wires (figure 5.4) have been located between transducer and conjugator. Wires have been fixed on the holder of two-co-ordinate system of positioning (figure 5.2) which moved in plane, perpendicular to direction of ultrasonic beams propagation. The sizes of scanning zone are 8×7 mm. Two-dimensional distribution of amplitudes of received conjugated signal has been registered with the resolution 80×70 points (figure 5.3). Thus, the size of a step of scanning was 100 microns.

In order to determine the resolution of the microscope the wire has been scanned in one section. From the cross-section line depicted in figure 5.5, which corresponds to one line of the image of the object, we can obtain the lateral resolution of our microscope.

The spatial resolution of obtained images is defined by the size of focal area of our ultrasonic transducer matched to air. Obtained lateral resolution is about 800 microns.

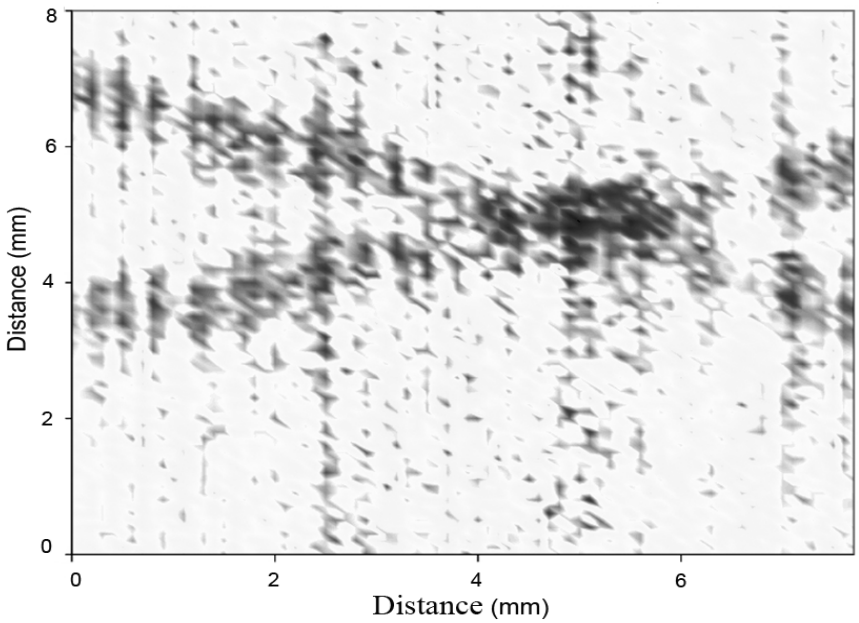

Figure 5.3. Acoustic image of crossed wires 200 microns in diameter.

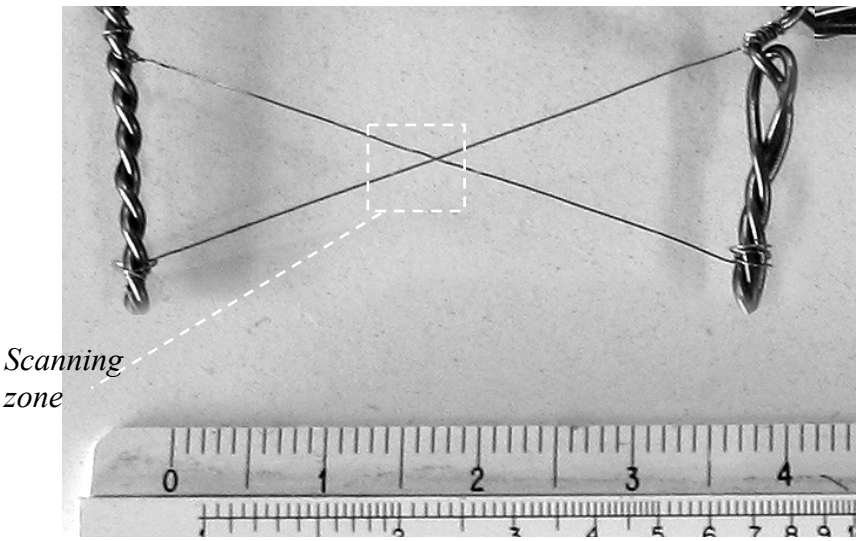

Figure 5.4. Photo of crossed wires 200 microns in diameter. Dashed line - scanning zone.

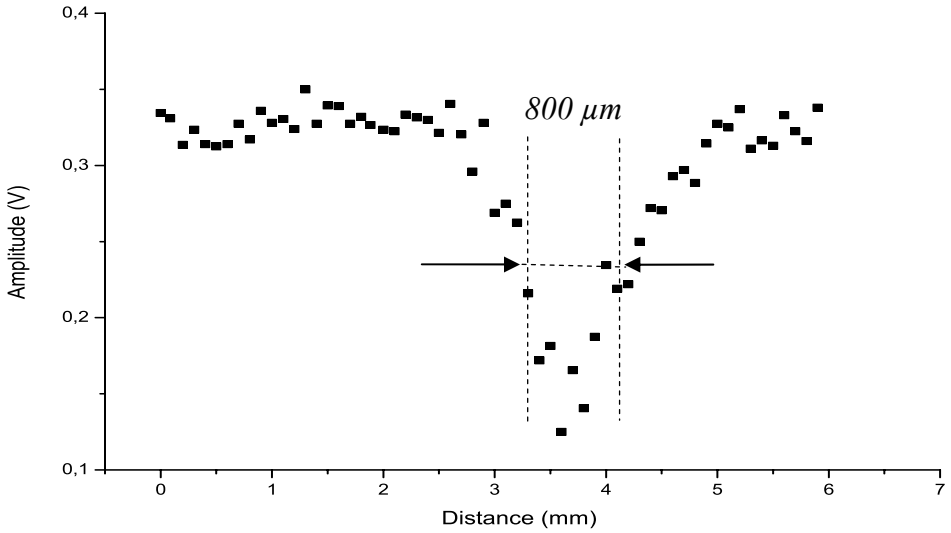

Figure 5.5. Variations of amplitudes of the signal along scanning line

Obtained lateral resolution is defined by the size of focal area of our ultrasonic transducer matched to air and was about 800 microns. We used transducer Imasonics IM-10-10-R30 with 30 mm focal length to provide a small angle of incident on ferrite. Focal area of Imasonics transducer in water is about 600 microns. To avoid the huge absorption in air on big focal length we used a cylinder made from agar with acoustic properties close to water. The thickness of agar was selected so that exit of ultrasonic wave was directly before the focal point, so that the ultrasonic beam was focused in air. Therefore the focal area of the transducer with attached cylinder made from agar became a little bit more than the focal area of Imasonics transducer in water.

5.3. Air flowmeter based on wave phase conjugation phenomena.

Medium motion violates the time invariance of an acoustic field that leads to distortions in an amplitude-phase distribution in a phase-conjugate wave with respect to the initial direct wave. In this case, in particular, the capability of a phase-conjugate wave to reconstruct independently of their propagation path, the phase of a direct wave at the radiation source is violated. As the result of wave propagation through moving regions of a medium an uncompensated phase shift is formed in a phase-conjugate wave. The value and sign of the phase shift give the information on the value and direction for the motion velocity of a medium that can be used for velocimetry and diagnostics of gas flows.

In this section is demonstrated that the presence of air flow in the propagation region leads to an uncompensated Doppler shift in the phase of a phase conjugate wave at the source, which may be used for measuring the flow velocity with the help of phase conjugation.

WPC - phenomena can also be used for detection and measuring velocity of flows. While direct wave passing through the flow with velocity v it obtains phase incursion

$$\Delta\varphi_i = k \cdot d \;/\; (1 - v / c) \; .$$

The backward PCW has the phase shift equal to

$$\Delta\varphi_c = k \cdot d \;/\; (1 + v / c)$$

As a result the phase of detected signal is equal to:

$$\Delta\varphi = \Delta\varphi_i - \Delta\varphi_c = \frac{2 \cdot k \cdot d \cdot \dfrac{v}{c}}{1 - \dfrac{v^2}{c^2}} \approx 2 \cdot k \cdot d \cdot \frac{v}{c}, \quad v \ll c$$

Thus the total phase shift is proportional to flow velocity and can be used for measuring its value and direction.

Preliminary calculation shows that sensitivity of a flowmeter is linear in the wide range of velocity and equal to 1.4 degree/(1 cm/s) when the slope of jet to the axis of confocal ultrasonic system equals 30 degrees, diameter of air flow is 4 mm, frequency of ultrasound is 6.3 MHz. Such high sensibility is due to a big ratio of flow and ultrasonic velocity. For example when flow velocity is more than 5m/s phase shift is more than 2π. It leads to difficulties to measure flow velocity when it exceeds the value of 10m/s, particularly in the case when velocity fluctuation is more than 1m/s.

To measure flow velocity exceeding 10 m/s using change of amplitude of the phase conjugate wave is proposed. Due to big difference between acoustical impedances of ferrite and air the critical angle for longitudinal wave is less than 3^0 and for shear wave is less than 6^0.

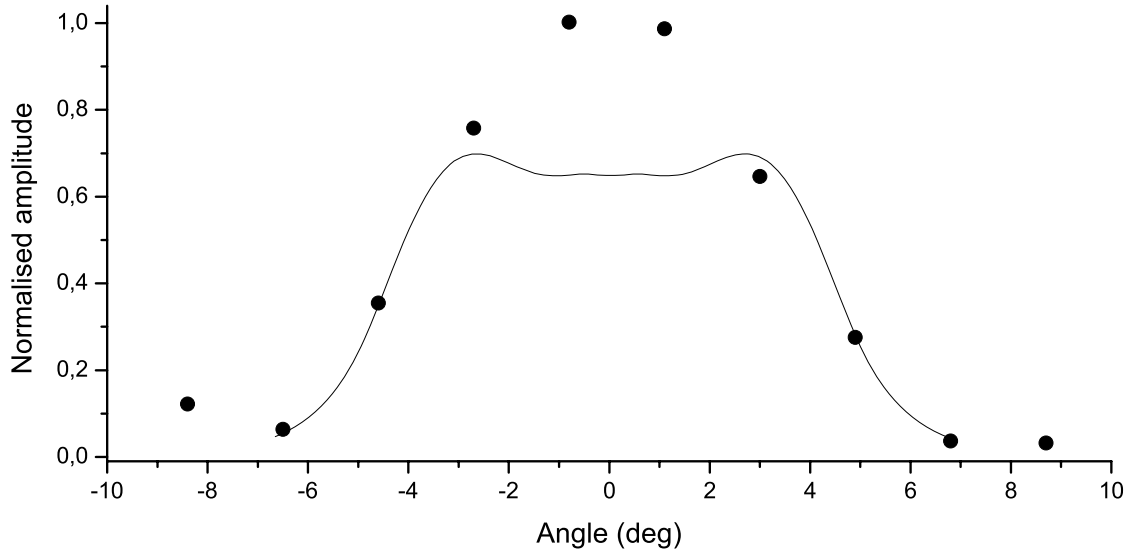

Figure 5.6 Angular dependence of WPC signal in the ultrasonic confocal system. Points – experimental data. Line - theoretical curve calculated in the frame of developed mathematical model.

Taking into account that the opening angle of confocal system in air is 4^0 one can obtain angular distribution of amplitude of phase conjugate wave in the frame of theoretical model describes in Part 3. Directivity pattern of ultrasonic phase conjugate confocal system is presented on figure 5.6.

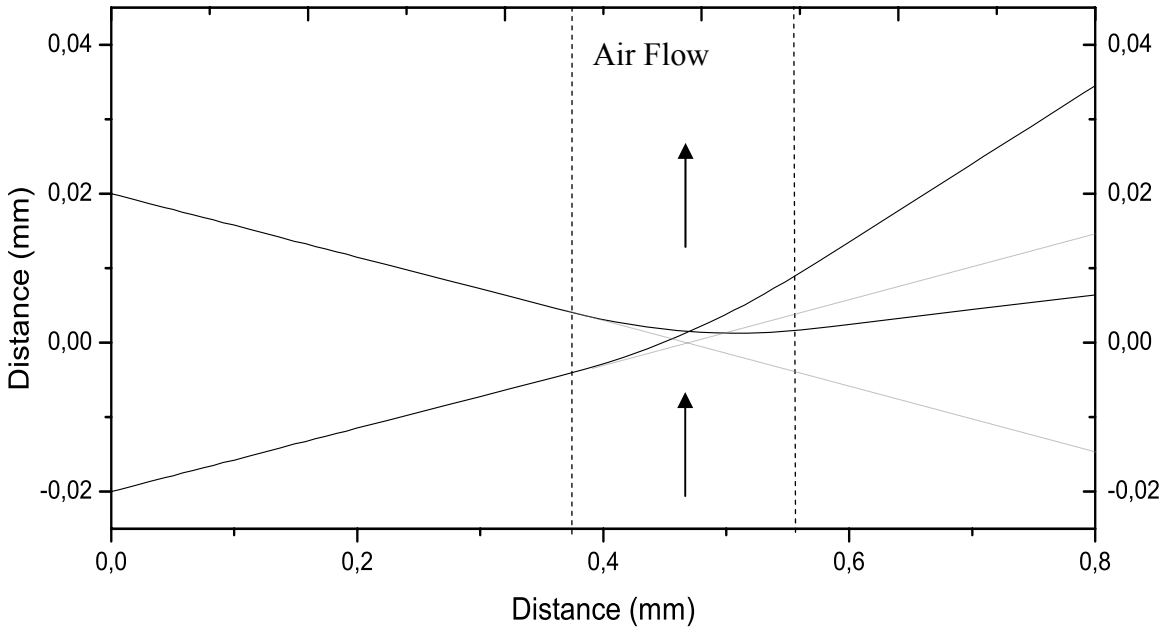

Figure 5.7 Ultrasonic ray paths in the aerial gap of confocal system at flow velocity of 25m/s. Dotted lines –ray paths without air flow. Dashed lines – boundaries of air flow.

The valley of the angular characteristics (solid line in figure 5.6) is formed because of the restrictions of applied mathematical model. Considering that the longitudinal wave in this model is perfectly plane, the phase conjugation of this wave in ferrite is negligible. But in the large the theoretical curve gives a good approximation of experimental data at least at angular width of directivity characteristics.

On the other hand relatively small air sound velocity leads to displacement of ultrasonic beam, even when flow velocity is not so high. Ultrasonic ray paths in the aerial gap of confocal system at flow velocity of 25m/s is shown in figure 5.7.

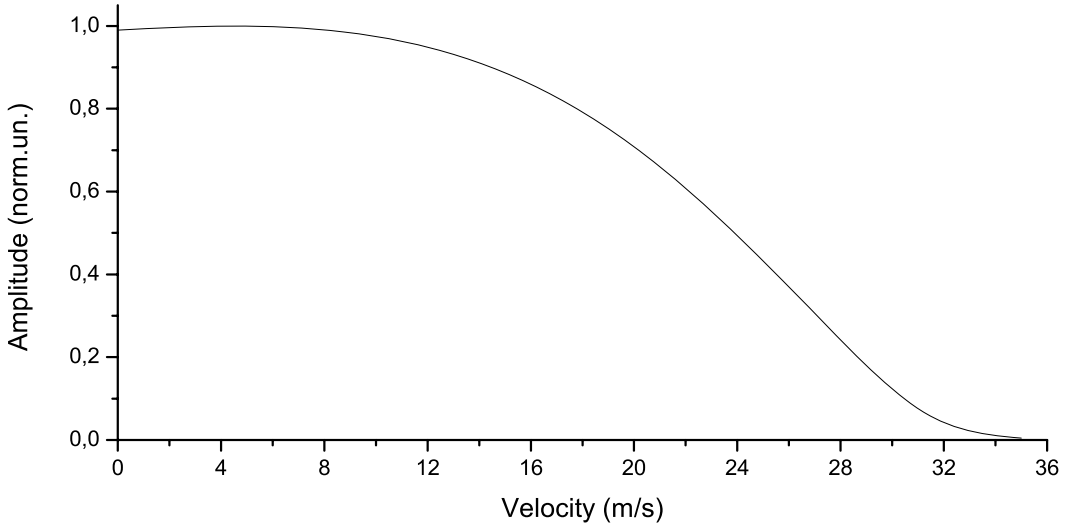

Figure 5.8 Amplitude of PCW vs velocity of aerial flow.

As results of this theoretical prediction the most part of acoustical beam exceeds critical angle at this value of flow velocity. It leads to decrease of amplitude in the whole of beam. The slope of the amplitude of PCW in the air confocal system, when flow velocity change up to 35 m/s, is shown in figure 5.8. Numerical calculations based on theoretical model described in the Part3 point to possibility of flow measurement in the range of 10-35(m/s). It is to note that in this case it is not necessary of obliquity of aerial jet relative to ultrasonic beam direction. This fact appreciably simplifies the method of measurement and the experimental setup.

Figure 5.9 show that WPC phenomena can be used for detection of velocity of air flows. In the figure are presented experimental data of changes of amplitude of conjugate wave at different velocities of air flow, and corresponding values of flow velocity calculated according the theoretical curve (figure 5.8) is shown on figure 5.10. Also it is

necessary to note that the amplitude noise level at the experiment was one order less compared to the Doppler velocimetry technique.

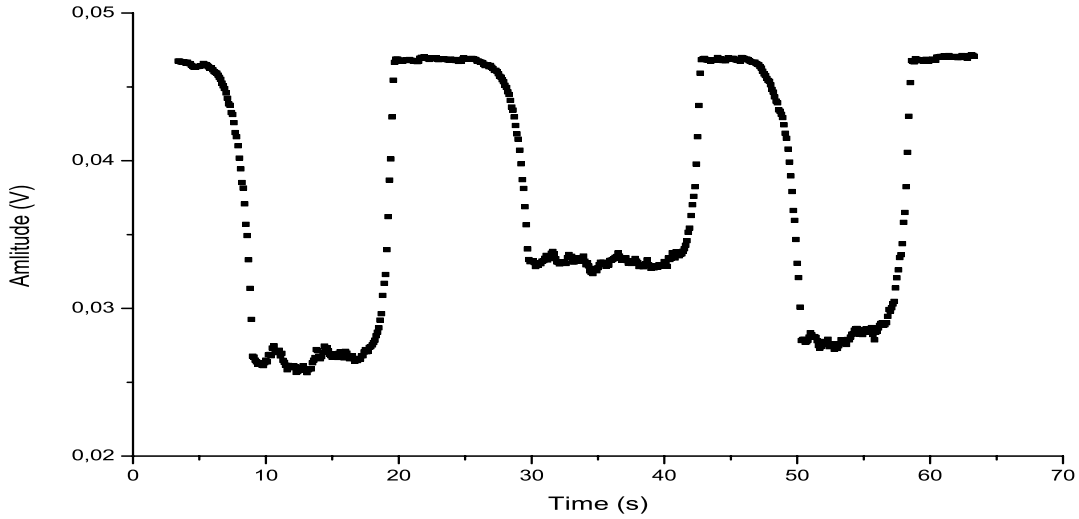

Figure 5.9. Amplitude dependence of PCW when turning on (off) of an air jet.

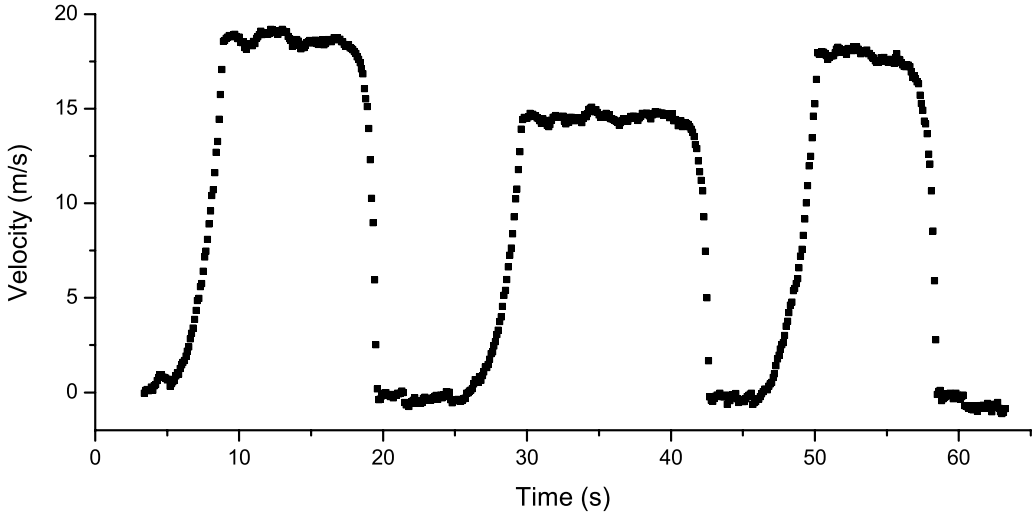

Figure 5.10. Flow velocity of PCW calculated according the theoretical curve.

5.4. Velocimetry of air flow by means of wave phase conjugation

Development of effective methods for ultrasonic phase conjugation in the megahertz frequency range stimulated interest to the use of phase conjugation processes in ultrasonic tomography and diagnostics of inhomogeneous acoustic media.

The phenomenon of phase conjugation of acoustic waves can be used for the super high sensitive detection of flow velocities in the medium of ultrasonic wave propagation.

The scheme of this experiment is presented on figure 5.1. The experiment geometry is presented in details in figure 5.11.

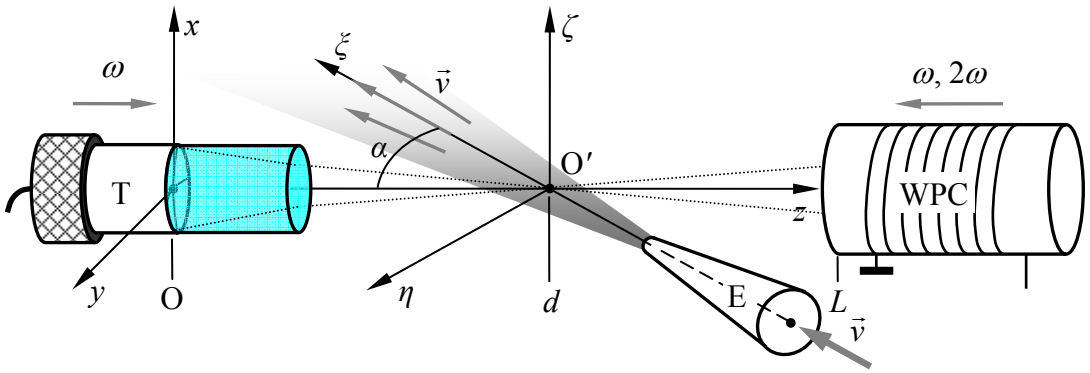

Figure 5.11. Flow mapping experiment geometry.

A nozzle 1 mm in diameter has been located between transducer and conjugator in the focal plane of the transducer as is shown on figure 5.12. Nozzle has been fixed on the holder of two-coordinate system of positioning (figure 5.2) controlled by computer which moved in planes, perpendicular to direction of ultrasonic beams propagation.

The angle of slope of a nozzle relative to the axis of ultrasonic beam propagation is $\alpha = 10\ °$. A variation of pressure in a hose in different experiments corresponds to variations of velocity from 0 to 35 m/s maximum in spatial distribution.

The sizes of scanning zone are 6×5 mm for low flow (figure 5.13) and 10×20 mm for turbulent flow (figure 5.14). Two-dimensional distribution of velocities has been registered experimentally with the resolution 12×20 points (fig. 5.13) and 20×40 (fig. 5.14) points. Thus, the size of a step of scanning has 500 microns for one axis and 200 microns for other axis for figure 5.13 and 500 microns for all axis for figure 5.14.

The acoustical image of air flow has been constructed from amplitude and phase of the correlation function (see part II) which were sensitive to changes of amplitude and phase of the conjugate wave passed through the air flow. The velocity of the flow was then derived. The distribution of velocity in the air jet calculated from phase(a) and amplitude(b) distribution of ultrasonic PCW is presented on figure 5.13 and figure 5.14. It is necessary to note that the spatial distribution of velocity in the air jet, obtained from the

amplitude distribution of PCW is in agreement with the spatial distribution obtained from measurements of velocity with the help of Dantec hot-wire anemometer.

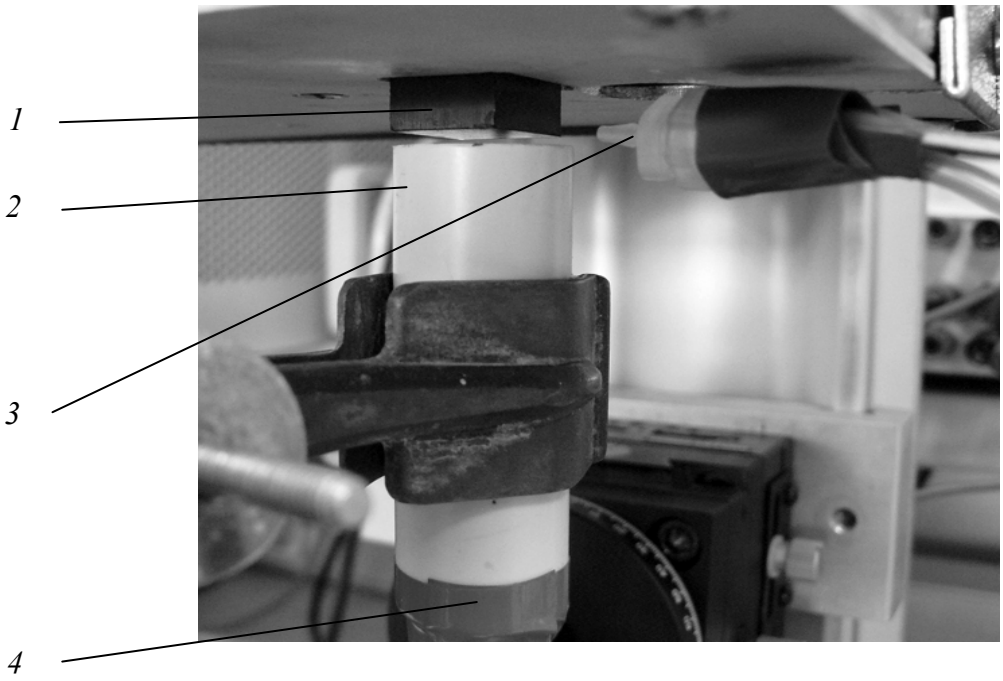

Figure 5.12. Photo of experimental installation for velocimetry of air flow. 1 – Active element of WPC system; 2 – Tube with agar; 3 – Nozzle 1mm in diameter; 4 – Transducer clinged close to agar.

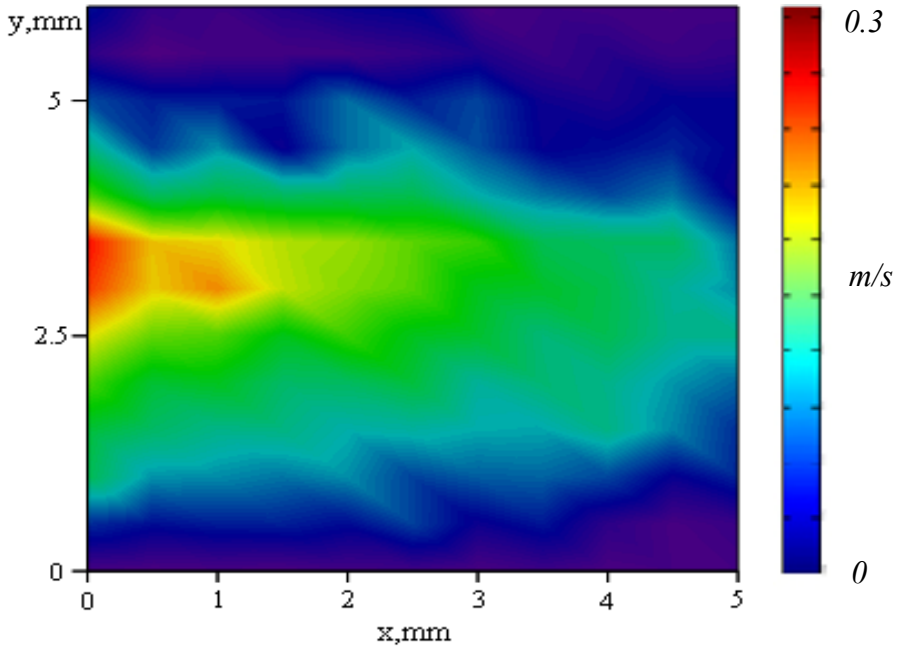

Figure 5.13. The distribution of velocities in the air jet calculated from phase distribution of ultrasonic PCW for non turbulent flow.

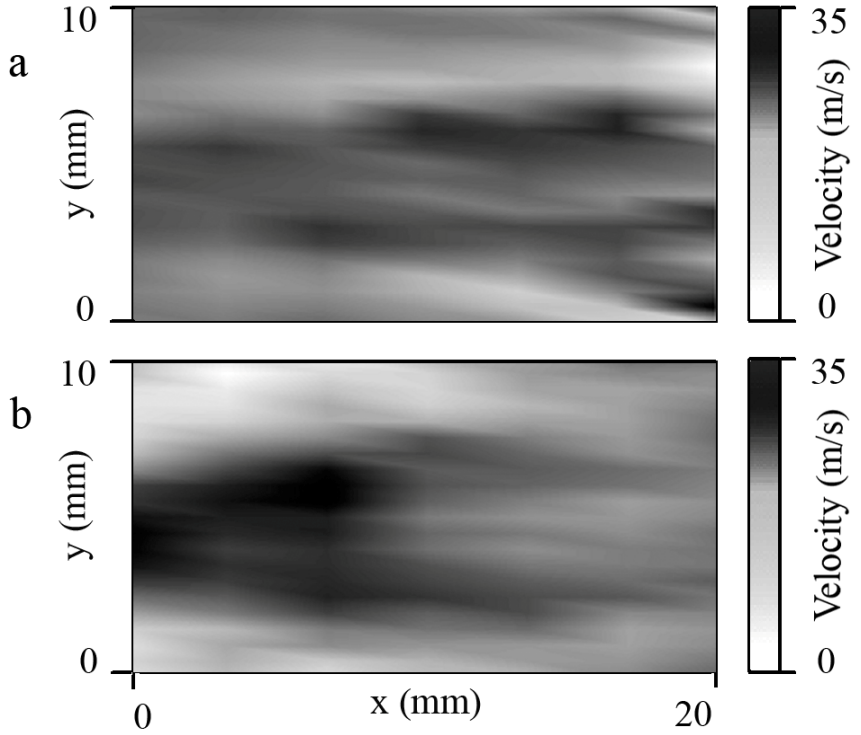

Figure 5.14. The distribution of velocity in the air jet calculated from phase(a) and amplitude(b) distribution of ultrasonic PCW for turbulent flow.

The distribution of velocities in the air jet has been numerically simulated (figure 5.15c) by a method of final elements on the basis of compressible Navier-Stokes equations in software package Comsol Multiphysics 3.2. Simulation was carried out in the same geometry of a problem and at the same values of velocities of flow that in the experiment. In the numerical modeling parabolic distribution of velocities in flow has been set.

The received velocities distribution in air jet has been imported to Mathcad package where on the basis of the model considered in chapter 3 and presented by the system of equations (3.2.5)–(3.2.7), (3.2.10)–(3.2.13) has been carried out a calculating of the phase shifts (figure 5.11b) got by phase conjugate wave passing through the air flow.

Results of simulation and experimental data of velocities distribution in air jet are presented in figure 5.15c. Results of simulation and experimental data for two cross-section of air flow stream (on distances of 5 and 8 mm from a nozzle) are shown on fig. 5.16. The cross-sections are marked by dotted lines on figure 5.15.

The general character of distribution of velocity in the air jet for two cross-section is in agreement with model of parabolic distribution of velocity.

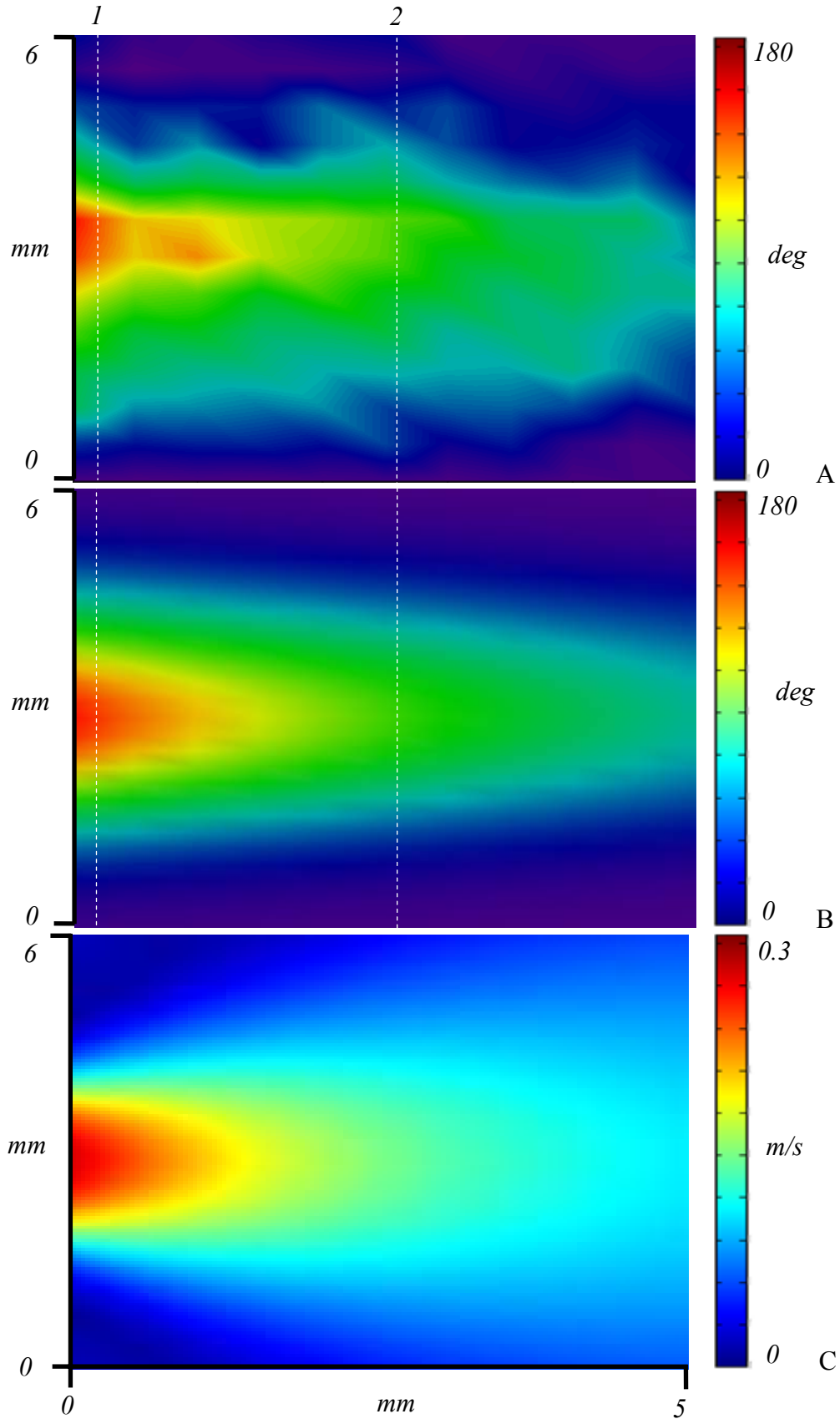

Figure 5.15. Results of simulation and experimental data of velocities distribution and phase shift in air jet. A - experimental data of phase shift of phase conjugate wave passed through air flow; B - numerical modeling of phase shift of phase conjugate wave passed through air flow; C –l numerical modeling of distribution of flow velocities.

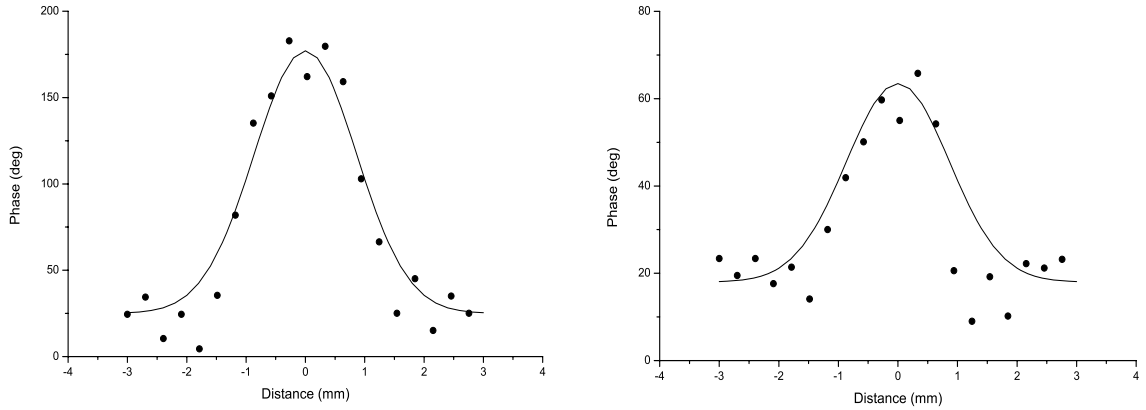

1 2

Figure 5.16. Phase shift distribution of the phase conjugate wave in cross-section of the flow received experimentally (points) and by means of numerical modeling (continuous lines): 1 — on distance about 5 mm from a nozzle (section 1 on fig. 5.15); 2 – on distance about 8 mm from a nozzle (section 2 on fig. 5.15).

Conclusion

The obtained results show the possibility of application of supercritical magneto-elastic phase conjugation to imaging in C-scan acoustic air-coupled microscopy. Obtained lateral resolution is defined by the size of focal area of our ultrasonic transducer matched to air and was about 800 microns.

Also it is shown that the WPC phenomena can be used for detection of velocity of air flows. It is shown a significant advantage of flow measurement using cross-correlation measuring techniques and phase conjugation.

Application of the phase-conjugation technique opens new opportunities in phase velocimetry and flow mapping. These opportunities are connected with the provision of automatic confocality in the case of spatial flow scanning by focused acoustic beams.

Obtained experimental sensibility of WPC air flowmeter is ~ 1 grad/m/s.

General conclusion

The goal of this thesis is to establish the novel air-coupled non-contact technique for velocimetry by means of WPC based on magnetostrictive ceramics. This study demonstrates the ability of air-coupled WPC for drawing up of new methods of ultrasonic velocimetry and microscopy. The elaborated methods expands limits of applications and can be used for design of devices of ultrasonic microscopy, tomography and velocimetry of gas microstreams, which do not require precision adjustment, providing automatic confocality of measuring schemes, and allow realizing cartography of flow. As a result of accomplishment of this work experimental setup allowing the observation of PC waves propagated in air has been created.

As the previous researches in air-coupled NDT have shown, the general problems to create the air-coupled WPC system are great differences in the impedances of the solid-state active medium (polycrystalline nickel ferrite) and gaseous medium, very high attenuation of ultrasound in air in the megahertz frequency range and very low critical angle of reflection.

For losses minimization all the experimental setup was retuned to 6.3 MHz frequency. Features of operation modes of ultrasonic wave phase conjugation system in air media have been studied in order to analyze the efficiency of WPC. Some materials with low acoustic impedance have been found, analyzed and investigated for acoustical matching reasons. To provide a small angle of incident on ferrite, transducer with long focal distance was used. To avoid the huge absorption in air on big focal length a cylinder made from agar was used. Length of cylinder made from agar was a little bit smaller than the focal distance of transducer to minimize the distance of wave propagation with high

attenuation. Also advanced technique for data processing and signals aquisition of weak signals (enhancing signal-to-noise ratio) has been created.

Main results of this investigation are:

1 In the frame of ray acoustics the base system of equations for mathematical model of phase conjugate wave passage through the interface active element of con-focal WPC system – medium of propagation is developed. This model has allowed calculating the power loss per each passage of the air–ferrite (active element of WPC) and agar–air interfaces, the intensity of ultrasonic beams with WPC, total angular dependence of transmission coefficient of ultrasound PC wave, trajectories of acoustical rays in con-focal system, phase shift of phase conjugate wave propagating in moving air media.

2 It is developed and realized the phase coding technique by pseudonoise M-sequence for registration of weak acoustical phase conjugate signals. This method has allowed to work more effectively with strong noisy and being under noise level phase conjugate signals. Also this method has allowed improving a gas flow velocimetry method.

3 It is developed and realized the technology of acoustical matching on base of thin polycorbonate porous membrane filters impregnated by oil. This technology has allowed optimising the conditions of wave transmission through the interface air–ferrite in the low megahertz frequency range.

4 On the basis of the developed model phase shift of phase conjugate wave propagating in moving air media is calculated. Experimental results of measurements of phase shift of phase conjugate wave propagating in moving air media are in agreement with results of numerical simulation.

5 Possible applications of phase conjugate waves in air are shown. It is shown that a supercritical mode of parametric WPC can be successfully used in air-coupled acoustic imaging systems. Also is shown that the WPC phenomena can be used for detection of velocity of air flows.

Bibliography

[1] B. Ya. Zel'dovich, N. F. Pilipetsky, and V. V. Shkunov, Principles of Phase Conjugation (Springer Verlag, Berlin, 1985).
[2] B. Y. Zel'dovich, V. I. Popovichev, V. V. Ragul'skii, and F. S. Faizullov, ''Connection between the wave fronts of the reflected and exciting light in stimulated Mandel'shtam-Brillouin scattering,'' Sov. Phys. JETP Lett. 15, 109–113 (1972).
[3] R. A. Fisher, Ed., Optical Phase Conjugation (Academic, New York, 1983).
[4] M. Nikoonahad and T. L. Pusateri, ''Ultrasonic phase conjugation,'' J. Appl. Phys. 66, 4512–4513 (1989).
[5] D. R. Jackson and D. R. Dowling, ''Phase conjugation in underwater acoustics,'' J. Acoust. Soc. Am. 89, 171–181 (1991).
[6] M. Fink, ''Time reversal of ultrasonic fields—Part I: Basic principles,'' IEEE Trans. Ultrason. Ferroelectr. Freq. Control 39, 555–566 (1992).
[7] Fink M., Prada C., Wu F., and Cassereau D. "Self-focusing with time reversal mirror in inhomogeneous media", Proc. IEEE Ultrason. Symp., Montreal, 1989, Vol. 2, pp 681–686.
[8] Fink M IEEE Trans. on Ultrasonics, Ferroelectrics and Frequency Control 39 555 (1996).
[9] Chakroun N., Fink M., Wu F. "Time reversal processing in ultrasonic nondestructive testing ", IEEE Trans. UFFC., 1995, Vol. 42, No. 6, pp 1087-1098.
[10] Zel'dovich B Ya et al. Dokl. Akad. Nauk SSSR 252 92 (1980) [Sov.Phys. Doklady 25 377 (1980)].
[11] Lyamshev L M, Sakov P V Akust. Zh. 34 127 (1988).
[12] Brysev A.P., Bunkin V.F., Vlasov D.V., Kazarov Yu.E. "Experimental realization of parametrical phase conjugating sound amplifier (PPCSA) on lithium niobate", Techn. Phys. Lett., 1982, Vol. 8, p. 554.
[13] F. V. Bunkin, D. V. Vlasov, and Y. E. Kravtzov, ''On wave phase conjugation of sound with amplification of the reversed wave,'' Kvant. Elektron. (Moscow) 8, 1144–1145 (1981). Translated in Sov. J. Quantum Electron. 11, 687–688 (1981).
[14] Bunkin F V, Vlasov D V, Kravtsov Yu A, in Obrashchenie Volnovogo Fronta Izlucheniya v Nelineinykh Sredakh (Optical Phase Conjugation in Nonlinear Media) (Ed. V I Bespalov) (Gor'kiy: IPF AN SSSR, 1982) pp. 63 – 90.
[15] Yariv A, Pepper DMOpt. Lett. 1 16 (1977).

[16] Brysev A P et al., in Problemy Akustiki Okeana (Problems of Ocean Acoustics) (Eds. L M Brekhovskikh, I B Andreeva) (Moscow: Nauka, 1984) p. 102.
[17] Rudenko O V, Soluyan S I Teoreticheskie Osnovy Nelineinoy Akustiki (Theoretical Foundations of Nonlinear Acoustics) (Moscow: Nauka, 1975) [Translated into English (New York: Plenum, Consultants Bureau, 1977)].
[18] Bunkin F V et al. Akust. Zh. 29 169 (1983).
[19] Kustov L M, Nazarov V E, Sutin AMAkust. Zh. 31 837 (1985).
[20] Bunkin F V et al. Pis'ma Zh. Tekh. Fiz. 7 560 (1981)
[21] Sato T, Kataoka H, Yamakoshi Y, in Problemy Nelineynoy Akustiki: Tr. XI Mezhdunar. Simp. po Nelineynoy Akustike (Problems of Nonlinear Acoustics: Proc. XIth International Symp. on Nonlinear Acoustics) Vol. 1 (Ed. V K Kedrinskiy) (Novosibirsk: GPNTB SO AN SSSR, 1987) p. 478.
[22] Bunkin F V, Vlasov D V, Kravtsov Yu A, Pis'ma Zh. Tekh. Fiz. 7 325 (1981).
[23] Andreeva N P et al. Pis'ma Zh. Tekh. Fiz. 8 104 (1982)
[24] Bunkin F V et al. Akust. Zh. 31 137 (1985)
[25] Bunkin F V, Vlasov D V Dokl. Akad. Nauk SSSR 272 839 (1983) [Sov. Phys. Doklady 28 876 (1983)].
[26] Van de Vaart H., Lyons D.H., Damon R.W. “Parametric excitation and amplification of magnetoelastic waves”, J. Appl. Phys., 1967, Vol. 36, No. 1, pp 360-374.
[27] Smolenskiy G A et al. Fizika Segnetoelektricheskikh Yavleniy (Physics of Ferroelectric Phenomena) (Leningrad: Nauka, 1985) pp. 263 – 279.
[28] Kopvillem U Kh, Prants S V Polyarizatsionnoe Ekho (Polarization Echo) (Moscow: Nauka, 1985) pp. 97 – 113.
[29] Fossheim K, Holt R M, in Physical Acoustics: Principles and Methods Vol. 16 (Eds W P Mason, R N Thurston) (New York: Academic Press, 1982) p. 221.
[30] L. O. Svaasand, ‘‘Interaction between elastic surface waves in piezoelectric materials,’’ Appl. Phys. Lett. 15, 300–302 (1969).
[31] Thomson R.B., Quate C.F. “Nonlinear interaction of microwave electric fields and sound in LiNbO3”, J. Appl. Phys., 1971, Vol. 42, No. 3, pp 907-919.
[32] A. P. Brysev, F. V. Bunkin, D. V. Vlasov, and Yu. E. Kazarov, Sov. Phys. Tech. Lett. 8, 237 (1982).
[33] V. I. Reshetzky, ‘‘Phase conjugate reflection and amplification of a bulk acoustic wave in piezoelectric cryatals,’’ J. Phys. C 17, 5887–5891 (1984).
[34] M. Ohno, ‘‘Generation of acoustic phase conjugate waves using nonlinear electroacoustic interaction in LiNbO3 ,’’ Appl. Phys. Lett. 54, 1979–1980 (1989).
[35] N. S. Shiren, R. L. Melcher, and T. G. Kazyaka, ‘‘Multiple-quantum phase conjugation in microwave acoustics,’’ IEEE J. Quantum Electron QE-22, 1457–1460 (1986).
[36] M. Ohno and K. Takagi, ‘‘Acoustic phase conjugation in highly nonlinear PZT piezoelectric ceramics,’’ Appl. Phys. Lett. 64, 1620–1622 (1993).
[37] M. Ohno and K. Takagi, ‘‘Enhancement of the acoustic phase conjugate reflectivity in nonlinear piezoelectric ceramics by applying static electric or static stress fields,’’ Appl. Phys. Lett. 69, 3483–3485 (1996).
[38] Andreeva I.N. et al. Electronical Technics, 1983, Vol. 179, No. 7. (in Russian).
[39] Belov K.P. et al. “Giant Magnetostriction”. Phys.-Uspekhi, 1983, Vol. 140, p 271. [Sov. Phys. Usp. 26 518 (1983)].
[40] Clark A E, in Ferromagnetic Materials (Handbook of Magnetic Materials, Ed. E P Wohlfarth) (Amsterdam: North-Holland, 1990) p. 531.
[41] Savage H.T., Adler C.J. “Magnetoelastic bifurcation in an amorphous ribbon”, JMMM, 1986, Vol. 58, p. 320.

[42] A. P. Brysev, F. V. Bunkin, D. V. Vlasov, L. M. Krutianskii, V. L. Preobrazhenskii, and A. D. Stakhovskii, ‘‘Parametric phase conjugation of an ultrasonic wave in a ferrite,’’ Sov. Phys. Acoust. 34, 642–643 (1989).
[43] A. P. Brysev, F. V. Bunkin, D. V. Vlasov, A. D. Stakhovsky, V. N. Streltsov, L. M. Krutiansky, V. L. Preobrazhensky, Yu. V. Pyl’nov, and E. A. Ekonomov, ‘‘Some recent findings on acoustic phase conjugation in parametric media,’’ Opt. Acoust. Rev. 1, 107–120 (1989).
[44] L. M. Krutiansky, V. L. Preobrazhensky, Yu. V. Pyl’nov, A. P. Brysev, F. V. Bunkin, and A. D. Stakhovsky, ‘‘Observation of ultrasonic waves in liquid under overthreshold parametric phase conjugation in ferrite,’’ Phys. Lett. A 164, 196–200 (1992).
[45] Krasilnikov V.A., Mamatova T.A., Prokoshev V.G. “Parametrical amplification while wave phase conjugation of magnetoelastic wave in haematite”, Sol. State Phys., 1986, Vol. 28, p. 615. (in Russian).
[46] Evtikhiev N N et al. Vopr. Radioelektron., Ser. Obshchetekh. 2 124 (1978).
[47] Lebedev A Yu, Ozhogin V I, Yakubovskiy A Yu Pis'ma Zh. Eksp. Teor. Fiz. 34 22 (1981) [JETP Lett. 34 19 (1981)].
[48] Ozhogin V.I. and Preobrazhenskii V.L., “Effective anharmonicity of the elastic subsystem of antiferromagnets”, JETP Lett., V. 46(3), pp. 523-529, 1977.
[49] A. P. Brysev, F. V. Bunkin, D. V. Vlasov, L. M. Krutyansky, V. L. Preobrazhensky, A. D. Stakhovsky. “Regenerative amplification mode of acoustic waves and phase conjugation in ferrite”, Acoust. Phys., 1988, Vol. 34, No. 6, pp 986-990.
[50] Yu. V. Pyl’nov, P. Pernod, and V. L. Preobrazhenskii, Detection of Moving Objects and Flows in Liquids by Ultrasonic Phase Conjugation, Acoustical Physics, Vol. 51, No. 1, 2005, pp. 105–109.
[51] Pyl'nov Yu.V., Pernod Ph., Preobrazhensky V.L. “Low Frequency Emission by Nonlinear Interaction of Phase Conjugate Ultrasound Waves”, Acta Acustica united with Acustica, 2003, Vol. 89, No. 6, pp 942-947.
[52] Pylnov Yu., Pernod P., Preobrazhensky V. “Low frequency emission by means of nonlinear interaction of phase conjugate ultrasound waves in water”, IEEE Ultras. Symp., 2001, Vol. 1, pp 397-399.
[53] Pyl’nov Yu., Pernod P., Preobrazhensky V., “Acoustic imaging by second harmonic of phase-conjugate wave in inhomogeneous medium”, Appl. Phys. Letts., V. 78(4), pp. 553-555, 2001.
[54] Krutyansky L., Pernod P., Brysev A., Bunkin F.V., Preobrazhensky V. “Supercritical parametric wave phase conjugation as an instrument for narrowband analysis in ultrasonic harmonic imaging”, IEEE Trans. UFFC., V. 49(4), pp. 409-414 2002.
[55] Ohno M Jpn. J. Appl. Phys. 29 Suppl. 29-1 299 (1990).
[56] Yamamoto K et al., in Proc. World Congress on Ultrasonics (Ed. K Takagi) (Yokohama: University of Tokyo, 1997) p. 1 LP1.
[57] F. Wu, J.-L. Thomas et M. Fink. "Time reversal of ultrasonic fields- Part II : Experimental results". IEEE Trans. Ultrason. Ferroel. Freq. Control 39, pp 567-578, 1992.
[58] Tanter M. “Application du retournement temporel à l'hyperthermie ultrasonore de cerveau”, Thèse de doctorat de l'université Paris 7. – 1999.
[59] Pyl'nov Yu, Preobrazhensky V, “Principles of Ultrasonic Velocimerty by Means of Nonlinear Interaction of Phase Conjugate Waves” in Proc. of the IEEE Ultrasonics Symp., Montreal, 2004 Vol. 3, p. 1612.
[60] Roux P., Fink M. “Experimental evidence in acoustics of the violation of time reversal invariance induced by vorticity”, Europhys. Lett. – 1995. – Vol. 32. – P. 25-29.

[61] J. Appel, A. Brutre, F. Dunand and E. Haziza, IEEE Trans. Instrurn. Meas. 28 (1979) 263.
[62] F.I. Brand, The Acoustic Method for the Measurement of Flow Velocities, Voith Forschung and Konstruktion (21) Paper 6, Reprint 2120, 1987.
[63] C.A. Watson, in: Flow Measurement of Liquids, eds. H.H. Dijstelbergen and E.A. Spencer (North-Holland, Amsterdam, 1978) p. 571.
[64] V.K. Hamidullin, Ultrasonic Control and Measurement Equipments and Systems, ISBN 5-288 00208-8 (University of Leningrad, 1989) [in Russian].
[65] G.N. Bobrovnikov, B.M. Novozilov and V.G. Serafanov, Non-contact Flow-Meters (Mashinostroenie, Moscow, 1985).
[66] Takeda, Y., Velocity Profile Measurement by Ultrasound Doppler Shift Method, Int. J. Heat Fluid Flow 7(4) 313-318, 1986.
[67] Y. Takeda, ‘‘Velocity profile measurement by ultrasonic Doppler method,’’ Exp. Therm. Fluid Sci., 10, 444–453 (1995).
[68] IEEE Trans. Acoust. Speech, Signal Processing, Special Issue on Time Delay Estimation, vol. ASSP-29, June 1981.
[69] W. Siebert, “A radar detection philosophy,” IRE Trans. Inform. Theory, vol. IT-2, no. 3, pp. 204-221, 1956.
[70] J. Coulthard, “Cross-correlation flow measurement-A history and state of the art,” Measurement and Contr. , vol. 16, pp. 214-218, June 1983.
[71] H. J. McSkimin, “Pulse superposition method for measuring ultrasonic wave velocities in solids,” J. Acoust. Soc. Amer., vol. 33, no. 1, pp. 12-16, Jan. 1961.
[72] E. P. Papadakis, “Ultrasonic attenuation and velocity in three transformation products in steel,” J. Appl. Phys., vol. 35, no. 5, pp. 1474-1482, May 1964.
[73] J. Coulthard, “Ultrasonic cross-correlation flowmeters,” Ultrason., vol. 11, no. 2, pp. 83-88, Mar. 1973.
[74] K. H. Ong and M. S. Beck, ‘‘Slurry flow velocity, concentration, and particle size measurement using flow noise and correlation techniques,” Meas. and Contr., vol. 8, pp. 453461, Nov. 1975.
[75] J. S. Tornberg, M. Karras, E. M. Hrknen, and 0. Hirsimki, “Analysis of ultrasonic correlation flowmeters for pulp suspension,” IEEE Trans. Sonics Ultrason., vol. SU-30, pp. 264-269, July 1983.
[76] B. Castagnede, J. Roux, and B. Hosten, “Correlation method for normal mode tracking in anisotropic media using an ultrasonic immersion system,” Ultruson., vol. 27,- pp. 280-287, Sept. 1989.
[77] E. S. Furgason, V. L. Newhouse, N. M. Bilgutay, and G. R. Cooper, “Application of random signal correlation techniques to ultrasonic flaw detection,” Ultrason., vol. 13, no. 1, pp. 11-17, Jan. 1975.
[78] B. B. Lee and E. S. Furgason, “An evaluation of ultrasound NDE correlation flaw detection systems,” IEEE Trans. Sonics Ultrason., vol. SU-29, pp. 359-369, NOV. 1982
[79] Coulthard J. Ultrasonic cross-correlation flowmeters. Ultrasonics 1973; 11:83–8.
[80] Beck MS, Plaskowski A. Cross correlation flowmeters: Their design and application. Institute of Physics Publishing; 1987.
[81] M. Bassini, D. Dotti, E. Gatti, P. L. Pizzolati, and V. Svelto, “An ultrasonic noninvasive blood flowmeter based on cross-correlation techniques,’’ Ultrason. Int. Proc., pp. 273-278, 1979.
[82] A. P. Brysev, L. M. Krutyansky, P. Pernod, and V. L. Preobrazhensky. "Nonlinear Ultrasonic Phase-Conjugate Beams and Their Application in Ultrasonic Imaging", Acoustical Physics, Vol. 50, No. 6, 2004, pp. 623–640. [Translated from Akusticheskiy Zhurnal, Vol. 50, No. 6, 2004, pp. 725–743].

[83] Pyl'nov Yu., Preobrazhensky V., Pernod Ph. and Smagin N. "Flow Velocity Measurements by Means of Nonlinear Interaction of Phase Conjugate Ultrasonic Waves", Proc. of IEEE Int. UFFC Conference, 2005, Rotterdam, Holland, pp. 1612-1615.
[84] Blitz, Jack; G. Simpson (1991). Ultrasonic Methods of Non-Destructive Testing. Springer-Verlag New York, LLC.
[85] Lüscher, Edgar. "Photoacoustic Effect in Condensed Matter—Historical Development" in Lüscher, Edgar, et al., eds. Photoacoustic Effect: Principles and Applications. Braunschweig: Friedr. Vieweg & Sohn, 1984. p. 1.
[86]. Rosencwaig, Allan. Photoacoustics and Photoacoustic Spectroscopy. New York: John Wiley & Sons, 1980. p. 12.
[87] H.M. Frost, "Electromagnetic ultrasonic transducers: Principles, Practice and Applications", in Physical Acoustics, Vol.XIV, W.P. Mason and R.N. Thurston (Eds.), Academic Press, New York, 179-276 (1979).
[88] M Hirao and H Ogi, "An SH-wave EMAT technique for gas pipeline inspection", NDT&E International 32 (1999) 127-132.
[89] Gori, M., Giamboni, S., D'Alessio, E., Ghia, S., and Cernuschi, F., "EMAT transducers and thickness characterization on aged boiler tubes," Ultrasonics, Vol. 34 , pp 311-314, 1996.
[90] Udpa, L., Mandayam, S., Udpa, S., Sun, Y., and Lord, W., "Developments in gas pipeline inspection", Materials Evaluation, pp. 467-472, April, 1996.
[91] R.M. White, Generation of elastic waves by transient surface heating, J. Appl. Phys. 34 (1963) 3559–3567.
[92] C.B. Scruby, R.J. Dewhurst, D.A. Hutchings, S.B. Palmer, Quantitative studies of thermally generated elastic waves in laser-irradiated metals, J. Appl. Phys. 51 (1980) 6210–6216.
[93] D.A. Hutchins, Ultrasonic generation by pulsed lasers, Phys. Acoust. 18 (1988) 21–23.
[94] R.D. Huber, R.E. Green Jr., Noncontact acousto-ultrasonics using laser generation and laser interferometric detection, Mater. Evaluat. 49 (1991) 613–618.
[95] F. Lanza di Scalea, R.E. Green Jr., Experimental observation of the intrusive effect of a contact transducer on ultrasound propagation, Ultrasonics 37 (1999) 179–183.
[96] B. Audoin, Non-destructive evaluation of composite materials with ultrasonic waves generated and detected by lasers, Ultrasonics 40 (2002) 735–740.
[97] Kessler, L.W., "Acoustic Microscopy", Metals Handbook, Vol. 17 - Nondestructive Evaluation and Quality Control, ASM International, 1989, pp. 465–482.
[98] T. Gudra, Z. Kojro, M. Schmachtl, C. Lier, M. Schubert, W.Grill, Ultrasonics 34 (1996) 711.
[99] Z. Kojro, T.J. Kim, G. Lippold, T. Gudra, W. Grill, Ultrasonics 35 (1998) 563.
[100] T.J. Kim, Z. Kojro, M. Pluta, M. Schmachtl, M. Schubert, T. Gudra, W. Grill., Confocal scanning acoustic microscopy in air at normal conditions at frequencies close to the phonon cut-off regime, Physica B 263-264 (1999) 588-594
[101] D. A. Hutchins and D. W. Schindel, "Advances in non-contact and air-coupled transducers," in Proc. IEEE Ultrason. Symp., 1994, pp. 1245–1254.
[102] W. A. Grandia and C. M. Fortunko, "NDE applications of aircoupled ultrasonic transducers," in Proc. IEEE Ultrason. Symp., 1995, pp. 697–709.
[103] D. A. Hutchins, D. W. Schindel, A. G. Bashford, and W. M. D. Wright, "Advances in ultrasonic electrostatic transduction," Ultrasonics, vol. 36, pp. 1–6, 1998.
[104] T. E. Gomez, "A non-destructive integrity test for membrane filters based on air-coupled ultrasonic spectroscopy," IEEE Trans. Ultrason., Ferroelect., Freq. Contr., vol. 50, no. 6, pp. 676–685, 2003.

[105] R. Stoessel, N. Krohn, K. Pfleiderer, and G. Busse, “Air-coupled ultrasound inspection of various metals,” Ultrasonics, vol. 40, pp. 159–163, 2002.
[106] E. Blomme, D. Bulcaen, and F. Declercq, “Recent observations with air-coupled NDE in the frequency range of 650 kHz to 1.2 MHz,” Ultrasonics, vol. 40, pp. 153–157, 2002.
[107] E. Blomme, D. Bulcaen, and F. Declercq, “Air-coupled ultrasonic NDE: Experiments in the frequency range 750 kHz– 2 MHz,” NDT& E Int., vol. 35, pp. 417–426, 2002.
[108] M. Castaings, P. Cawley, R. Farlow, and G. Hayward “Single Sided Inspection of Composite Materials Using Air Coupled Ultrasound”, Journal of Non Destructive Evaluation, vol. 17(2), p. 37-45, 1998.
[109] R. Hickling and S.P. Marin, “The use of ultrasonics for gauging and proximity sensing in air“, JASA 79(4), April 1986, pp, 1151-1159.
[110] H.E. Bass, L.C. Sunderland, Joe Percy, and Landan Evans, ”Absorption of Sound in the Atmosphere”, in Phys. Acoust. Vol. XVII, W.P. Masan ed. (Academic Press, New York, 1984) pp. 145-232.
[111] E.H. Brown and S.F. Clifford, “On the Attenuation of Sound by Turbulence”, JASA 60(4), 1976, pp. 788-794.
[112] H.J. Bass, L.C. Sutherland, and A.J Zuckerwar, “Atmospheric Absorption of Sound: Update,” JASA88 (8), 1990, pp. 2019-2021.
[113] H.E. Bass, L.C. Sutherland, and A.J. Zuckerwar, “Atmospheric Absorption of Sound Further Developments”, JASA 97(l) 1995, pp.680-683.
[114] L.J. Bond, C-H. Chiang. and C.M. Fortunko, “Absorption of Ultrasonic Waves in Air at High Frequencies (10-20 MHz)”, JASA 92(4), 1992, pp. 2006-2015.
[115] J. Sdlard, “Ultrasonic Testing, Non-conventional Testing Techniques” (Wiley, New York,1 982) pp. 400-402.
[116] Castaings, M. and Hosten, B., “The use of Electrostatic, Ultrasonic, Air-coupled Transducers to Generate and Receive Lamb Waves in Anisotropic, Viscoelastic Plates,” Ultrasonics, v. 36, pp. 361-365 (1998).
[117] J. Loschberger and V. Magori, "Ultrasonic robotic sensor with lateral resolution", Proc. 1987 IEEE Ultrason. Symp.
[118] M.K. Brown, "Controlling a robot with sonic and ultrasonic means", Proc. 1987 IEEE Ultrason. Symp., 553- 561, (1987).
[119] H. Carr and C. Wykes, "Diagnostic measurements in capacitance transducers", Ultrasonics 31, 13-20, (1993).
[120] D.W. Schindel, D.A. Hutchins, L. Zou and M. Sayer, "Capacitance Devices for the Generation of Air-Borne Ultrasonic Fields", Proc. 1992 IEEE Ultrason. Symp., Tucson, 843-846, (1992).
[121] D.W. Schindel, D.A. Hutchins, L. Zou and M. Sayer, "The design and characterization of micromachined air-coupled capacitance transducers", IEEE Trans. Ultrason. Ferroelec. Freq. Contr., in press.
[122] Schindel, D.W., Hutchins, D.A., Zou, L., and Sayer, M., "The Design and Characterisation of Micromachined Air-Coupled Capacitance Transducers," IEEE Trans. Ultrason. Ferroelect. Freq. Control., v. 42, pp. 42-51 (1995).
[123] Ladabaum, I., Khuri-Yakub, B.T., and Spoliansky, D., "Micomachined Ultrasonic Transducers (MUTS): 11.4MHz Transmission in Air and More," App. Phys. Lett., v. 68, pp. 7-9 (1996).
[124] D.S. Dean, “Towards an Air Sonar”, Ultrasonics, Jan. 1968, pp. 29-38
[125] V. Magori, “Ultrasonic Senson in Air”in, Proc. 1994 Ultrasonics Symp., B.R. McAvoy ed. (IEEE,NewYork, 1994)pp.471-481.

[126] L.C. Lynnworh, “Ultrasonic Impedance Matching from Solids to Gases”, IEEE Trans. Sonics and Ultrasonics, SU-12(2), June 1965, pp. 37-48
[127] F. Massa “Ultrasonic Tranrducen for Use in Air” IEEE Proc. 53(10) Oct. 1965,pp.1363-1371.
[128] W. Kuhl, G.R. Schmdder, and F.-K. Schroeder, “Condenser Transmitters and Microphones with Solid Dielectric for Airborne Transducers” Acustica 4(5), Apr. 1954, pp. 519-532.
[129] W.W. Wright, “High Frequency Electrostatic Transducers for use in Air” , IRE National Conv Rec. 10(6), 1962, pp. 95-100.
[130] W.M. Wright, D.W. Schindel, D.A. Hutchins, P.W. Carpenter, D.P. Jansen, Ultrasonic tomographic imaging of temperature and flow fields in gases using air-coupled capacitance transducers, J. Acoust. Soc. Am. 104 (1998) 3446.
[131] B.T. Khuri-Yakub, J.H.Kim, C-H. Chou, P. Parent, and G .S. Kino, “A New Design for Air Transducers”, in Proc. 1988 Ultrasonics.
[132] D. Reilly and G. Hayward, "Through air transmission for ultrasonic non-destructive testing", Proc. I991 IEEE Ultrason. Symp., Florida, 763-766, (1991).
[133] M.I. Haller and B.T. Khuri-Yakub, "1-3 composites for ultrasonic air transducers", Proc. I992 IEEE Ultrason.
[134] W. Manthey, N. Kroemer and V. MBgori, "Ultrasonic transducers and transducer arrays for applications in air", Meas. Sci. Techn. 3, 249-261, (1992).
[135] V.I. Zddyukovskii and G.T. Kartsev“, Use of Piezoelectric Transducers for Cantactless Ultrasonic Product Inspection”, Defektoskopiya (Sov. J. NDT) 3, Mar. 1978, pp. 28-34.
[136] W.A. Grandia, “Advances in Nondestructive Testing - Noncontact Ultrasonic Inspection of Composites”, in Proc.39th International SAMPE Symp., Vol. 39, Book I, K. Drake, J.Bauer, T. Serafini, and P.Cheng eds., 1994,pp. 1308-1315.
[137] M. Deka, “Air-coupled Ultrasonic Transducer for NDE, in 1987 Ullrasonics Symp. Pm., B.R. McAvoy ed. (IEEE, New York, 1987) pp. 543-546.
[138] Brunk, J.A., Valenza, C.J., and Bhardwaj, M.C., "Applications and Advantages of Dry Coupling Ultrasonic Transducers for Materials Characterization and Inspection," in Acousto-Ultrasonics, Theory and Applications, John C. Duke, Jr., Editor, Plenum Press, New York (1988), pp. 231-238.
[139] Bhardwaj, M.C. and Bhalla, A., "Ultrasonic Characterization of Ceramic Superconductors," J. Mat. Sci. Lett., v. 10 (1991).
[140] Kulkarni, N., Moudgil, B. and Bhardwaj, M., "Ultrasonic Characterization of Green and Sintered Ceramics: I, Time Domain," Am. Cer. Soc., Cer. Bull, Vol. 73, No. 6, (1994).
[141] O. Krauss, R. Gerlach, and J. Fricke, “Experimental and theoretical investigations of SiO2-aerogel matched piezotransducers,” Ultrasonics, vol. 32, no. 3, pp. 217–222, 1994.
[142] T. E. Gomez, F. Montero, E. Rodriguez, A. Roig, and E. Molins, “Fabrication and characterisation of silica aerogel films for aircoupled piezoelectric transducers in the megahertz range,” in Proc. IEEE Ultrason. Symp., 2002, pp. 8–11.
[143] R. Gerlach, O. Kraus, J. Fricke, P. Eccardt, N. Kroemer and V. Magori. “Modified SiO2 aerogels as acoustic impedance matching layers in ultrasonic devices” J. Non-Cryst. Solids, 145, pp . 227-232, 1992.
[144] T. Yano, M. Tone, and A. Fukumoto, “Range finding and surface characterization using high-frequency air transducers,” IEEE Trans. Ultrason., Ferroelect., Freq. Contr., vol. 34, pp. 232–236, 1987.

[145] S. Schiller, C. K. Hsieh, C. H. Chou, and B. T. Khuri-Yakub, "Novel high frequency air transducers," Rev. Prog. QNDE, vol. 9, pp. 795–798, 1990.
[146] S. Takahashi, H. Ohigashi, Acoustic microscopy in air by the piezoelectric polymer (P(VDF/TrFE)) transducers. J. Acoust. Soc. Jpn. 59 (2003) 309–315.
[147] Fox, J.D., Khuri-Yakub, B.T., and Kino, G.S., "High Frequency Wave Measurements in Air, " 1983 IEEE Ultrasonics Symposium, pp. 581-592 (1983).
[148] T.E. Gomez, "Acoustic Impedance Matching of Piezoelectric Transducers to the Air", IEEE transactions on ultrasonics, ferroelectrics, and frequency control, vol. 51, no. 5, may 2004.
[149] T.E. Gomez, "Air-coupled ultrasonic spectroscopy for the study of membrane filters", Journal of Membrane Science 213 (2003) 195–207.
[150] A.P. Brysev, L.M. Krutyianskii, V.L. Preobrazhenskii, Physics-Uspekhi, (reviews of topical problems), 41 (8), 1998, p. 793
[151] Preobrazhensky V.L. "Overthreshold nonlinearity of parametric sound wave phase conjugation in solids", Jpn. J. Appl. Phys. 1993, 32 (1), 2247-2251.
[152] A.P. Brysev, L.M. Krutyansky, and V.L. Preobrazhensky ''Modern problems of the parametric ultrasonic wave phase conjugation'' Physics of Vibrations Vol. 9. Number 1,pp. 52 – 70 (2001).
[153] C. Elias, "An ultrasonic pseudorandom signal correlation system," IEEE Trans. Sonics Ultrason., vol. SU 27, no. 1, pp. 1-7, 1980.
[154] F. Lam and M. Hui, "An ultrasonic pulse compression system using maximal length sequences," Ultrason., vol. 20, no. 3, pp. 107-1 12, 1982.
[155] M. M. Bilgutary. E. S. Furgason, and V. L. Newhouse "Evaluation of random signal correlation for ultrasonic flaw detection," IEEE Trans. Sonics Ultrason., vol. SU 23, no. 5, pp. 329-333, 1976.
[156] M. O'Donnell, "Coded excitation system for improving penetration of real time phased array imaging systems," IEEE Trans. Ultrason., Ferroelec., Freq. Confr., vol. 39, pp. 341-351. 1992.
[157] B. B. Lee and E. S. Furgason, "High speed digital Golay code flaw detection system," Ultrason., vol. 21, pp. 153-161, 1983.
[158] W. H. Chen and J. L. Deng, "Ultrasonic non destructive testing using Barker code pulse compression techniques," Ultrason., vol. 26, pp. 23-26, 1987.
[159] E. E, Hollis, ''Comparison of combined Barker codes for Radar use." IEEE Trans. Aerosouce and Electron. Sysf., vol. AES-3, no. 1. pp. 141-144, 1967.
[160] D. V. Sarwate and M. B. Pursdey, "Crosscorrelation properties of pseudorandom and related sequences," Proc. IEEE, pp. 593-619, 1980.
[161] M. J. Golay. "Complementary series," IRE Tans. Inform. Theon, vol. IT-7. pp. 82-87, April 1961.
[162] E. E. Hollis, "A property of decomposable Golay codes which greatly simplifies sidelobe calculation," Proc. IEEE, pp. 1727-1728. 1975.
[163] R. L. Frank, "Polyphase codes with good nonperiodic correlation properties," IEEE Trans. Inform. Theory. vol. IT-9, no. I , pp. 4345, 1963.
[164] C. E. Cook and M. Bernfeld. Radur signals, An introducrion to theory and applications. New York: Academic, 1967
[165] M. H. Ackroyd, "The design of Huffman sequences." IEEE Truns. IRE Trans. Inform. Theory, vol. IT-8, pp, 10-16, 1962. Aerospace and Electron. Syst., vol. AES-6, pp. 790-796. 1970.
[166] F. F. Kretschmer and Lin, "Huffman coded pulse compression waveforms", RNL Rep. 8894. Naval Res. Lab., Wash.. DC, pp. 96108, Feb. 1985.

[167] W.P. Mason, R.N. Thurston, “Physical acoustics: principles and methods”, Volume 1, Methods and devices, London: Academic Press; New-York, 1964.
[168] Khokhlova V.A., Averianov M.V., Blanc-Benon PH., Cleveland R.O. “Propagation of nonlinear acoustic signals through inhomogeneous moving media”, Proc. IEEE UFFC Conf., Montreal, 2004, pp 533-536.
[169] Rosanov N.N, Sochilin G.B. “Sound channels and lenses in the madium with inhomogeneities of velocity of medium motion”, Pis'ma Zh. Tekh. Fiz. V. 30, №11. – pp. 85-88 (2004).
[170] Hayward, G. and Gachagan, A. “An evaluation of 1-3 connectivity composite transducers for air-coupled ultrasonic applications” J. Acoust. SOC. Am. 99 (4), pp 2148-2157, 1996.
[171] M. I. Haller and B. T. Khuri-Yakub, “Micromachined 1-3 composites for ultrasonic air transducers,” Rev. Sci. Instrum., vol. 65, no. 6, pp. 2095–2098, 1994.
[172] V. Gibiat, O. Lefeuvre, T. Woignier, J. Pelous, and J. Phalippou, “Acoustic properties and potential applications of silica aerogels,” J. Non-Cryst. Solids, vol. 186, pp. 244–255, 1995.
[173] S. P. Kelly, G. Hayward, and T. E. Gomez, “An air-coupled ultrasonic matching layer employing half wavelength cavity resonance,” in Proc. IEEE Ultrason. Symp., 2001, pp. 965–968.
[174] M. C. Bhardwaj, “High transduction piezoelectric transducers and introduction of noncontact analysis,” in Encyclopaedia of Smart Materials. J. A. Harvey, Ed. New York: Wiley, 2000.

RESUME :

Les méthodes de diagnostic ultrasonore sont largement développées aujourd'hui et sont appliquées avec succès en géophysique, en médecine et dans l'industrie pour le contrôle non-destructif. La mesure de la vitesse des écoulements gazeux représente un problème important pour les domaines industriels et scientifiques où les méthodes ultrasonores sont largement appliquées. Les méthodes ultrasons possèdent une série d'avantages qui les rendent seules applicables dans de nombreuses applications pratiques. Les méthodes modernes d'imagerie ultrasonore utilisent de nouveaux effets tels que l'interaction des ondes ultrasonores dans le milieu de propagation non-linéaire ainsi que l'interaction avec des champs de diverses natures ou encore, prennent en compte les effets non-linéaires.

L'apparition des transducteurs piézoélectriques a provoqué une large utilisation des ondes ultrasonores dans les applications pratiques. Le développement de moyens de mesure "sans contact" suscite toujours le plus grand intérêt. L'introduction récente du contrôle ultrasonore sans contact et sans milieu couplant intéresse un nombre croissant de fournisseurs dans le domaine du CND (contrôle non destructif) et ouvre la voie à des applications qu'il n'était pas possible d'envisager avec les techniques traditionnelles. L'ultrason aux fréquences basse dans la bande du MHz devient une possibilité réelle pour quelques applications particulières: dans le domaine du CND, en vélocimétrie, microscopie et tomographie ultrasonore des écoulements.

Parallèlement au développement des techniques de mesures ultrasonores dans les années 1960, l'invention de laser lance le développement de l'optique cohérente. A partir du fait que l'équation d'onde est invariante au changement de signe du vecteur d'onde, on a montré la possibilité d'obtenir des faisceaux optiques « retournés à fronts d'ondes » c'est-à-dire des faisceaux possédant la même distribution des phases et des amplitudes que des faisceaux initiaux mais se propageant en direction inverse. On a nommé cet effet la Conjugaison de Phase car cette transformation provoque l'inversement de la phase de l'onde. Dans les années 1970, on a obtenu expérimentalement la Conjugaison de Phase par la diffusion induite de la lumière. Son utilisation en optique cohérente a permis de résoudre un ensemble de problèmes complexes : autocompensation des distorsions de phase dans les dispositifs optiques et guides de lumière, autofocalisation de l'émission laser sur des cibles, contrôle et gestion de la structure spatio-temporelle des champs optiques.

Après la découverte de la Conjugaison de Phase en optique, on a commencé les tentatives de conjugaison de phase des faisceaux ultrasonores. Pourtant, l'application par analogie à l'optique des mécanismes basés sur les principes du mélange à quatre ondes de type holographique ou paramétrique n'a pas donné de résultat positif. La difficulté principale qui complique l'utilisation de ces principes est l'absence de la dispersion des ultrasons en acoustique non-linéaire.

Une approche plus efficace a été trouvée, consistant en l'utilisation d'un pompage de type non-acoustique pour le retournement paramétrique du son dans les milieux électro- et magnéto-acoustiquement actifs. L'existence d'un régime de génération de l'onde inverse au dessus de seuil d'instabilité absolue des ondes ultrasonores dans un solide permet d'effectuer l'opération de la conjugaison de phase avec une amplification géante (qui excède 80 dB pour la céramique magnétostrictive). Cette méthode est appelée la conjugaison de phase paramétrique.

L'approche alternative suivante consiste en l'utilisation du fait qu'en acoustique, contrairement à l'optique, il existe une possibilité de mesurer la phase de signal. Ainsi on peut enregistrer la distribution du champ acoustique dans une certaine région de l'espace, pour ensuite la retourner temporellement par traitement électronique et la réémettre dans l'espace. A la fin des années 1980 cette approche a été réalisée techniquement : la distribution du champ acoustique est enregistrée par un réseau de transducteurs et réémise dans l'espace en chronologie inverse. Cette méthode est appelée Renversement Temporel. En effet, le renversement de temps provoque le même résultat que la conjugaison de phase : l'onde réémise se propage en sens inverse et possède une surface d'onde inversée par rapport à celle de l'onde initiale.

Ces deux méthodes sont développées actuellement dans les travaux de recherches et possèdent de nombreuses possibilités d'applications pratiques. Leurs utilisations permettent d' améliorer considérablement les caractéristiques des systèmes ultrasonores et de réaliser des effets complètement nouveaux. L'effet d'autocompensation des distorsions de phases trouve de nombreuses applications dans les domaines du contrôle non-destructif, de l'imagerie acoustique et des communications sous-marines. L'autofocalisation des faisceaux acoustiques inverses peut être utilisée en thérapie médicale, contrôle non-destructif et détection acoustique sous-marine où elle permet de résoudre les problèmes de la focalisation et de la détection des objets dans les milieux fortement inhomogènes. L'amplification géante de l'onde inverse rend possible l'utilisation des effets de l'acoustique non linéaire tels que la génération des harmoniques

supérieures et la diffusion Brillouin ce qui permet d'augmenter la résolution et la sensibilité des systèmes d'imagerie acoustique.

La poursuite du développement des méthodes de vélocimétrie des écoulements par la mesure du décalage de phase non-compensé des faisceaux ultrasonores conjugués en phase est prometteuse. Ainsi le développement des méthodes modernes de la conjugaison de phase ultrasonore et la demande de l'amélioration des moyens de vélocimétrie ultrasonore des écoulements conditionnent l'actualité de l'investigation des ondes ultrasonores conjuguées en phase dans les milieux mobiles et l'élaboration de méthodes de diagnostique des écoulements par l'effet de la conjugaison de phase.

Actualité du sujet. Les problèmes de l'utilisation des ondes ultrasonores conjuguées en phase dans le domaine du contrôle non-destructif ultrasonore (compris vélocimétrie, microscopie et tomographie ultrasonore des écoulements gazeux) sans contact sont assez urgent. Pour la développement de nouveaux applications pratiques du système de conjugaison de phase à la mode sans contact il est très important de connecter les nouvelles opportunités dans la vélocimétrie et la tomographie ultrasonore des écoulements qui donne la technique de la conjugaison de phase (les avantages de l' autocompensation des distorsions et de l'amplification géante de l'onde conjuguée ; les systèmes de vélocimétrie à base de CdP n'exige pas le réglage de précision, en assurant le confocalité automatique des schémas de mesure) avec les possibilités d'ultrasons couplé par l'air aux fréquences basse dans la bande du mégahertz.

But de la recherche. Le but principal de la recherche est la realisation de la technique de la conjugaison de phase ultrasonore à couplage par l'air pour la microscopie et la vélocimétrie de micro écoulements. Pour atteindre le but posé, on a défini les **tâches de recherche** suivantes :

1. Les investigations théoriques et expérimentales des particularités de la propagation des ondes ultrasonores conjuguées en phase dans les milieux gazeux.
2. Développement dans le cadre de l'acoustique géométrique un système d'équations pour décrire mathématiquement le passage par l'interface entre l'élément actif du système de conjugaison de phase confocale – milieu de propagation.

3. Les investigations théoriques et expérimentales de modes du fonctionnement du conjugateur avec des faibles signaux acoustiques et différent temps du pompage électromagnétique.

4. Choix de techniques avancées de traitement du signal pour augmenter le rapport signal-bruit.

5. Les investigations théoriques et expérimentales d'adaptation d'impédance acoustique entre le capteur et l'air, l'élément actif du système de conjugaison de phase et l'air.

6. Les investigations de la possibilité d'application de l'effet de conjugaison de phase paramétrique à la vélocimétrie des écoulements gazeux et à la microscopie à couplage par l'air.

7. Création d'un dispositif expérimental et réalisation des expériences de la mesure des vitesses des écoulements gazeux à l'aide de la conjugaison paramétrique de phase. Comparaison des données obtenues avec les résultats de calculs numériques réalisés en utilisant le modèle théorique.

Méthodologies de la recherche. Pour atteindre les buts posés, on a utilisé les méthodes d'intégration numérique des systèmes d'équations différentielles de l'acoustique géométrique. Les méthodes d'automatisation basées sur la conception d' instruments virtuels ont été utilisées pendant la réalisation des expériences. Ce travail a pu être réalisé en s'appuyant sur de la conjugaison de phase paramétrique du son en mode supercritique dans une céramique magnétostrictive.

Nouveautés scientifiques de la recherche. Dans le travail pour la première fois :

1. La conjugaison de phase ultrasonore à couplage par l'air basée sur une céramique magnétostrictive et une membrane de filtration poreuse pour la microscopie et la vélocimétrie de micro écoulements a été développée.

2. Une technique d'adaptation d'impédance acoustique basée sur la membrane de filtration poreuse imprégnée par de l'huile a été développée et réalisé. Cette technique a permis d'optimiser les conditions de transmission de l'onde à l'interface air–ferrite aux fréquences basse dans la bande du MHz.

3. Une technique de codage de phase par m-séquence pour l'enregistrement des faibles signaux conjugués en phase a été développée et réalisé. Cette technique a permis de travailler plus efficacement avec le fort bruit et les signaux qui se trouvent sous le niveau de bruit. Aussi cette technique a permis d'améliorer une méthode de vélocimétrie des écoulements gazeux.

Thèses de soutenance.

1. Le modèle mathématique de processus de propagation d'onde conjugué en phase dans le système confocal avec l'espace aérien. Ce modèle permet de calculer les pertes en passage les surface de milieux de propagation et les dépendances angulaire de coefficient de transmission d'onde ultrasonore sur la surface de différentes parties du système de conjugaison de phase.

2. Une technique d'adaptation d'impédance acoustique basée sur la membrane de filtration poreuse imprégnée par de l'huile. Cette technique a permis d'optimiser les conditions de transmission de l'onde à l'interface air–ferrite aux fréquences basse dans la bande du MHz.

3. Une technique de codage de phase par m-séquence pour l'enregistrement des faibles signaux conjugués en phase. Cette technique a permis de travailler plus efficacement avec le fort bruit et des signaux qui se trouvent sous le niveau de bruit. Aussi cette technique a permis d'améliorer une méthode de vélocimétrie des écoulements gazeux.

4. Les résultats de la mesure expérimentale du décalage de phase dans le milieu mobile. Ces résultats expérimentaux permettent de restaurer la distribution des vitesses dans écoulement gazeux et de créer des images de cette distribution.

5. Les résultats des mesures expérimentales de phase et d'amplitude de l'onde conjuguée en phase en système de microscopie à couplage par l'air. Les résultats montrent que le mode supercritique de WPC paramétrique peut être utilisé avec succès dans des systèmes d'imagerie acoustique à couplage par l'air.

Validité des résultats. La validité des résultats obtenus dans le travail est confirmée par la concordance des données expérimentales avec les résultats de calculs

numériques, par les expériences de vérification et par la fondation physique et mathématique des calculs théoriques et des prototypes expérimentaux.

Portée pratique du travail. Les résultats des investigations de propagation des ondes conjuguées en phase dans les milieux mobiles peuvent servir pour l'élaboration de nouvelles méthodes de vélocimétrie ultrasonore dans les applications industrielles.

La propriété unique des ondes conjuguées en phase de reconstruire la distribution initiale de phase sur la source d'émission peut être utilisée pour la création de nouvelles techniques avec de meilleures caractéristiques des systèmes d'imagerie acoustique.

Sensibilité de phase aux déviations de la vitesse de mouvement du milieu du système de la conjugaison de phase ultrasonore à couplage par l'air permettent de créer de nouvelles dispositifs avec de meilleures caractéristiques.

Les méthodes élaborées a repoussé les limites d'applications pratiques de l'effet de conjugaison de phase et peuvent être utilisées pour le développement des dispositifs en vélocimétrie, microscopie et tomographie ultrasonore des écoulements gazeux.

Contenu du travail.

Le manuscrit de thèse se compose de 5 chapitres. Chaque chapitre commence par sa propre brève introduction et finit par un résumé. Le volume total du mémoire de thèse est de 128 pages, comprenant 51 illustrations. La liste bibliographique contient 174 références.

Dans l'introduction nous discutons sur le choix du sujet étudié, l'actualité de ce sujet, son importance scientifique et pratique et sa nouveauté. Puis nous présentons les principaux points de la thèse et nous montrons la validité des résultats obtenus.

Le premier chapitre présente les généralités du sujet. Il contient les notions, les concepts et les bases théoriques concernant les phénomènes de l'effet de conjugaison de phase en acoustique et les différentes approches de sa réalisation et ses applications. On réalise également un état de l'art de la vélocimétrie et CND ultrasonore dans les applications industrielles.

Le deuxième chapitre est consacré aux problèmes de fonctionnement du système de conjugaison de phase avec des faibles signaux acoustiques. On parle de fonctionnement du conjugateur avec des faibles signaux et différent temps du pompage électromagnétique. On parle d'une technique de codage de phase par m-séquence pour l'enregistrement des faibles signaux conjugués en phase. Cette technique a permis de

travailler plus efficacement avec le fort bruit et des signaux qui se trouvent sous le niveau de bruit, d'améliorer une méthode de vélocimétrie des écoulements gazeux. Aussi dans cette partie il s'agit d'une technique d'adaptation d'impédance acoustique basée sur la membrane de filtration poreuse imprégnée par de l'huile. Cette technique a permis d'optimiser les conditions de transmission de l'onde à l'interface air–ferrite aux fréquences basse dans la bande du MHz.

Le troisième chapitre est consacré aux aspects théoriques de la propagation des ondes conjuguées en phase dans l'air et du modèle théorique de la propagation des ondes acoustiques conjuguées en phase dans un milieu mobile dans le cadre de l'acoustique géométrique. Ce modèle permet calculer les pertes en passage les surface de milieux de propagation, les marches de rayon près de la tache de focalisation du système confocale et les dépendances angulaire de coefficient de transmission d'onde ultrasonore sur la surface de différentes parties du système de conjugaison de phase et calculer la modification de phase et d'amplitude des faisceaux acoustiques ultrasonores pendant leurs propagations dans le milieu mobile.

Dans le chapitre 4 il s'agit d'adaptation acoustique du système de la conjugaison onde de phase ultrasonique. On parle de problème d'utilisation de l'ultrasons aux fréquences dans la bande du MHz dans l'air, d'investigation de membranes de filtration pour l'adaptation acoustique du système de la conjugaison de phase. On presente une technique d'adaptation d'impédance acoustique basée sur la membrane de filtration poreuse imprégnée par de l'huile. Cette technique a permis d'optimiser les conditions de transmission de l'onde à l'interface air–ferrite aux fréquences basse dans la bande du MHz.

Le cinquième chapitre contient des exemples d'applications pratiques de l'effet de la conjugaison de phase paramétrique à la vélocimétrie ultrasonore des écoulements gazeux et à la microscopie à couplage par l'air.

La dernière partie du travail est consacrée à une conclusion générale. Nous y discutons sur l'ensemble des résultats numériques et expérimentaux. Nous développons aussi les différentes perspectives que ce travail a amenées.